SCIENTIFIC COMMITTEE
FIFTEENTH REGULAR SESSION
Pohnpei, Federated States of Micronesia
12–20 August 2019

Background analyses for the 2019 stock assessment of SW Pacific striped marlin

WCPFC-SC15-2019/SA-IP-07

N. Ducharme-Barth[1], **G. Pilling**[1]

[1]Oceanic Fisheries Programme, The Pacific Community

Contents

1 Executive summary

This information paper provides details of the supplementary analyses and descriptions of information that support the 2019 assessment of southwest (SW) Pacific striped marlin. These include:

- Description of the 14 fisheries used in the assessment. Though a single region model, a fleets-as-areas structure was used to partition catch and composition data into 4 sub-regions of the assessment region.
- The traditional CPUE standardization approach used in the 2012 assessment is described and compared to the geostatistical CPUE standardization used in the current assessment. Key changes include the movement to a "delta" CPUE standardization approach and inclusion of a species targeting covariate.
- Development of the maturity-at-length ogive used in the current assessment.
- Description of the sex disaggregated composition and growth information used in the development of the sex disaggregated one-off sensitivity model.
- Description of the spatial structure, movement rates, fisheries definitions, and CPUE used to develop the spatially disaggregated one-off sensitivity model.

2 Background information

The stock assessment model presented to the Scientific Committee (SC) of the Western & Central Pacific Fisheries Commission (WCPFC) is a product of the integration of multiple data-sources and analyses. This paper provides additional detail and description of the data preparation and analyses undertaken in support of the 2019 SW Pacific striped marlin (*Kajikia audax*) stock assessment and is meant to be read in conjunction with the main assessment report (Ducharme-Barth et al., 2019a).

The 2019 SW Pacific striped marlin assessment is unique in that there has been a larger than normal time gap back to the previous assessment, relative to other species undergoing regular WCPFC stock assessments. Though the main structure of the model remains similar to the 2012 assessment (Davies et al., 2012), there have been substantial changes in terms of MULTIFAN-CL model development (Davies et al., 2013, 2015, 2017, 2018, 2019), and methodological advances for preparing and incorporating data into the assessment model. Many of the changes relating to the stock assessment model specification will be described in Ducharme-Barth et al. (2019a), however changes that pertain to the analyses preparing catch, catch-per-unit-effort (CPUE), size composition, and biological information for inclusion in the assessment model, will be described in greater detail in this document. Additionally, two substantive one-off sensitivities were undertaken in the 2019 assessment. This document will also cover the data preparation and background analyses done in support of those sensitivity models.

Briefly, this paper will adhere to the following structure. The first section (3) contains a description of the fisheries definitions used for the 2019 regional structure. The second section (4) describes the analyses done to prepare the CPUE data and compares the indices generated using the methods used in the 2012 assessment with the indices produced by the geostatistical methods used in more recent assessments (Tremblay-Boyer et al., 2018a; Vincent et al., 2019). In the third section (5), the development of a maturity-at-length ogive is described. Finally, the last two sections lay-out

the background analyses required for the development of the sex-disaggregated (6) and spatially disaggregated sensitivity models (7).

3 Fisheries definitions

Similar to the two previous striped marlin stock assessments (Langley et al., 2006; Davies et al., 2012), the 2019 assessment assumed a single region with a well-mixed stock. Based on analyses of the spatial patterns in the catch, effort, CPUE and composition data; four sub-regions (Figure 1) were used to define a total of 14 fisheries (12 longline and 2 recreational fisheries) in the assessment model (Langley et al., 2006). These definitions were preserved in the current iteration of the assessment (Table 1).

Japanese longline vessels historically dominated both total longline fishing effort and striped marlin catches within the model region and have had a continued presence since the beginning of the assessment period (1952). Given this, a separate Japanese fishery was defined in each of the four model sub-regions (Fisheries 1-4; Figures 2-5). Japanese longline fishing effort was quite patchy in sub-region 4, and by the 1980s was virtually non-existent. In order to account for this, a separate fishery was defined for Chinese Taipei longline vessels as their effort and catches of striped marlin increased in sub-region 4 post-1970 (Fishery 5; Figure 6). Since the mid-1990s, major longline fisheries for Australia (Fisheries 6-7; Figures 7-8) and New Zealand (Fishery 8; Figure 9) developed in sub-regions 2 & 3 off of eastern Australia and extended south into the Tasman Sea. In order to account for the remaining longline fishing effort and striped marlin catch, four additional longline fisheries were defined in each of the model sub-regions (Fisheries 11-14; Figures 12-15). These fisheries grouped together the effort, catch, and composition data of the other distant-water fishing nations (DWFNs) and Pacific Island countries and territories (PICTs) operating in the assessment region.

In addition to the longline fisheries, individual fisheries were defined in sub-region 3 to account for the two major recreational fisheries targeting striped marlin in the assessment region: Australia (Fishery 9; Figure 10) and New Zealand (Fishery 10; Figure 11). Though the magnitude of catches is dwarfed by total longline removals of striped marlin, these two fisheries are historically significant with catch records dating back prior to 1940 for the Australian recreational fishery and weight composition records dating back to 1925 for the New Zealand recreational fishery. Additional recreational fisheries for striped marlin exist throughout the assessment region (Whitelaw, 2001). However, these fisheries are relatively small and poorly documented compared to the more established fisheries in Australia and New Zealand.

4 CPUE

4.1 Overview

Standardized CPUE indices are critical inputs to stock assessments conducted using integrated models (Fournier and Archibald, 1982). Based on the previously described fisheries definitions, standardized CPUE indices were constructed from catch and effort records for two of the major DWFNs operating in the model region: Japan and Chinese Taipei.

Both the Japanese and Chinese Taipei distant water longline fleets (JPDW & TWDW) have long histories operating in the Pacific region, and particularly in the assessment region for SW Pacific striped marlin. For Japanese longline fishing activity, aggregate monthly catch and effort data,

provided at $5^\circ \times 5^\circ$ grid cells by the Japan Fisheries Agency were available from the beginning of the assessment period in 1952. Beginning in 1967, daily operational logbook catch and effort records were available at $1^\circ \times 1^\circ$ grid cells. Fishing by Chinese Taipei in the SW Pacific ocean provided another key source of information for the assessment model. The development of their TWDW fleet began in the 1960s, with operational logbook catch and effort records available from the Chinese Taipei Fisheries Agency at $1^\circ \times 1^\circ$ grid cells beginning in 1964. These operational datasets are a part of the larger Pacific-wide operational data set which was described by McKechnie et al. (2015). Additionally, smaller "offshore" longline fleets exist for both Japan and Chinese Taipei (JPOS & TWOS). These fleets developed in the 1970's and typically operated in PICT territorial waters pursuant to access agreements.

During the long period of both Japanese and Chinese Taipei fishing operations in the SW Pacific, systematic changes to fishing practices (change in number of hooks between floats, *HBF*), target species, and areas fished (Figure 16) occurred. These systematic changes manifested themselves on top of a background of gradual, persistent increase in vessel efficiency due to technological innovation or improved fisher knowledge. All of these may, independently or cumulatively, result in catchability changes and thus changes in the catch rates of striped marlin by these fleets. In order to account for these spatial and temporal changes in catchability, nominal CPUE data are typically standardized using a statistical model (Maunder and Punt, 2004).

The number of HBF is a commonly used variable in longline CPUE standardization as it is often assumed to be representative of the depth of the fishing gear. This assumption is based on the theoretical catenary geometry of a longline and that more HBF would add more weight to the line causing it to sink deeper. For a relatively shallow swimming species like striped marlin, this is an important covariate to consider as deeper longline sets may not be representatively sampling the population. Unfortunately, HBF was not recorded until the 1970s in the Japanese data and the mid-1990s by Chinese Taipei. Similar to what was done previously (Hoyle et al., 2012), this analysis assumed that Japanese longline sets prior to 1970 had a similar gear configuration to that deployed in the early 1970s (5 HBF), and assumed that Chinese Taipei sets prior to 1995 had a gear configuration similar to that fished in the late-1990s (10 HBF).

Not unlike the evolution of fishing practices in the Pacific, CPUE standardization practices used in WCPFC stock assessments have changed since the last striped marlin stock assessment. In 2012, a generalized linear model (GLM) was used to standardize CPUE for the striped marlin assessment (Hoyle et al., 2012); this approach gave way to the two-step delta-GLM model (McKechnie et al., 2016, 2017; Tremblay-Boyer et al., 2017), and more recently geostatistical delta generalized linear mixed models (delta-GLMMs) (Tremblay-Boyer et al., 2018a; Vincent et al., 2019). In preparation for this assessment, each iteration of the standardization models listed above was compared in order to span the methodological improvements made since 2012. Ultimately, based on the simulation work done by Ducharme-Barth et al. (2019b), indices produced by the geostatistical delta-GLMMs were used for the 2019 assessment.

In addition to comparing the choice of standardization model type, this analysis also considered fitting data at either the monthly-$5^\circ \times 5^\circ$-HBF aggregate level (*cell-month-HBF*) or the daily $1^\circ \times 1^\circ$ operational logbook level. The cell-month-HBF aggregation scheme is a slight modification to what was done previously in 2012 which aggregated the data at the cell-quarter-HBF level. In this particular case, there are benefits to analyzing the data at either the aggregate cell-month-HBF or operational logbook level. Using the aggregated data allows for the creation of an index spanning the entire assessment period. This is an important consideration given that the largest annual catches occur prior to the availability of the operational logbook data. However, previous

studies (Ahrens, 2010; Hoyle et al., 2010) noted that the analysis of aggregate data may limit the ability to identify or correct for fine scale patterns in fishing strategy. Additionally, using the operational level data allows for the estimation of individual vessel effects which can potentially account for biases introduced via effort creep and technological innovation.

Prior to undertaking the CPUE analysis, data (both the aggregated cell-month-HBF and the operational logbook) were filtered to match the protocol used in Hoyle et al. (2012). Data were removed if the number of hooks fished were ≤ 0, if no catches were reported, and if HBF were greater than 40 or missing after 1970. Data from trips pertaining to OS vessels (both for Japan and Chinese Taipei) were also removed for the majority of the models considered in this analysis. A special run of models added the OS data back in to explore the effect of including these data. The net result of each data processing step can be seen in Figure 17.

Standardized CPUE indices were calculated at a year-quarter time step to match the temporal resolution of the fisheries catch data provided to the assessment model. CPUE was defined as catch of striped marlin in numbers per 100 hooks fished. Separate indices were calculated for each of the 4 assessment sub-regions. In the case of the geostatistical model the 4 sub-region indices were estimated simultaneously using a single estimation model. The conventional approaches fit a separate, independent estimation model to data within each of the 4 sub-regions. It is important to note that though Chinese Taipei data are present in all 4 model regions; it is only defined as an independent fishery in the assessment for sub-region 4 and therefore only the index calculated for sub-region 4 is considered in the assessment. Indices were calculated for Chinese Taipei in the other 3 model sub-regions for completeness.

4.2 Targeting clusters

In order to account for changes in striped marlin CPUE arising from subtle modifications in gear configuration designed to increase the catchability of desired species, target species were identified via a clustering analysis for each aggregate or operational record. The key assumption being that fishing effort directed towards a particular species should have a high proportion of the total catch of the target species. This analysis is in line with what has previously been done in CPUE standardization analyses supporting WCPFC stock assessments (Bigelow and Hoyle, 2012; Tremblay-Boyer et al., 2015, 2018b).

Target species were identified at the monthly-$5^\circ \times 5^\circ$ (*cell-month*) aggregate level using a k-means (Hartigan and Wong, 1979) clustering analysis in R (R Core Team, 2018) following the approach of McKechnie et al. (2015). Aggregating the catch to this scale was thought to better represent the overall targeting strategy for vessels operating within that cell since it removed potential set-to-set variability, and it allowed for clustering to be defined in the same way for both the aggregate and operational logbook data. The k-means clustering algorithm was selected since it is able to efficiently cluster large data sets, though it is worth noting that other clustering algorithms could be used which could lead to different results. The proportion of total catches of striped marlin (STM), albacore tuna (ALB), bigeye tuna (BET), yellowfin tuna (YFT), and swordfish (SWO) was used to define the cluster membership of each cell-month. k-means clustering requires an *a priori* definition of the number of clusters so partitions of 2, 3, 4 and 5 were explored. It was found that a two-cluster partitioning of cell-months into either albacore or tropical tuna (BET/YFT) clusters best captured the key spatial and temporal patterns in species targeting as it pertained to striped marlin. Cluster identity was then mapped back to both the aggregate and operational logbook data based on cell-month and this variable was included in the CPUE standardization as

a covariate.

Clustering results are shown here as the temporal pattern in proportion of the total catch of each species for each cluster (Figure 18), and the number of cell-months classified as each cluster across space, time, and fleet group (Figure 19). In the albacore cluster (k2 in Figure 18) species proportion remained fairly constant over time. However, in the tropical tuna cluster (k1 in Figure 18), the proportion of bigeye tuna gradually increased over time at the expense of yellowfin. Spatiotemporal patterns in clustering were present. Vessels operating in the equatorial sub-region 1 typically were classified as having higher proportions of tropical tuna catch, while vessels in the other sub-regions were classified as having higher proportions of albacore in the catch. An exception to this is the TWDW fleet operating in region 1 which appeared to undergo a switch in targeting from albacore to tropical tunas around the year 2000.

4.3 Traditional CPUE models

4.3.1 GLM

In the 2012 stock assessment, a log offset GLM was used to standardize CPUE for both the Japanese and Chinese Taipei fleets. This model was defined according to Hoyle et al. (2012) as follows:

$$log(C_i + 1) \sim YearQtr_i + Cell_i + g(HBF_i) + g(log(hhooks_i)) + \epsilon; \epsilon \sim Normal \tag{1}$$

where C is the i^{th} observation of striped marlin caught (in numbers), $YearQtr$ is the fixed effect for year-quarter, $Cell$ is the fixed effect for the $5^\circ \times 5^\circ$ spatial cell, $g(HBF)$ is a cubic spline of degree 7 for the HBF, and $g(log(hhooks))$ is a cubic spline of degree 10 for the natural logarithm of hundred hooks fished.

4.3.2 delta-GLM

A conventional delta-GLM was fit for the purpose of model comparison. Delta-GLMs are the combination of two underlying GLMs: a logistic model (binomial component) predicting the probability of a positive catch occurring and a second model (positive component) predicting the magnitude of the positive catch rate (Lo et al., 1992; Stefansson, 1996). The two models are defined as follows:

$$p_i \sim YearQtr_i + Cell_i + p(HBF_i) + \epsilon; \epsilon \sim Binomial \tag{2}$$

$$C_i > 0 : log\left(\frac{C_i}{hhooks_i}\right) \sim YearQtr_i + Cell_i + p(HBF_i) + \epsilon; \epsilon \sim Normal \tag{3}$$

where the model terms are defined as above for the GLM. The exception is $p(HBF_i)$ which is defined as a polynomial spline of degree 7.

4.4 Geostatistical delta-GLMM model

A geostatistical delta-GLMM is an extension of the delta-GLM described above, the key difference being how space is modeled. An interactive relationship between space and time, as opposed to an additive one, is specified using Gaussian random fields to define the spatial and spatiotemporal components of the model (Thorson et al., 2015). These Gaussian random fields are defined with a Matern covariance function. Using the estimated correlation structure of the data, geostatistical

delta-GLMMs can simultaneously interpolate abundance of unobserved strata. The delta-GLMM structure was implemented in R using the VAST package (Thorson, 2019) and is defined below:

$$p_i \sim YearQtr + \omega_1(x_i) + \phi_1(x_i, t_i) + SpeciesCluster^* + p(HBF) + \xi_1(x_i, t_i) + \epsilon \quad (4)$$

$$log\left(\frac{C_i}{hhooks_i}\right) \sim YearQtr + \omega_2(x_i) + \phi_2(x_i, t_i) + SpeciesCluster^* + p(HBF) + \xi_2(x_i, t_i) + \epsilon \quad (5)$$

$^*SpeciesCluster$ *excluded in the model used for comparison with the GLM and delta-GLM.*

where $YearQtr$ is the fixed effect for year-quarter, $\omega(x_i)$ is the spatial random effect at knot x, $\phi(x_i, t_i)$ is the spatiotemporal random effect at time t and location x, $SpeciesCluster$ is the fixed effect for target species, $p(HBF)$ is a polynomial spline of degree 5 for the HBF and $\xi(x_i, t_i)$ is the quadratic effect of sea surface temperature (SST) at $YearQuarter$ t and knot x. Both ω and ϕ are described by multivariate normal spatial random fields $MVN(0, R)$ where R is a Matern correlation function. In the case of ϕ, temporal independence across $YearQtr$ was assumed. One-hundred-forty-four spatial knots were used to define the spatial structure of the model. Three different methods were used to distribute the knots defining the spatial structure of the model: proportional to the density of the observations (knot type 0), proportional to the $1^\circ \times 1^\circ$ grid cells within the assessment region (knot type 1), and proportional to the sampled $1^\circ \times 1^\circ$ grid cells within the assessment region (knot type 2). Please consult the *Technical Annex* of Ducharme-Barth et al. (2019b) for a more thorough discussion of both the model structure and description of the process used to allocate observations to spatial knots.

One of the benefits of the geostats framework is that it can use the estimated spatial correlation structure of the data, along with any estimated relationships with environmental covariates, to interpolate abundance into un-sampled areas. However, for a sub-tropical species like striped marlin, it is particularly important that biomass is not interpolated into areas that are biologically unfeasible (i.e. too cold). Previous geostats analyses used in WCPFC stock assessments made modifications to the model to only use biomass from grid cells that met a biologically realistic minimum temperature threshold for the creation of the abundance index (Tremblay-Boyer et al., 2018b; Kinoshita et al., 2019). The same approach was taken in this analysis by not interpolating abundance into cells with SST below the minimum thermal threshold from each quarter. This threshold was defined as the minimum observed temperature for striped marlin in each quarter (Figure 20) based on matching up the (x_i, t_i), specified for the geostats model that striped marlin were caught in with the appropriate quarterly temperature from the NOAA ERRST model (Smith and Reynolds, 1981).

4.5 Model comparisons

In the development of the final indices used in the 2019 stock assessment, a number of different side analyses were undertaken to assess the impacts of changing the data inputs, model structure or model type.

Given the progression in CPUE standardization models since the last assessment; GLM, delta-GLM, and geostats models were used to calculate indices for the JPDW and TWDW fleets in each of the 4 sub-regions. This served a dual purpose of comparing the effect of model type on the estimated index, but also to calculate a baseline index with the GLM to use as input in the stepwise development of the 2019 assessment model. These models were configured according to Hoyle et al. (2012) to have the same formulation ($YearQtr_i + Cell_i + g(HBF_i)$), and were fit to data aggregated at the quarterly, $5^\circ \times 5^\circ$, and HBF category level. The results of this are shown in Figure 21. All

indices were standardized to a mean of 1 prior to plotting. Generally speaking, the GLM and the geostats indices showed similar trends across sub-regions and fleet groups. The exception to this was sub-region 4 for Japan. Spatial sampling deteriorated substantially after the 1970s and this was reflected in the volatility and discontinuity of the GLM estimated index. The delta-GLM index (calculated solely for completeness of the comparison) appeared quite volatile, and in two instances (JP-4 and TW-3) was not able to be calculated. This was driven by a sensitivity to the number of observations in a given temporal stratum. The large spikes in the index occured in instances where there were very few observations, the binomial component was predicted to be very close to 1, and the observed positive cpue was quite high. When the two components of the delta-GLM model were multiplied together to form the index, this resulted in a value that was much larger than in the adjacent periods. Going forwards, the rest of the indices presented were calculated using the geostats model.

As discussed earlier, availability of the operational logbook data presented the opportunity for analyzing data at a finer spatiotemporal scale and accounting for individual vessel effects. However, there was a tradeoff with the length of data availability, particularly in the case of the Japanese data. Unique vessel ID for Japan was largely incomplete prior to the 1980s. Tremblay-Boyer et al. (2018b) tried to account for this by fitting a block vessel effect for the missing vessels. However, this had an undesireable effect in the estimated indices and so data coming from vessels with missing ID were removed from their analysis. Following that approach, data from vessels with missing IDs were removed from the current analysis which limited estimating an index to post-1979 for the Japanese data. Vessel ID was not an issue for the Chinese Taipei data as it was available back to 1964. In this particular analysis, there did not appear to be much of a difference in modeling the data at an aggregated scale versus using the operational level data (Figure 22). The estimated trend was very similar between the two types, though perhaps shifted up a little in the case of the indices estimated from the Japanese data. Given that using aggregated data allowed for the estimation of an index for the entire model period, aggregate data were used to estimate the indices presented in the remaining analyses and in the assessment.

The effect of including the OS data, as well as modeling all of the data (JP/TW and DW/OS) together was also considered (Figure 23). In sub-regions 1-3 the combined JPTW.DW index followed the same trend as the index derived solely from JP.DW data. In sub-region 4, the combined index seemed to follow the JP.DW before switching to more closely follow the TW.DW index post-1970. This result is unsurprising given the scarcity of JP.DW fishing effort in sub-region 4, and is specifically addressed in the assessment model with the creation of Fishery 5 (TW longline sub-region 4). Overall, the combined index did not appear to differ from the indices of the dominant fleet in each sub-region. Given this, and the fisheries structure defined for the assessment, the combined index was not given further consideration. Since the indices for the individual fleets were retained, choice of the standardized index (JP or TW) used in the assessment was included as an axis in the structural uncertainty grid. The inclusion of OS data did not appear to make much of a difference to the estimated index and was not considered further.

Using a geostatistical model estimated from JPDW data as a baseline, Figure 24 shows the impact on the index of sequentially adding the SST and catchability related covariates (HBF and SpeciesCluster). The first row of Figure 24 shows the effect of modeling the data with a geostatistical model, and the revision from the nominal catch rates especially in sub-regions 1 and 4. In the model periods where spatial sampling coverage was lower (early period for sub-region 1 and later period for sub-region 4) the estimated index was strongly influenced by data in adjacent sub-regions via the estimated model correlation structure. This resulted in a departure from the nominal trend.

In time periods that had more thorough spatial sampling, the index more closely related to the nominal catch rate of the region. Including SST did not change the index much except in sub-region 4 (2^{nd} row, Figure 24). This result makes intuitive sense. Spatiotemporal sampling in sub-region 4 was quite patchy, and as a result the index from this region would be heavily influenced by the interpolated biomass estimates derived from the spatial correlation structure and the SST relationship. Lastly, inclusion of the catchability covariates resulted in a large downwards revision of the index in the first two years (3^{rd} row, Figure 24).

Finally, the method used for defining the spatial knot structure was explored using a geostatistical model estimated from JPDW data(Figure 25). Similar to what was seen in the previous comparison, in sub-regions where spatial sampling was patchier (sub-region 4) the choice of method for defining the spatial knot structure made the most difference. Additionally, across all model sub-regions, knot structure definition caused differences in the index in the first year. This could impact the overall level of depletion implied by the index. To account for this, sensitivity to the choice of method for defining the knot structure was considered in the stepwise development of the 2019 diagnostic case model.

4.6 Diagnostic case index

In the 2019 striped marlin diagnostic case, Fishery 2 (Figure 3) was used as the fishery for which catchability was assumed to be constant over time and was the standardized CPUE index the assessment model was fit to. This standardized CPUE time series was estimated from aggregated Japanese distant-water data using a geostatistical model with 144 spatial knots distributed spatially according to the type 2 structure (Figure 26). Though indices were calculated for all 4 sub-regions, the presentation of the results will focus on sub-region 2 as this was the index used in the diagnostic case. The standardized index in sub-region 2 (Figure 27) appeared to decrease fairly rapidly from a peak in the mid-1950s, before rising briefly in the early 1970s. Following this, the index gradually declined for the rest of the time series resulting in an approximately 8-fold decrease in CPUE. Additionally, the index in sub-region 2 did not appear to be overly influenced by data from the other model sub-regions.

The included catchability covariates did not have the same effect on the binomial and positive (Figure 28) components of the assessment model. In the binomial component, both *SpeciesCluster* (denoted k2 in Figure 28) and *HBF* (denoted hbf in Figure 28) had similar magnitudes of influence on the index. However, in the positive component the effect of *SpeciesCluster* was negligible in comparison. Additionally, it is possible that *HBF* is temporally confounded with catch rate as both follow largely monotonic trends over the model period (HBF increasing and catch rate decreasing).

In terms of the spatiotemporal structure of the estimated quantities, both the predicted encounter probability and the predicted standardized CPUE showed similar patterns and a strong E-W spatial correlation structure (Figure 29). A persistent band of encounter probability exists between 20°S and 30°S, with the highest encounter probability west of 160°E (Figure 30). This hotspot of encounter probability coincides with the predicted CPUE hotspot (Figure 31), though the magnitude of predicted CPUE decreases overtime. Striped marlin in the SW Pacific Ocean are believed to form a spawning aggregation in this encounter and CPUE hotspot during the 4^{th} quarter of the year (Kopf et al., 2012). High levels of effort, and associated removals, during the spawning aggregation could explain the decline seen in the standardized index.

The choice of CPUE index to fit to was included as an axis in the structural uncertainty grid. In addition to fitting to the CPUE for Fishery 2, fitting to the CPUE for Fishery 5 (Figure 6) was

also considered. This index was estimated using the same geostatistical model structure that was just described for Fishery 2 except that aggregated Chinese Taipei distant-water data were used. Again, indices were calculated for all 4 model sub-regions but only the index from sub-region 4 was used (Figure 32).

5 Maturity-at-length

The maturity ogive (ρ) typically used in assessment models is a fixed vector of age-specific values. However, a recent development in MULTIFAN-CL (Davies et al., 2019) allows for the maturity ogive to be input as a function of length (ρ_ℓ). This is then mapped back to age, with respect to the growth function, internal to the model assessment model. The length based maturity ogive used to develop the 2019 diagnostic case was calculated as:

$$\underset{\ell=1}{\overset{\ell=52}{(\rho_\ell)}} = PF_\ell \times PMF_\ell \tag{6}$$

$$PF_\ell = 0.035 + \left(\frac{1.06 - 0.035}{1 + \left(\frac{LJFL_\ell}{2322} \right)^{-15.25}} \right) \tag{7}$$

$$PMF_\ell = -0.002 + \left(\frac{1.17 + 0.002}{1 + \left(\frac{LJFL_\ell}{2100} \right)^{-12.60}} \right) \tag{8}$$

$$LJFL_\ell = 1.16 \times EFL_\ell \times 10 \tag{9}$$

where PF and PMF are the proportion female and proportion females that are mature at length bin ℓ. For the stock assessment, length frequency measurements were aggregated into 52, 6cm bins beginning at 20cm. Calculations of PF and PMF at length were done based on the midpoint of each length bin using Equation 7 and Equation 8 which come from Kopf et al. (2012). Equations 7 & 8 were calculated based on the lower-jaw-fork length ($LJFL$) measurement taken in mm. However, the length frequency data used in the assessment were recorded as eye-orbital fork length (EFL) in cm so these were converted to $LJFL$ mm using Equation 9 (Williams and Smith, 2018).

The calculated curve for proportion female at length (Figure 33) showed very low proportions of females at length for smaller individuals (< 150cm). Striped marlin are not known to be protandrous hermaphrodites so this was thought to be unrealistic. The proportion female at length was modified so that a 50:50 sex ratio at length was assumed up to the inflection point of the curve described in Kopf et al. (2012). Therefore the maturity at length ogive, ρ_ℓ, used in the stock assessment is a product of the modified PF curve and PMF, rescaled so the maximum is 1 (Figure 34). Sensitivity to using the modified versus non-modified PF in the calculation of ρ_ℓ was considered in the stepwise development of the diagnostic case. Compared to the maturity at age ogive that was used in the 2012 stock assessment, the ρ_ℓ used in the current assessment shifted the spawning potential to older individuals.

6 Sex disaggregated model

Previous research has found some evidence of sexual dimorphism in striped marlin. Kopf et al. (2011) showed sex specific differences in the length-at-age and weight-at-length relationships for SW

Pacific striped marlin, with females growing to be larger than males. An accompanying study on reproductive behavior and characteristics noted that the sex-ratio at larger lengths tended to skew towards females (Kopf et al., 2012). One of the recommendations made in the 2012 stock assessment was to consider an alternative sex-disaggregated model structure in order to more appropriately account for these sex-specific processes. This sex-disaggregated model builds off of the work done by Takeuchi et al. (2018) for SW Pacific Ocean swordfish.

6.1 Biological parameterization

The 2019 striped marlin stock assessment assumed the "back-calculation 1" growth model from Kopf et al. (2011), averaged between sexes. The sex-disaggregated sensitivity models considered the sex specific growth from the "back-calculation 1" (Equations 10 & 11) and "back-calculation 2" models (Equations 12 & 13) from Kopf et al. (2011). Since Kopf et al. (2011) calculated growth in terms of *LJFL* mm, the parameters had to be recalculated in terms of *EFL* cm for use in the assessment model.

$$LJFL_{M,BK_1} = 2615(1 - e^{-0.44(Age+0.81)}) \tag{10}$$

$$LJFL_{F,BK_1} = 2628(1 - e^{-0.46(Age+0.71)}) \tag{11}$$

$$LJFL_{M,BK_2} = 2535(1 - e^{-0.51(Age+0.68)}) \tag{12}$$

$$LJFL_{F,BK_2} = 2580(1 - e^{-0.51(Age+0.59)}) \tag{13}$$

These growth curves are shown relative to the growth assumed for the 2019 diagnostic case in Figure 35.

The sex specific weight-at-length relationships calculated by Kopf et al. (2011), Equations 14 & 15, were also considered for the sex-disaggregated sensitivity runs. Again as these were calculated in terms of *LJFL* mm, the parameters were recalculated in terms of *EFL* cm. These are shown in terms of weight-at-age in Figure 36.

$$W_M = 1.902 \times 10^{-9} \times LJFL^{3.16} \tag{14}$$

$$W_F = 4.171 \times 10^{-11} \times LJFL^{3.67} \tag{15}$$

6.2 Sex-specific composition data

Sex-specific length and weight composition data for each fishery were compiled from data provided by: the National Research Institute for Far Seas Fisheries (NRIFSF) (Fisheries 1-4), the Fisheries Agency - Chinese Taipei (Fishery 5), the Australian Fisheries Management Authority (AFMA) (Fisheries 6-7), the Ministry of Fisheries - New Zealand (Fishery 8), Julian Pepperell (Pepperell Research & Consulting Pty Ltd) (Fishery 9), John Holdsworth (Blue Water Research Ltd.) (Fishery 10), and regional observer programs (Fisheries 11-14). Where necessary, measurements were converted to whole weight in kg and *EFL* in cm. A summary of the sex-specific composition data that was used in the analysis is shown in Figures 37 (length) & 38 (weight). There does appear to be a pattern of females being larger, however the dimorphism observed is much less than that observed for SW Pacifc Ocean swordfish (Takeuchi et al., 2018). For the recreational fisheries, paired length-weight measurements for unique individuals were available and these data are shown in Figure 39. Again, females appear to grow larger than males, however it is also apparent that fish sampled off of the east coast of Australia are smaller than those sampled in New Zealand.

7 Spatially disaggregated model

In addition to the sex disaggregated sensitivity model described above, a spatially disaggregated one-off sensitivity was also explored. In this model the outer boundaries of the assessment region in the SW Pacific Ocean were kept the same, but the assessment region was divided into two regions at 165°E similar to what was done for SW Pacific Ocean swordfish (Takeuchi et al., 2017). Previous tagging research conducted on striped marlin, using both conventional and electronic tags, appears to indicate different patterns of movement on either side of the 165°E boundary (Ortiz et al., 2003; Domeier, 2006; Sippel et al., 2011). Fish tagged off of the east coast of Australia (west of boundary) appear to show higher residence times and lower levels of dispersion relative to fish tagged off of the North Island of New Zealand (east of the boundary). These contradictory signals appear to challenge the assumption of a single homogeneous, well-mixed population made by the single region structure assumed in the 2019 striped marlin stock assessment. A series of two-area models with different levels of movement between the two assessment regions were run to evaluate the model sensitivity to the assumption of a single assessment region.

7.1 Spatial structure

As mentioned before, the two-region spatially disaggregated model was created by dividing the assessment region along 165°E. As a result, the existing sub-regions used to define fisheries in the model (1, 2, and 3) were bisected. This resulted in 7 sub-regions being defined with sub-regions 1, 3, and 5 contained in model region 1, and sub-regions 2, 4, 6, and 7 contained in model region 2 (Figure 40).

7.2 Movement rates

Given the limited knowledge about movement across the 165°E boundary, movement of striped marlin between the two assessment regions was defined in terms of quarterly bulk transfer rates (Δ) based up a range of diffusion rates (δ) agreed to at the 2019 Pre-Assessment Workshop (Pilling and Brouwer, 2019). Three diffusion scenarios were proposed: no movement ($\delta = 0$), moderate movement ($\delta = 0.1$), and high movement ($\delta = 0.4$). Diffusion was defined as longitudinal degrees traveled per day in the E-W direction following (Kolody and Davies, 2008). These diffusion rates were then converted to bulk transfer rates (defined as proportion of numbers moving per quarter) according to Kolody and Davies (2008) which allowed for the calculation of directional transfer rates east to west (Δ_{EW}) and west to east (Δ_{WE}).

- $\delta = 0$

  $\Delta_{EW} = 0$

  $\Delta_{WE} = 0$

- $\delta = 0.1$

  $\Delta_{EW} = 0.0285$

  $\Delta_{WE} = 0.07$

- $\delta = 0.4$

  $\Delta_{EW} = 0.0544$

  $\Delta_{WE} = 0.1373$

For reference the 2017 swordfish diagnostic case (Takeuchi et al., 2017) used bulk transfer rates of 7.5% and 2.5% for the same regional structure so the ones used in these sensitivity model runs are comparable.

7.3 Fisheries definitions

As a result of the new spatial structure, a number of the fisheries had to be redefined. The same fisheries that existed in the 2019 stock assessment were redefined according to the new sub-regional structure. Old Fishery 1 split into new Fisheries 1 (Figure 41) and 2 (Figure 42). The same happened for old Fisheries 2 (new Fisheries 3 and 4, Figures 43 and 44), 3 (new Fisheries 5 and 6, Figures 45 and 46), 11 (new Fisheries 14 and 15, Figures 54 and 55), 12 (new Fisheries 16 and 17, Figures 56 and 57), and 13 (new Fisheries 18 and 19, Figures 58 and 59). Additionally, old Fishery 4 was renumbered as new Fishery 7 (Figure 47). The same happened for old Fishery 5 (Fishery 8, Figure 48), 6 (Fishery 9, Figure 49), 7 (Fishery 10, Figure 50), 8 (Fishery 11, Figure 51), 9 (Fishery 12, Figure 52), 10 (Fishery 13, Figure 53), and 14 (Fishery 20, Figure 60).

7.4 CPUE

For the spatially disaggregated sensitivity runs, Fishery 3 (Figure 42) was selected as the fishery for which catchability was assumed to be constant over time and was the standardized CPUE index that the assessment model was fit to. This fishery was roughly equivalent to Fishery 2 which was used in the 2019 diagnostic case. The standardized CPUE for this fishery was estimated from aggregated Japanese distant-water data using the same geostatistical model used to calculate the index used in the 2019 diagnostic case and described in Section 4.6. Though the geostatistical model estimated indices for all of the sub-regions in the spatially disaggregated assessment structure, only the index in sub-region 3 was used (Figure 61).

References

Ahrens, R. (2010). *A global analysis of apparent trends in abundance and recruitment of large tunas and billfishes inferred from Japanese longline catch and effort data*. PhD thesis, University of British Columbia, Vancouver.

Bigelow, K. A. and Hoyle, S. D. (2012). Standardized CPUE for South Pacific albacore. Technical Report WCPFC-SC8-2012/SA-IP-14, Busan, Republic of Korea, 7–15 August 2012.

Davies, N., Fournier, D., and Hampton, J. (2019). Developments in the MULTIFAN-CL software 2018-2019. Technical Report WCPFC-SC15-2019/SA-IP-02, Pohnpei, Federated States of Micronesia.

Davies, N., Fournier, D. A., Hampton, J., and Bouye, F. (2015). Recent developments and future plans for MULTIFAN-CL. Technical Report WCPFC-SC11-2015/SA-IP-01, Pohnpei, Federated States of Micronesia, 5–13 August 2015.

Davies, N., Fournier, D. A., Hampton, J., Hoyle, S., Bouye, F., and Harley, S. (2013). Recent developments in the MULTIFAN-CL stock assessment software. Technical Report WCPFC-SC09-2013/SA-IP-07, Pohnpei, Federated States of Micronesia, 6–14 August 2013.

Davies, N., Fournier, D. A., Takeuchi, Y., Bouye, F., and Hampton, J. (2017). Developments in the MULTIFAN-CL software 2016-2017. Technical Report WCPFC-SC13-2017/SA-IP-05, Rarotonga, Cook Islands, 9–17 August 2017.

Davies, N., Fournier, D. A., Takeuchi, Y., Bouye, F., and Hampton, J. (2018). Developments in the MULTIFAN-CL software 2017-2018. Technical Report WCPFC-SC14-2018/SA-IP-02, Busan, South Korea, 9–17 August 2018.

Davies, N., Hoyle, S., and Hampton, J. (2012). Stock assessment of striped marlin (Kajikia audax) in the Southwest Pacific Ocean. Technical Report WCPFC-SC8-2012/SA-WP-05, WCPFC Scientific Committee, Busan, Republic of Korea, 7–15 August 2012.

Domeier, M. (2006). An analysis of Pacific striped marlin (Tetrapturus audax) horizontal movement patterns using pop-up satellite archival tags. *Bulletin of Marine Science*, 79(3):811–825.

Ducharme-Barth, N., Pilling, G., and Hampton, J. (2019a). Stock assessment of SW Pacific striped marlin in the WCPO. Technical Report WCPFC-SC15-2019/SA-WP-07, Pohnpei, Federated States of Micronesia.

Ducharme-Barth, N., Vincent, M., Pilling, G., and Hampton, J. (2019b). Simulation analysis of pole and line CPUE standardization approaches for skipjack tuna in the WCPO. Technical Report WCPFC-SC15-2019/SA-WP-04, Pohnpei, Federated States of Micronesia 12-20 August 2019.

Fournier, D. and Archibald, C. P. (1982). A general-theory for analyzing catch at age data. *Canadian Journal of Fisheries and Aquatic Sciences*, 39(8):1195–1207.

Hartigan, J. and Wong, M. (1979). A K-means clustering algorithm. *Applied Statistics*, 28:9.

Hoyle, S., Davies, N., and Pilling, G. (2012). CPUE standardisation for striped marlin in the western and central Pacific Ocean. Technical Report WCPFC-SC8-2012/SA-IP-09, Busan, Republic of Korea, 7-15 August 2012.

Hoyle, S., Shono, H., Okamoto, H., and Langley, A. (2010). Analyses of Japanese longline operational catch and effort for bigeye tuna in the WCPO. Technical Report WCPFC-SC6-2010/SA-WP-02.

Kinoshita, J., Aoki, Y., Ducharme-Barth, N., and Kiyofuji, H. (2019). Standardized catch per unit effort (CPUE) of skipjack tuna of the Japanese pole-and-line fisheries in the WCPO from 1972 to 2018. Technical Report WCPFC-SC15-2019/SA-WP-14, Pohnpei, Federated States of Micronesia.

Kolody, D. and Davies, N. (2008). Spatial structure in South Pacific swordfish stocks and assessment models. Technical Report WCPFC-SC4-2008/SA-IP-2, Port Moresby, Papua New Guinea, 11–22 August 2008.

Kopf, R., Davie, P., Bromhead, D., and Young, J. (2012). Reproductive biology and spatiotemporal patterns of spawning in striped marlin Kajikia audax. *Journal of Fish Biology*, (81):1834–1858.

Kopf, R. K., Davie, P. S., Bromhead, D., and Pepperell, J. G. (2011). Age and growth of striped marlin (Kajikia audax) in the Southwest Pacific Ocean. *ICES Journal of Marine Science*, 68(9):1884–1895.

Langley, A., Molony, B., Bromhead, D., Yokawa, K., and Wise, B. (2006). Stock assessment of striped marlin (Tetrapturus audax) in the southwest Pacific ocean. Technical Report WCPFC-SC2-2006/SA-WP-6, Manila, Philippines, 7–18 August 2006.

Lo, N. C., Jacobson, L. D., and Squire, J. L. (1992). Indices of Relative Abundance from Fish Spotter Data based on Delta-Lognormal Models. *Canadian Journal of Fisheries and Aquatic Sciences*, 49:2515–2526.

Maunder, M. N. and Punt, A. E. (2004). Standardizing catch and effort data: a review of recent approaches. *Fisheries Research*, 70(2-3):141–159.

McKechnie, S., Hampton, J., Pilling, G. M., and Davies, N. (2016). Stock assessment of skipjack tuna in the western and central Pacific Ocean. Technical Report WCPFC-SC12-2016/SA-WP-04, Bali, Indonesia, 3–11 August 2016.

McKechnie, S., Pilling, G., and Hampton, J. (2017). Stock assessment of bigeye tuna in the western and central Pacific Ocean. Technical Report WCPFC-SC13-2017/SA-WP-05, Rarotonga, Cook Islands, 9–17 August 2017.

McKechnie, S., Tremblay-Boyer, L., and Harley, S. J. (2015). Analysis of Pacific-wide operational longline CPUE data for bigeye tuna. Technical Report WCPFC-SC11-2015/SA-WP-03, Pohnpei, Federated States of Micronesia, 5–13 August 2015.

Ortiz, M., Prince, E. D., Serafy, J. E., Holts, D. B., Davy, K. B., Pepperell, J. G., Lowry, M. B., and Holdsworth, J. C. (2003). Global overview of the major constituent-based billfish tagging programs and their results since 1954. *Marine and Freshwater Research*, 54(4):489.

Pilling, G. and Brouwer, S. (2019). Report from the SPC Pre-assessment Workshop, Noumea, April 2019. Technical Report WCPFC-SC15-2019/SA-IP-01, Pohnpei, Federated States of Micronesia.

R Core Team (2018). *R: A Language and Environment for Statistical Computing*. R Foundation for Statistical Computing, Vienna, Austria.

Sippel, T., Holdsworth, J., Dennis, T., and Montgomery, J. (2011). Investigating Behaviour and Population Dynamics of Striped Marlin (Kajikia audax) from the Southwest Pacific Ocean with Satellite Tags. *PLoS ONE*, 6(6):e21087.

Smith, T. and Reynolds, R. (1981). NOAA Smith and Reynolds Extended Reconstructed Sea Surface Temperature (ERSST) Level 4 Monthly Version 5 Dataset in netCDF.

Stefansson, G. (1996). Analysis of groundfish survey abundance data: Combining the GLM and delta approaches. *Ices Journal of Marine Science*, 53(3):577–588.

Takeuchi, Y., Davies, N., Fournier, D., Pilling, G., and Hampton, J. (2018). Testing MULTIFAN-CL developments for multispecies/multi-sex assessments, using SW Pacific swordfish. Technical Report WCPFC-SC14-2018/SA-IP-10, Busan, South Korea, 8-16 August 2018.

Takeuchi, Y., Graham, P., and Hampton, J. (2017). Stock assessment of swordfish (Xiphias gladius) in the southwest Pacific Ocean. Technical Report WCPFC-SC13-2017/SA-WP-13, Rarotonga, Cook Islands, 9-17 August 2017.

Thorson, J. T. (2019). Guidance for decisions using the Vector Autoregressive Spatio-Temporal (VAST) package in stock, ecosystem, habitat and climate assessments. *Fisheries Research*, 210:143–161.

Thorson, J. T., Shelton, A. O., Ward, E. J., and Skaug, H. J. (2015). Geostatistical delta-generalized linear mixed models improve precision for estimated abundance indices for West Coast groundfishes. *Ices Journal of Marine Science*, 72(5):1297–1310.

Tremblay-Boyer, L., Hampton, J., McKechnie, S., and Pilling, G. (2018a). Stock assessment of South Pacific albacore tuna. Technical Report WCPFC-SC-14-2018/SA-WP-05, Busan, South Korea, 8-16 August 2018.

Tremblay-Boyer, L., McKechnie, S., and Harley, S. J. (2015). Standardized CPUE for south Pacific albacore tuna (\emphThunnus alalunga) from operational longline data. Technical Report WCPFC-SC11-2015/SA-IP-03, Pohnpei, Federated States of Micronesia, 5–13 August 2015.

Tremblay-Boyer, L., McKechnie, S., and Pilling, G. (2018b). Background Analysis for the 2018 stock assessment of South Pacific albacore tuna. Technical Report WCPFC-SC14-2018/ SA-IP-07, Busan, South Korea, 8-16 August 2018.

Tremblay-Boyer, L., McKechnie, S., Pilling, G., and Hampton, J. (2017). Stock assessment of yellowfin tuna in the Western and Central Pacific Ocean. Technical Report WCPFC-SC13-2017/SA-WP-06, Rarotonga, Cook Islands, 9-17 August 2017.

Vincent, M., Pilling, G., and Hampton, J. (2019). Stock assessment of skipjack tuna in the WCPO. Technical Report WCPFC-SC15-2019/SA-WP-05, Pohnpei, Federated States of Micronesia.

Whitelaw, W. (2001). Country Guide to Gamefishing in the Western and Central Pacific. Technical report, SPC-OFP, Noumea.

Williams, P. and Smith, N. (2018). Requirements for enhancing conversion factor information. Technical Report WCPFC-SC14-2018/ST-WP-05, Busan, South Korea, 8-16 August 2018.

8 Tables

Table 1: Definition of fisheries for the 2019 MULTIFAN-CL SW Pacific striped marlin stock assessment.

Fishery	Nationality	Gear	Sub.region
1: JP 1 LL	JP	Longline	1
2: JP 2 LL	JP	Longline	2
3: JP 3 LL	JP	Longline	3
4: JP 4 LL	JP	Longline	4
5: TW 4 LL	TW	Longline	4
6: AU 2 LL	AU	Longline	2
7: AU 3 LL	AU	Longline	3
8: NZ 3 LL	NZ	Longline	3
9: AU 3 REC	AU	Recreational	3
10: NZ 3 REC	NZ	Recreational	3
11: OTHER 1 LL	DWFN/PICT	Longline	1
12: OTHER 2 LL	DWFN/PICT	Longline	2
13: OTHER 3 LL	DWFN/PICT	Longline	3
14: OTHER 4 LL	DWFN/PICT	Longline	4

9 Figures

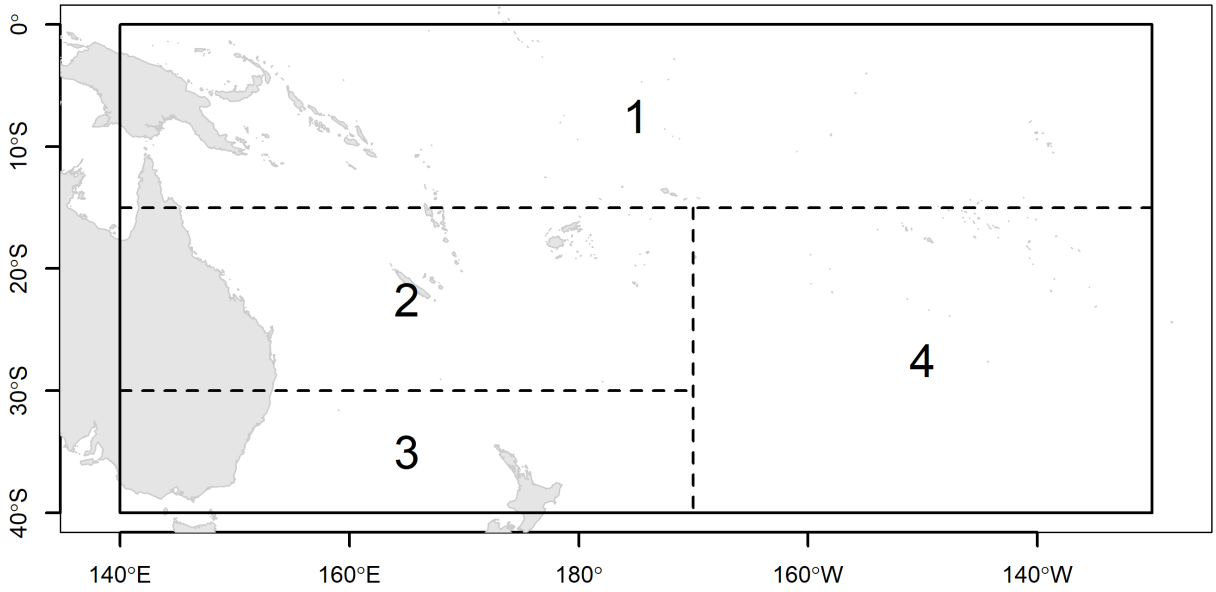

Figure 1: The 2019 striped marlin stock assessment model region with sub-regions used to define the fishery definitions.

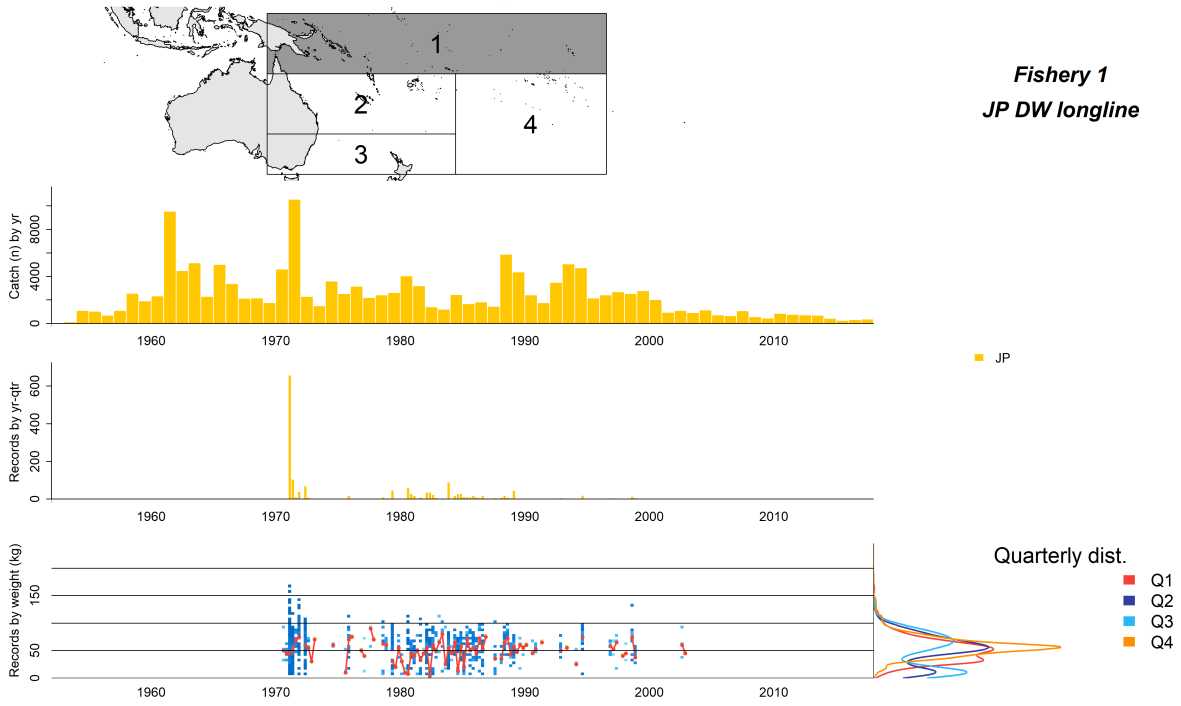

Figure 2: Summary plot showing the characteristics of the fisheries defined for the 2019 striped marlin stock assessment. The top panel indicates the sub-region the fishery was defined in. The middle two panels indicate the annual catch by country and the quarterly size composition records by country for the fishery (middle-top and middle-bottom, respectively). The lower panel shows the size composition data for the fishery by whole weight (kg) bin at a quarterly time scale with the median in each time period shown in red. To the right of this are the cumulative size composition distributions by quarter.

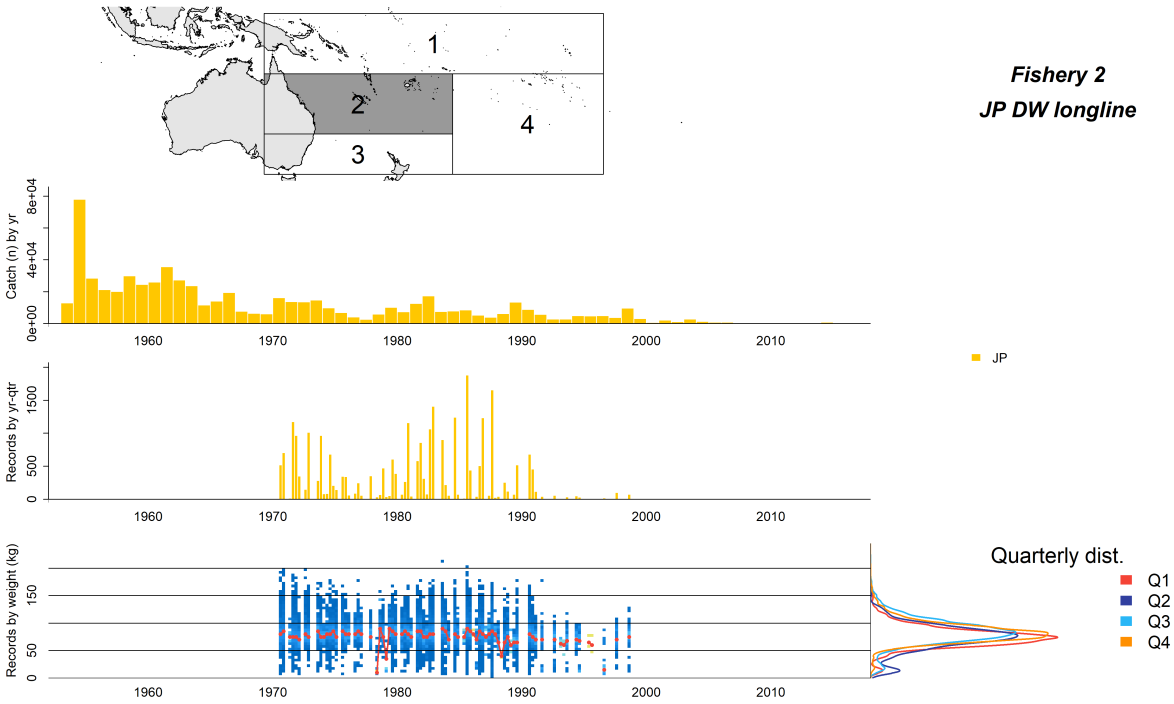

Figure 3: Summary plot showing the characteristics of the fisheries defined for the 2019 striped marlin stock assessment. The top panel indicates the sub-region the fishery was defined in. The middle two panels indicate the annual catch by country and the quarterly size composition records by country for the fishery (middle-top and middle-bottom, respectively). The lower panel shows the size composition data for the fishery by whole weight (kg) bin at a quarterly time scale with the median in each time period shown in red. To the right of this are the cumulative size composition distributions by quarter.

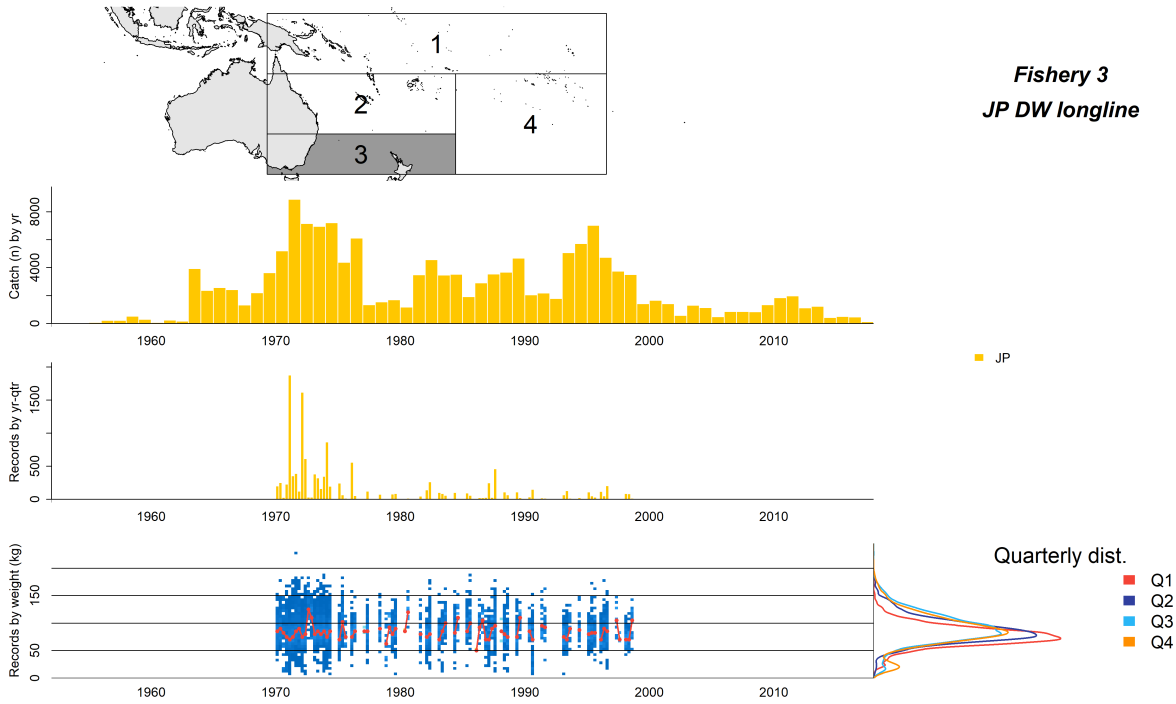

Figure 4: Summary plot showing the characteristics of the fisheries defined for the 2019 striped marlin stock assessment. The top panel indicates the sub-region the fishery was defined in. The middle two panels indicate the annual catch by country and the quarterly size composition records by country for the fishery (middle-top and middle-bottom, respectively). The lower panel shows the size composition data for the fishery by whole weight (kg) bin at a quarterly time scale with the median in each time period shown in red. To the right of this are the cumulative size composition distributions by quarter.

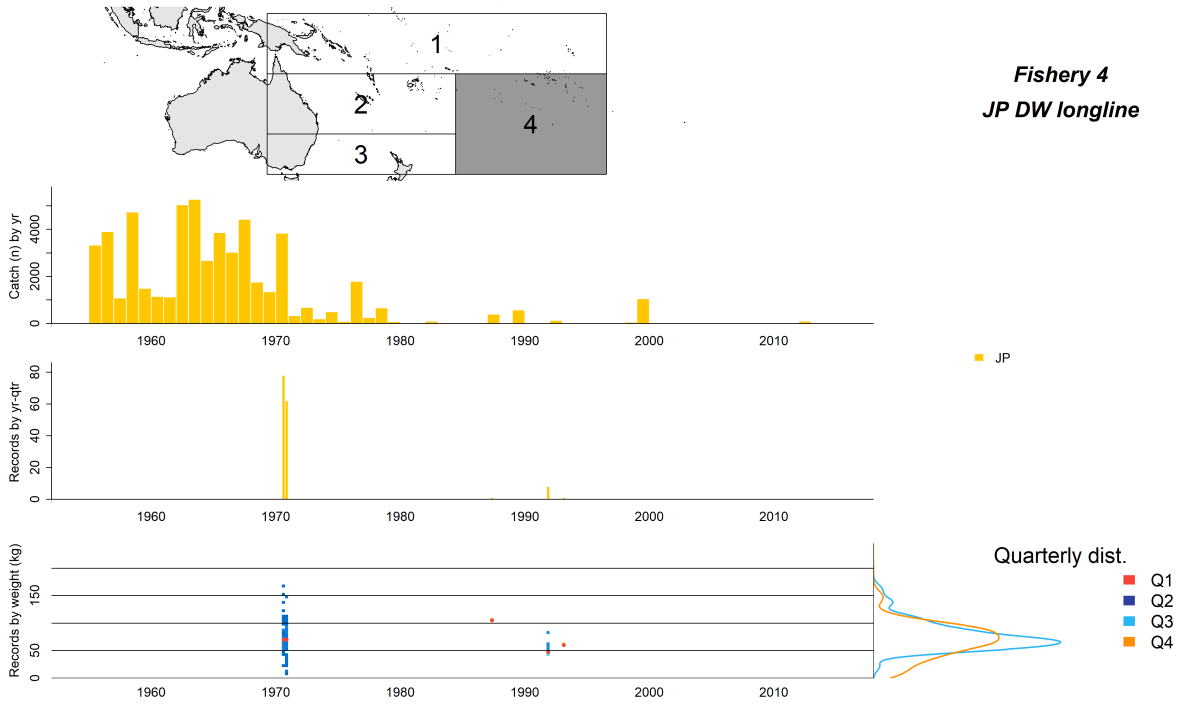

Figure 5: Summary plot showing the characteristics of the fisheries defined for the 2019 striped marlin stock assessment. The top panel indicates the sub-region the fishery was defined in. The middle two panels indicate the annual catch by country and the quarterly size composition records by country for the fishery (middle-top and middle-bottom, respectively). The lower panel shows the size composition data for the fishery by whole weight (kg) bin at a quarterly time scale with the median in each time period shown in red. To the right of this are the cumulative size composition distributions by quarter.

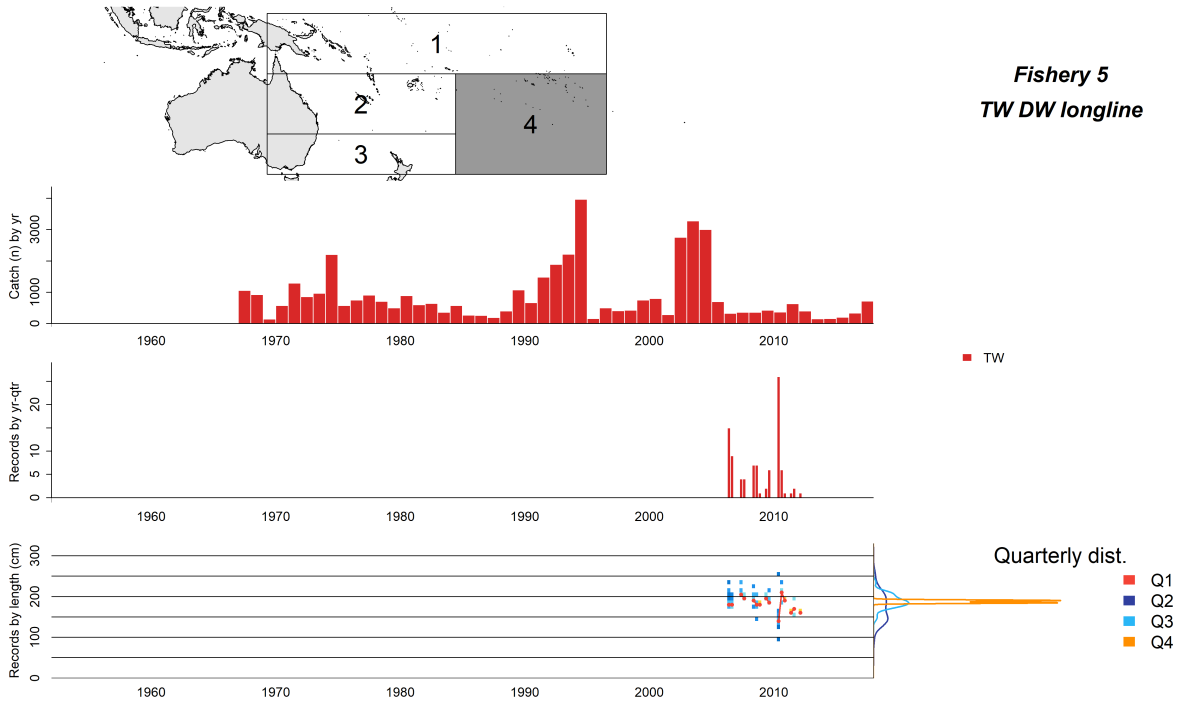

Figure 6: Summary plot showing the characteristics of the fisheries defined for the 2019 striped marlin stock assessment. The top panel indicates the sub-region the fishery was defined in. The middle two panels indicate the annual catch by country and the quarterly size composition records by country for the fishery (middle-top and middle-bottom, respectively). The lower panel shows the size composition data for the fishery by eye-fork length (cm) bin at a quarterly time scale with the median in each time period shown in red. To the right of this are the cumulative size composition distributions by quarter.

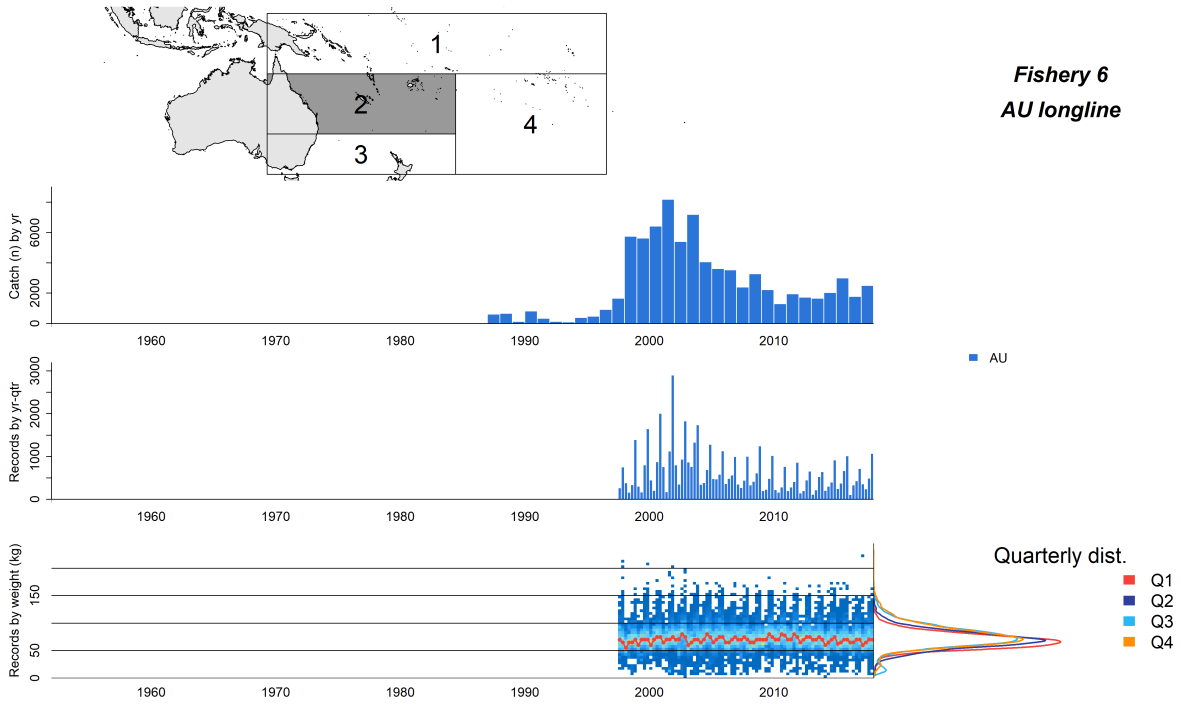

Figure 7: Summary plot showing the characteristics of the fisheries defined for the 2019 striped marlin stock assessment. The top panel indicates the sub-region the fishery was defined in. The middle two panels indicate the annual catch by country and the quarterly size composition records by country for the fishery (middle-top and middle-bottom, respectively). The lower panel shows the size composition data for the fishery by whole weight (kg) bin at a quarterly time scale with the median in each time period shown in red. To the right of this are the cumulative size composition distributions by quarter.

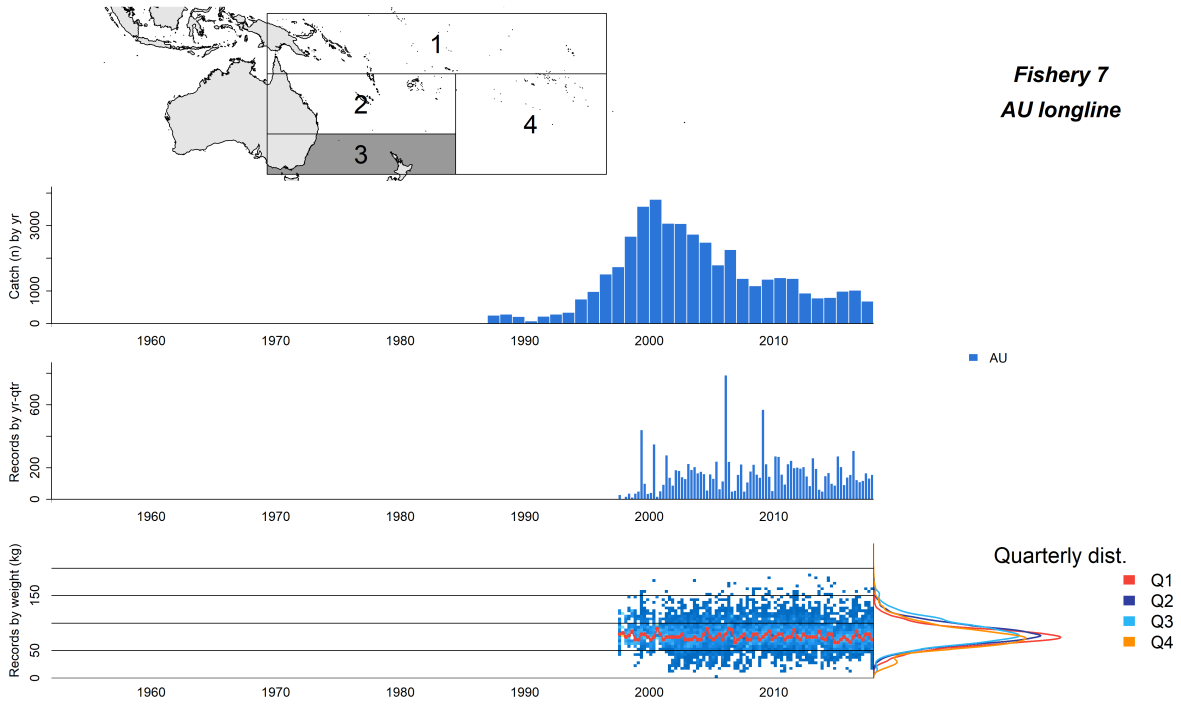

Figure 8: Summary plot showing the characteristics of the fisheries defined for the 2019 striped marlin stock assessment. The top panel indicates the sub-region the fishery was defined in. The middle two panels indicate the annual catch by country and the quarterly size composition records by country for the fishery (middle-top and middle-bottom, respectively). The lower panel shows the size composition data for the fishery by whole weight (kg) bin at a quarterly time scale with the median in each time period shown in red. To the right of this are the cumulative size composition distributions by quarter.

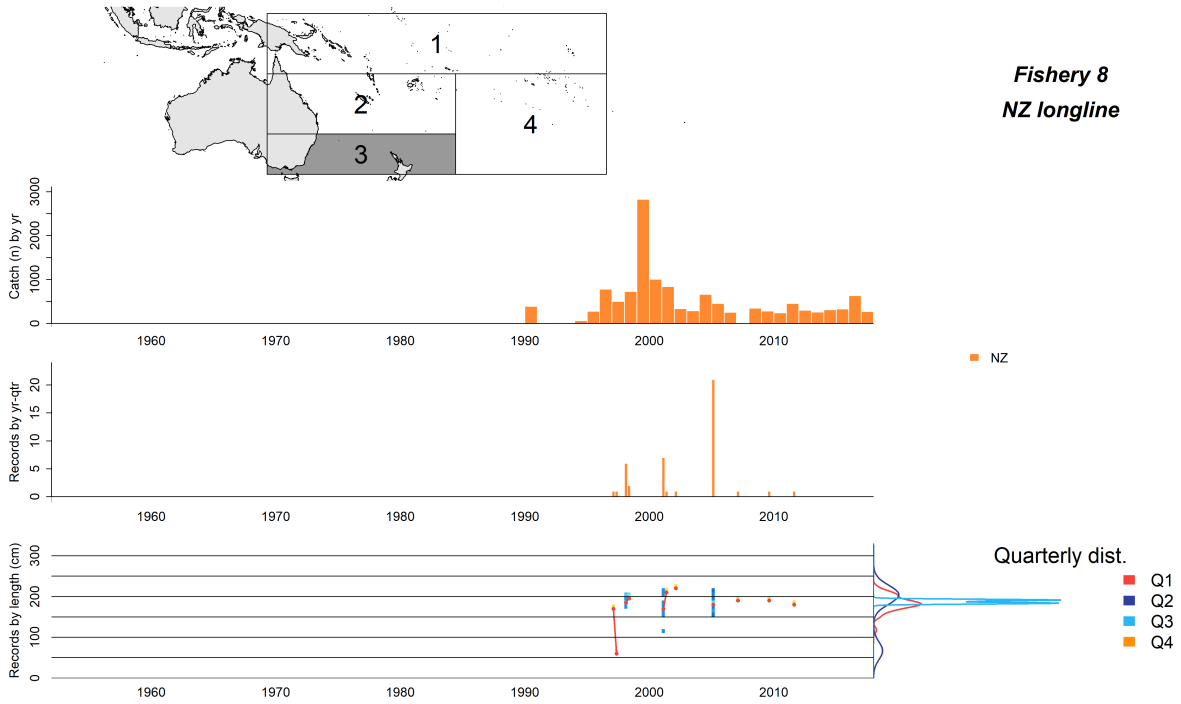

Figure 9: Summary plot showing the characteristics of the fisheries defined for the 2019 striped marlin stock assessment. The top panel indicates the sub-region the fishery was defined in. The middle two panels indicate the annual catch by country and the quarterly size composition records by country for the fishery (middle-top and middle-bottom, respectively). The lower panel shows the size composition data for the fishery by whole weight (kg) bin at a quarterly time scale with the median in each time period shown in red. To the right of this are the cumulative size composition distributions by quarter.

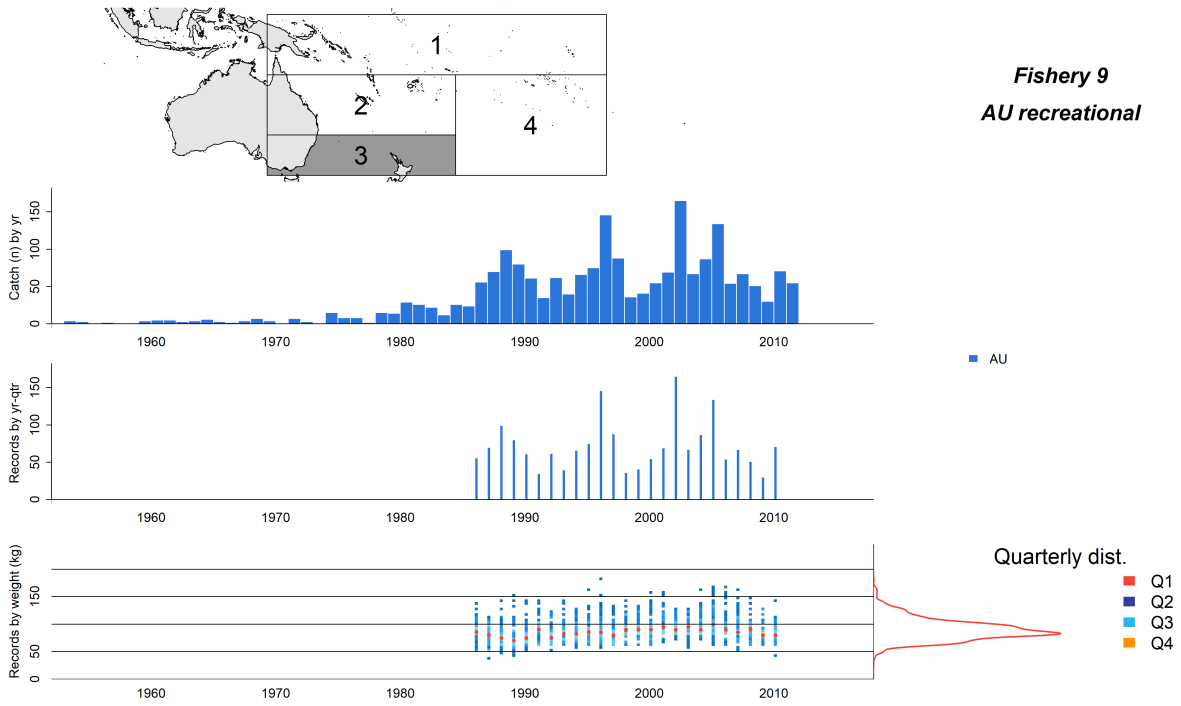

Figure 10: Summary plot showing the characteristics of the fisheries defined for the 2019 striped marlin stock assessment. The top panel indicates the sub-region the fishery was defined in. The middle two panels indicate the annual catch by country and the quarterly size composition records by country for the fishery (middle-top and middle-bottom, respectively). The lower panel shows the size composition data for the fishery by whole weight (kg) bin at a quarterly time scale with the median in each time period shown in red. To the right of this is the cumulative size composition distributions by quarter. Note that in the model the recreational fisheries are assumed to occur only in the first quarter of each year.

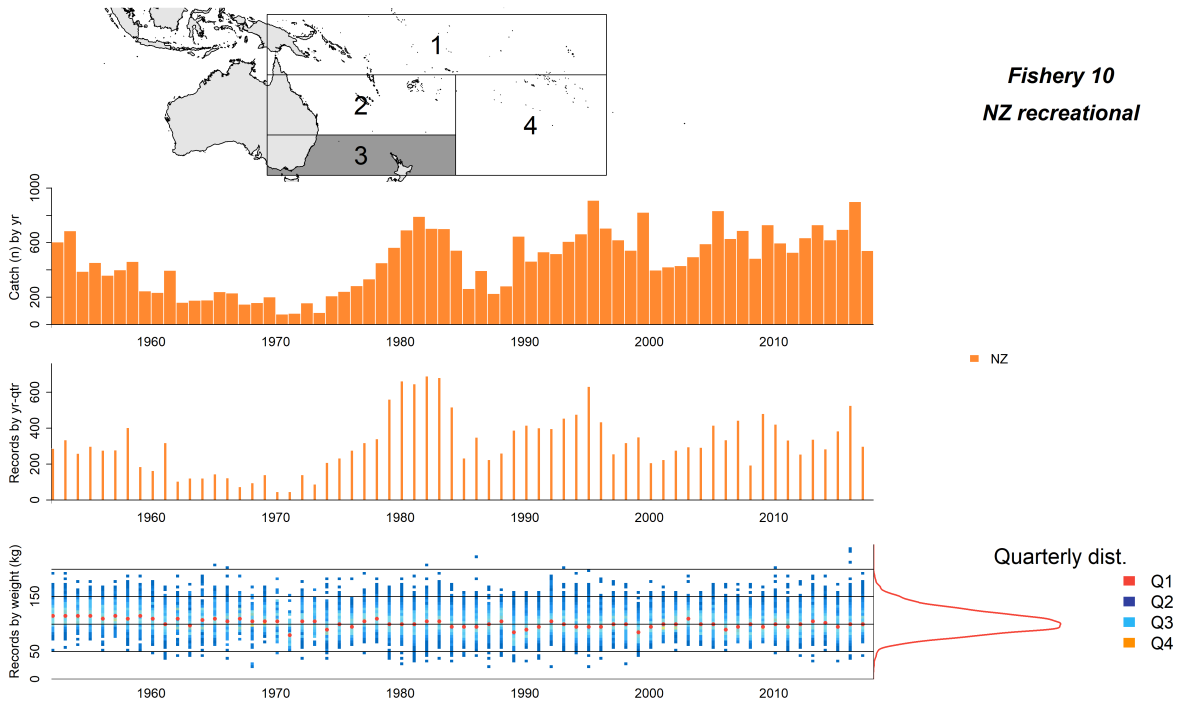

Figure 11: Summary plot showing the characteristics of the fisheries defined for the 2019 striped marlin stock assessment. The top panel indicates the sub-region the fishery was defined in. The middle two panels indicate the annual catch by country and the quarterly size composition records by country for the fishery (middle-top and middle-bottom, respectively). The lower panel shows the size composition data for the fishery by whole weight (kg) bin at a quarterly time scale with the median in each time period shown in red. To the right of this is the cumulative size composition distributions by quarter. Note that in the model the recreational fisheries are assumed to occur only in the first quarter of each year.

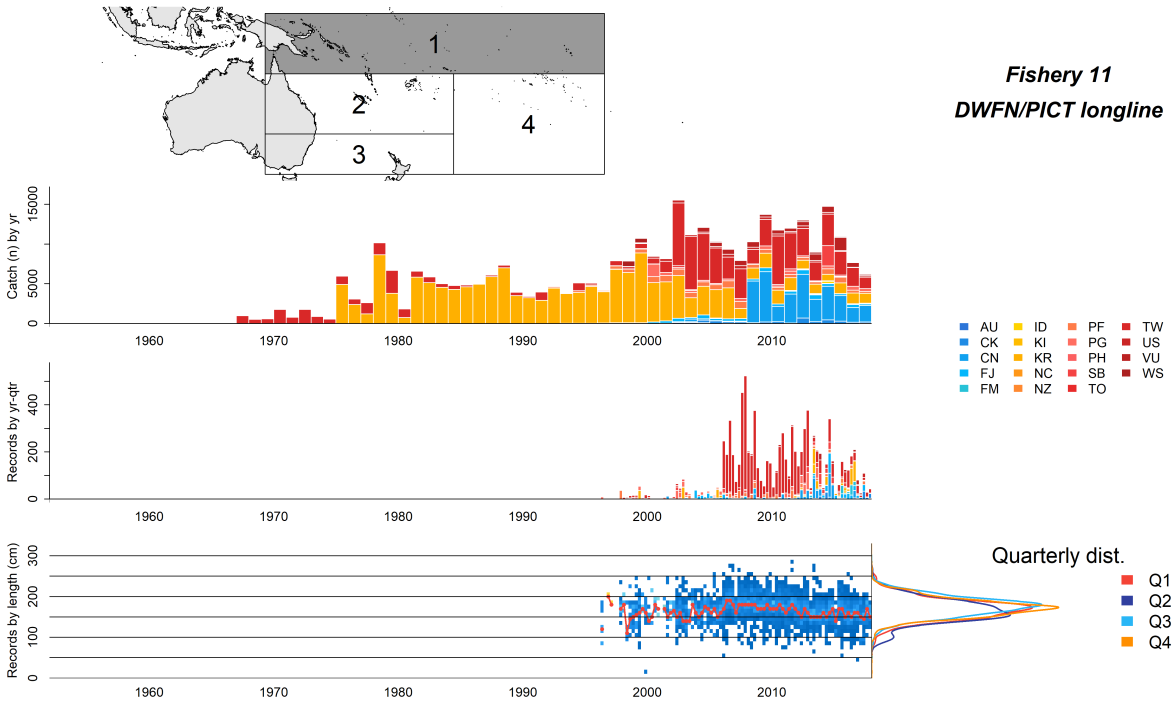

Figure 12: Summary plot showing the characteristics of the fisheries defined for the 2019 striped marlin stock assessment. The top panel indicates the sub-region the fishery was defined in. The middle two panels indicate the annual catch by country and the quarterly size composition records by country for the fishery (middle-top and middle-bottom, respectively). The lower panel shows the size composition data for the fishery by whole weight (kg) bin at a quarterly time scale with the median in each time period shown in red. To the right of this are the cumulative size composition distributions by quarter.

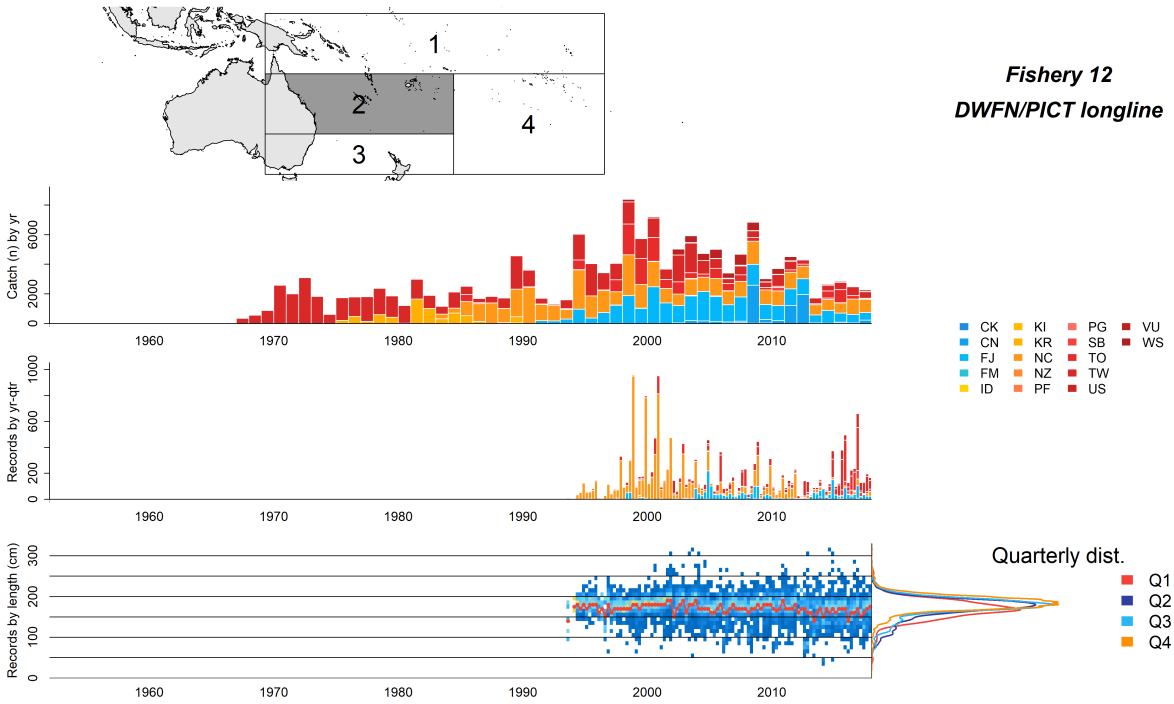

Figure 13: Summary plot showing the characteristics of the fisheries defined for the 2019 striped marlin stock assessment. The top panel indicates the sub-region the fishery was defined in. The middle two panels indicate the annual catch by country and the quarterly size composition records by country for the fishery (middle-top and middle-bottom, respectively). The lower panel shows the size composition data for the fishery by whole weight (kg) bin at a quarterly time scale with the median in each time period shown in red. To the right of this are the cumulative size composition distributions by quarter.

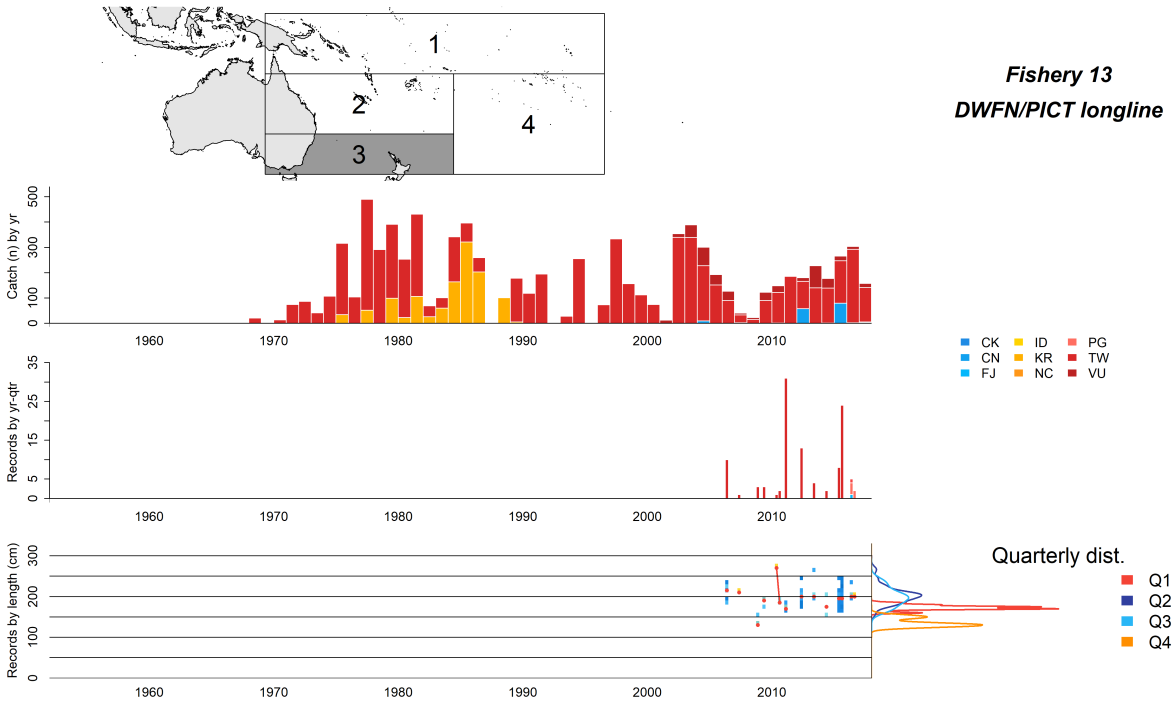

Figure 14: Summary plot showing the characteristics of the fisheries defined for the 2019 striped marlin stock assessment. The top panel indicates the sub-region the fishery was defined in. The middle two panels indicate the annual catch by country and the quarterly size composition records by country for the fishery (middle-top and middle-bottom, respectively). The lower panel shows the size composition data for the fishery by whole weight (kg) bin at a quarterly time scale with the median in each time period shown in red. To the right of this are the cumulative size composition distributions by quarter.

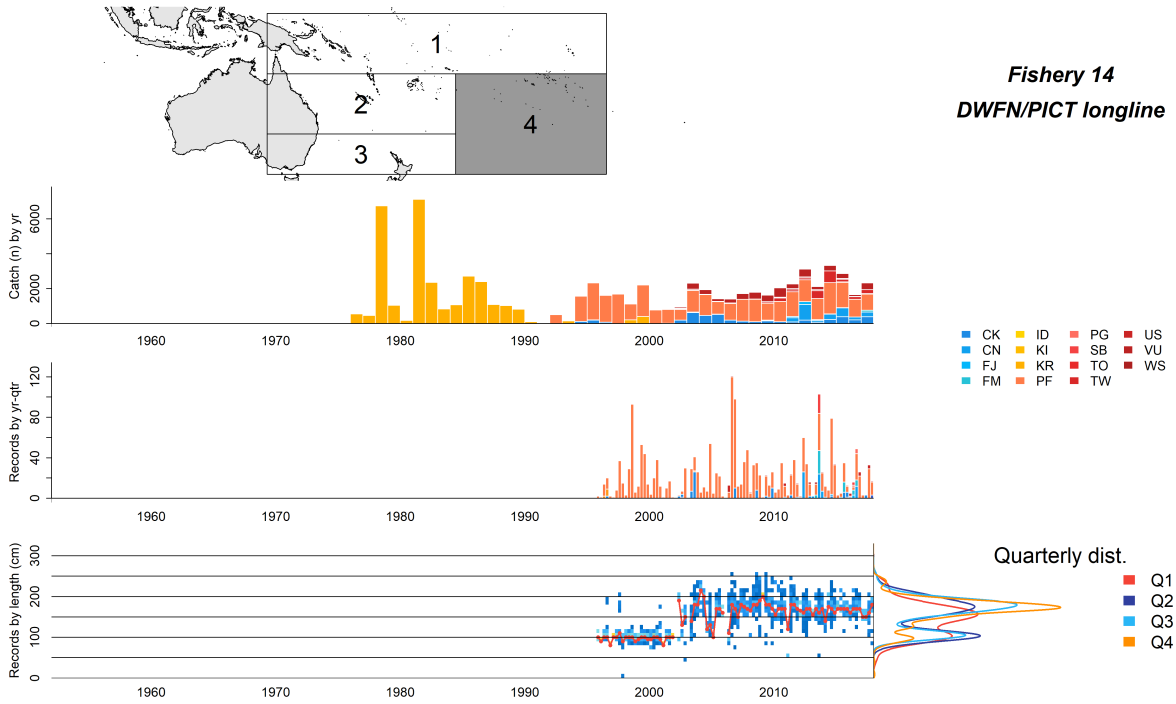

Figure 15: Summary plot showing the characteristics of the fisheries defined for the 2019 striped marlin stock assessment. The top panel indicates the sub-region the fishery was defined in. The middle two panels indicate the annual catch by country and the quarterly size composition records by country for the fishery (middle-top and middle-bottom, respectively). The lower panel shows the size composition data for the fishery by whole weight (kg) bin at a quarterly time scale with the median in each time period shown in red. To the right of this are the cumulative size composition distributions by quarter.

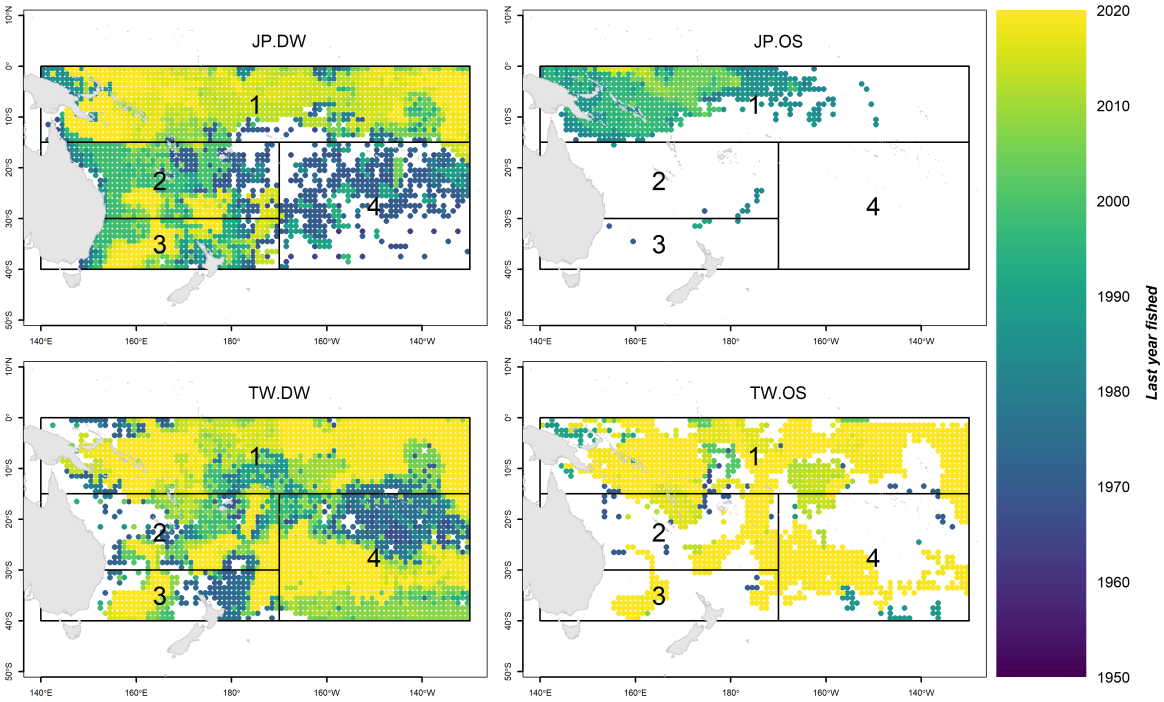

Figure 16: The spatiotemporal distributions of longline fishing effort for the distant-water (DW) and offshore (OS) components of the Japanese (JP) and Chinese Taipei (TW) fleets. Lighter colors indicate the $1^\circ \times 1^\circ$ grid cells have been fished more recently while darker colors indicate that the grid cell was last fished earlier in the model period.

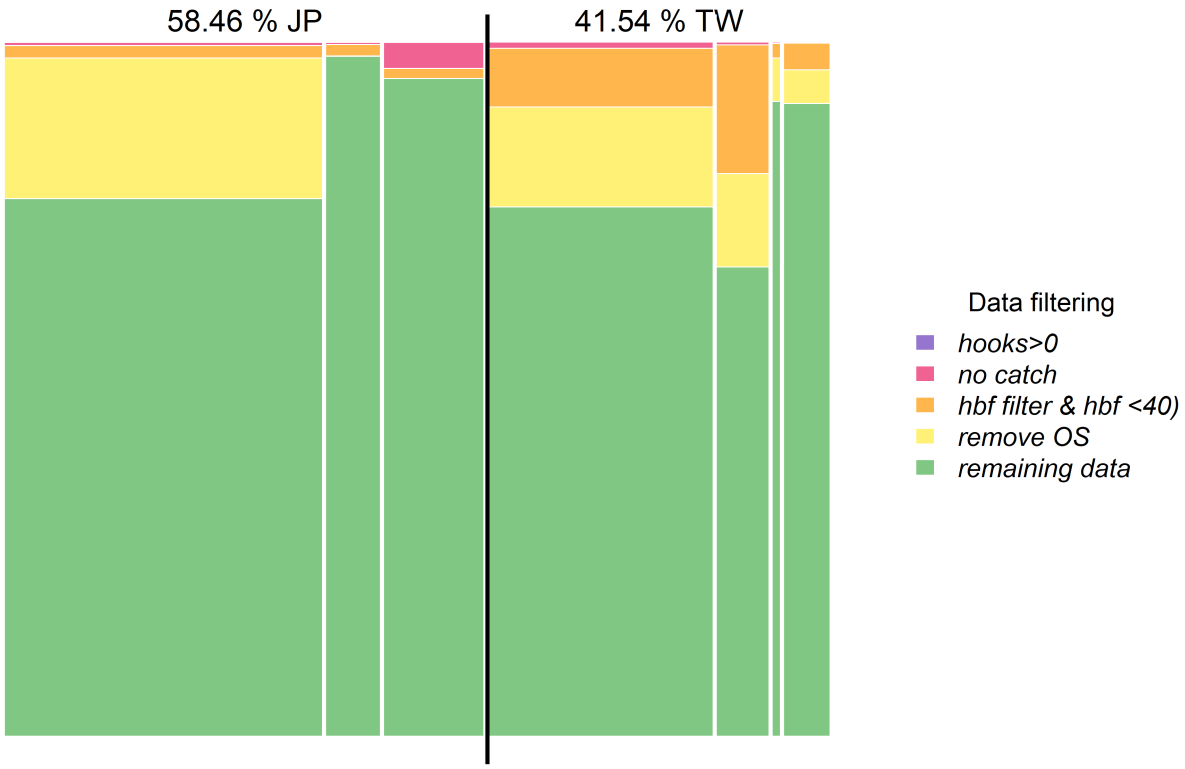

Figure 17: Depiction of the data remaining after each step of the filtering protocol used for preparing the catch rate data for CPUE standardization in each of the 4 sub-regions (denoted by white partitions with sub-region 1 being the furthest left). The percentages indicate how much of the total records used in the analysis came from Japan (JP) or Chinese Taipei (TW) (paritioned by the black line). Note that the proportion of JP data in model sub-region 4 is too small to be visible in the figure.

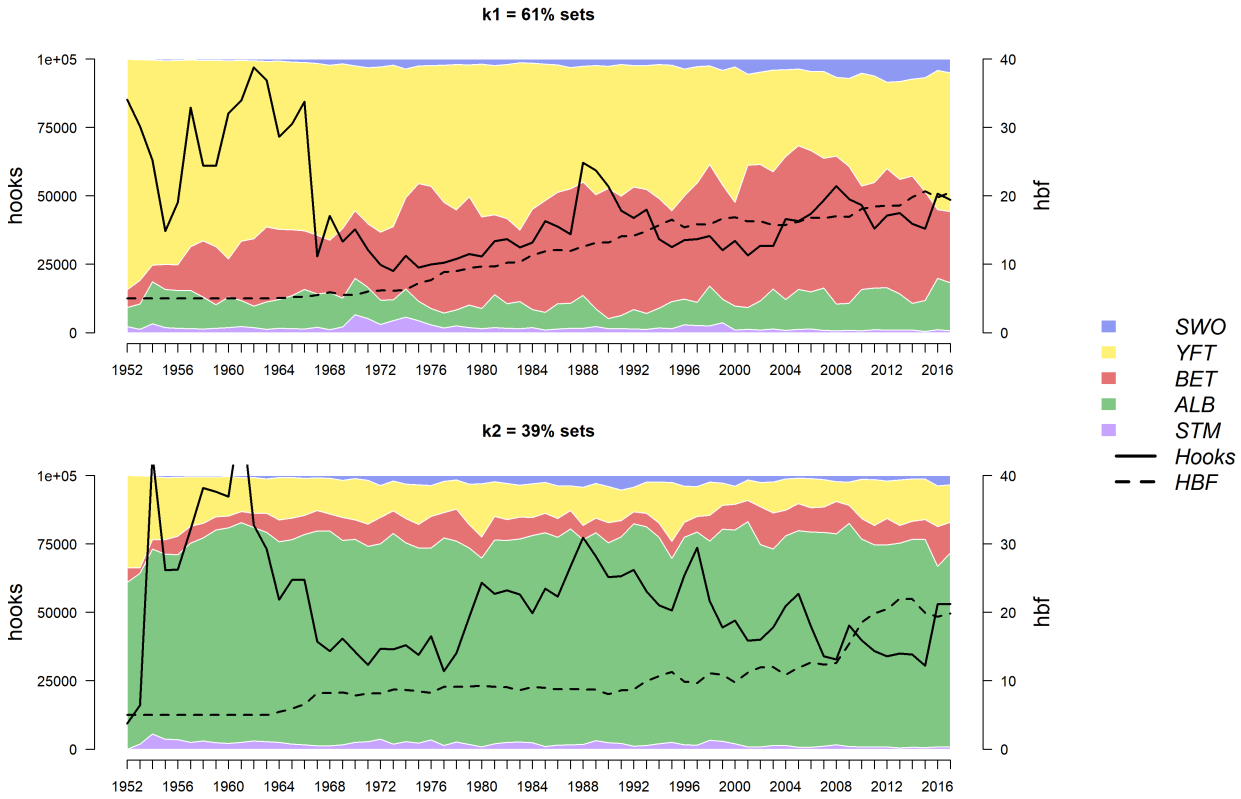

Figure 18: The proportion of total catch of each species for each cluster over time. Additionally, the average number of hooks fished (solid line, left axis) and HBF (dotted line, right axis) over time is shown for each cluster.

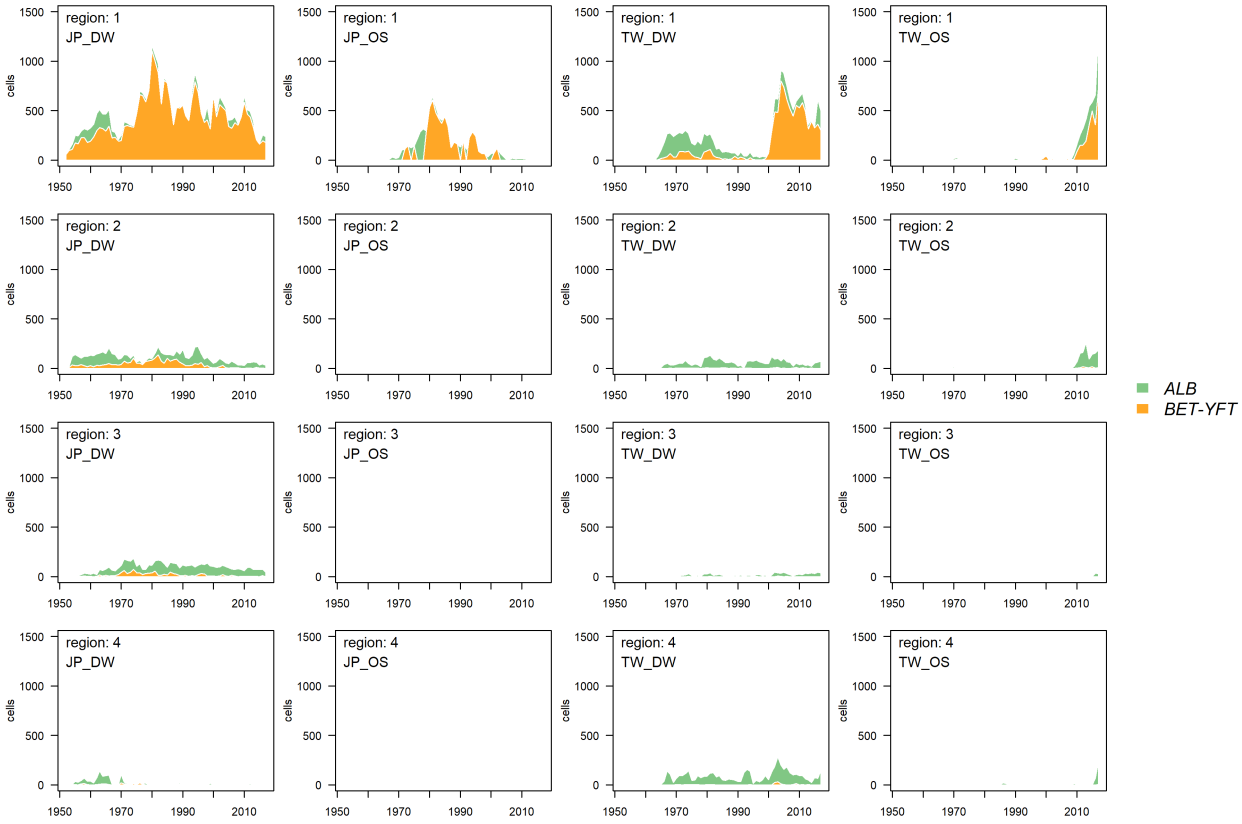

Figure 19: The number of cell-months classified as each cluster across space, time, and fleet group.

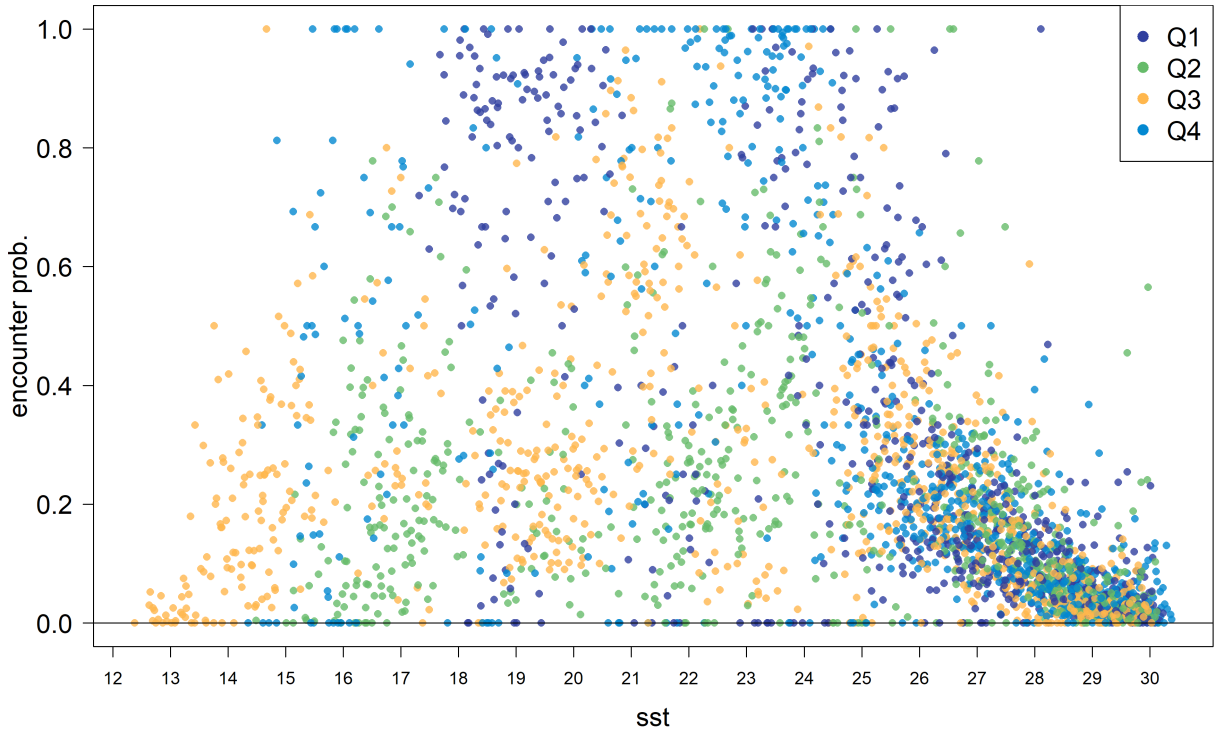

Figure 20: The empirical encounter probability of striped marlin by temperature and quarter based on the spatiotemporal locations of operational logbook sets for the longline fleets operating in the 2019 striped marlin assessment region.

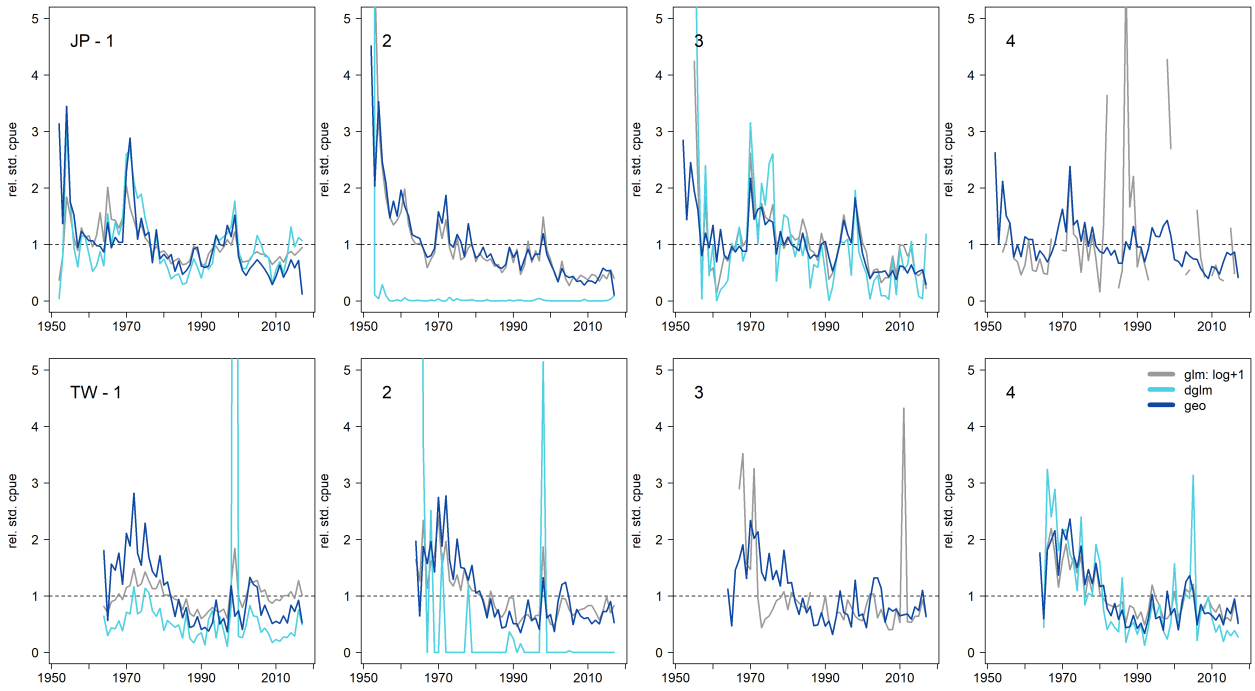

Figure 21: Standardized CPUE indices estimated from JPDW and TWDW data in each of the 4 model sub-regions using the three standardization frameworks: GLM (gray), delta-GLM (light blue), and geostats (dark blue). All indices were rescaled to a mean of 1.

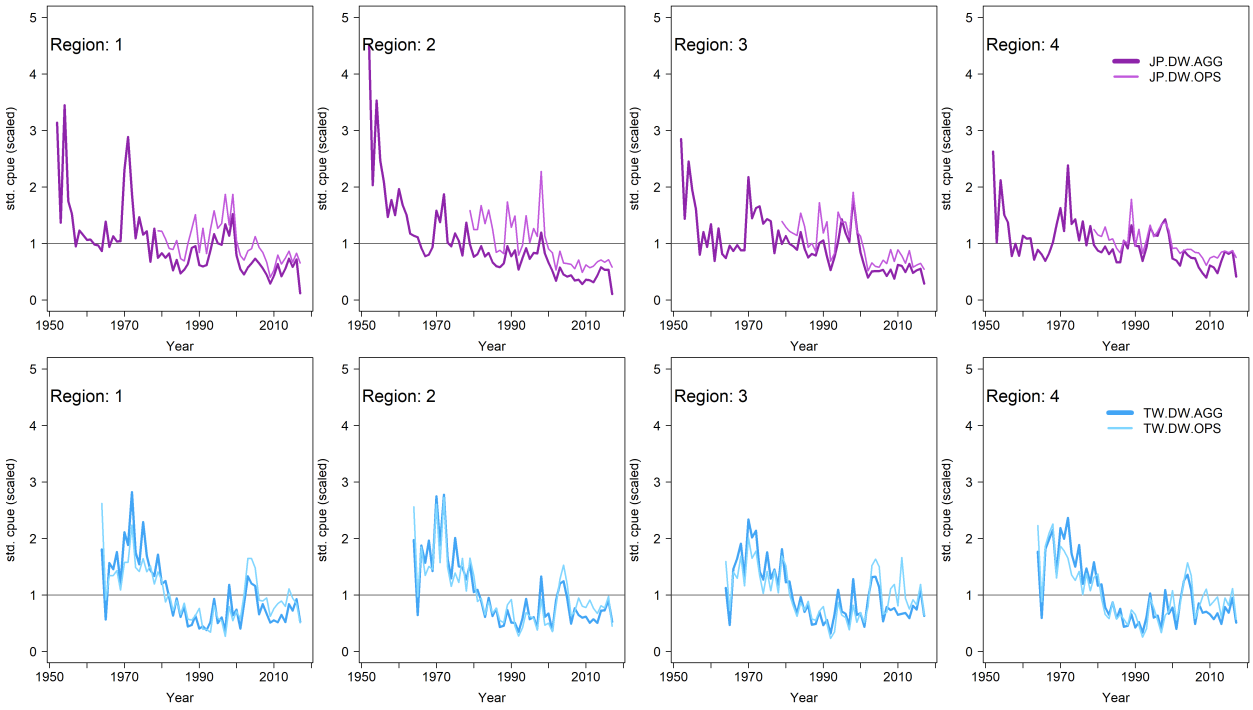

Figure 22: Standardized CPUE indices estimated from JPDW and TWDW data in each of the 4 model sub-regions using either aggregate (thick line) or operational logbook (thin line) data. All indices were rescaled to a mean of 1.

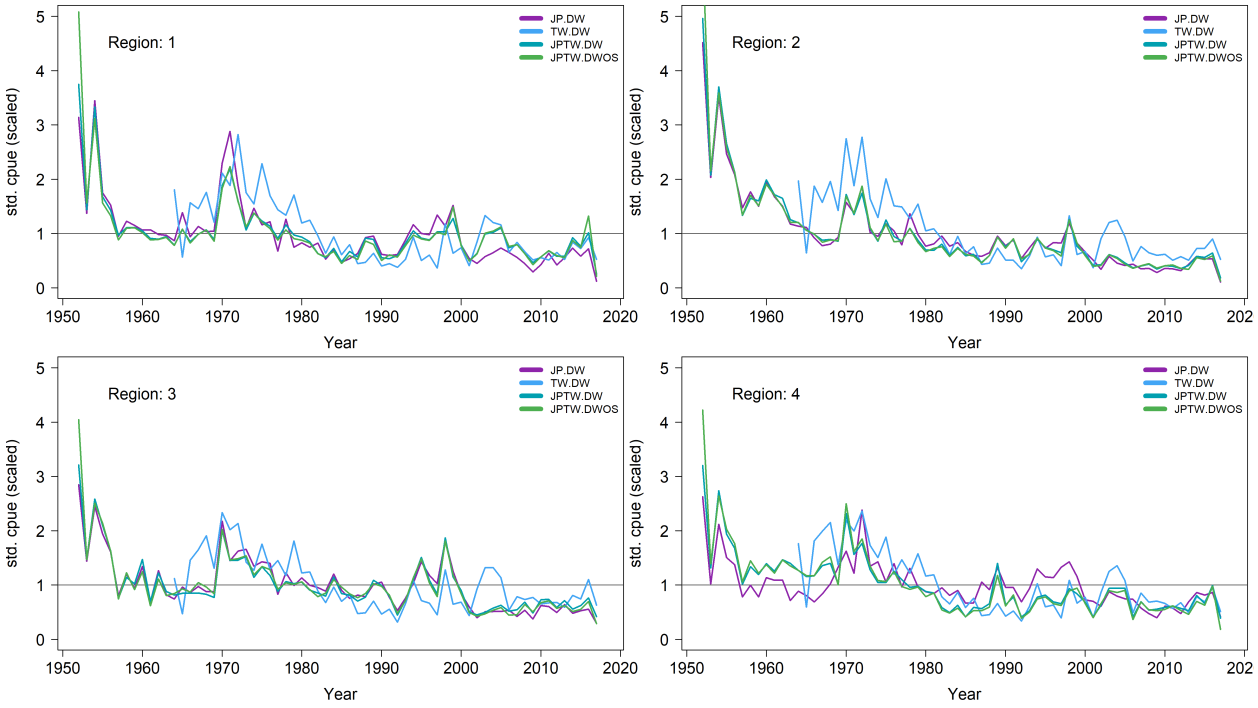

Figure 23: Standardized CPUE indices estimated from aggregated JPDW (purple), TWDW (blue), combined JP-TW DW (teal), and combined JP-TW DW-OS (green) data in each of the 4 model sub-regions. All indices were rescaled to a mean of 1.

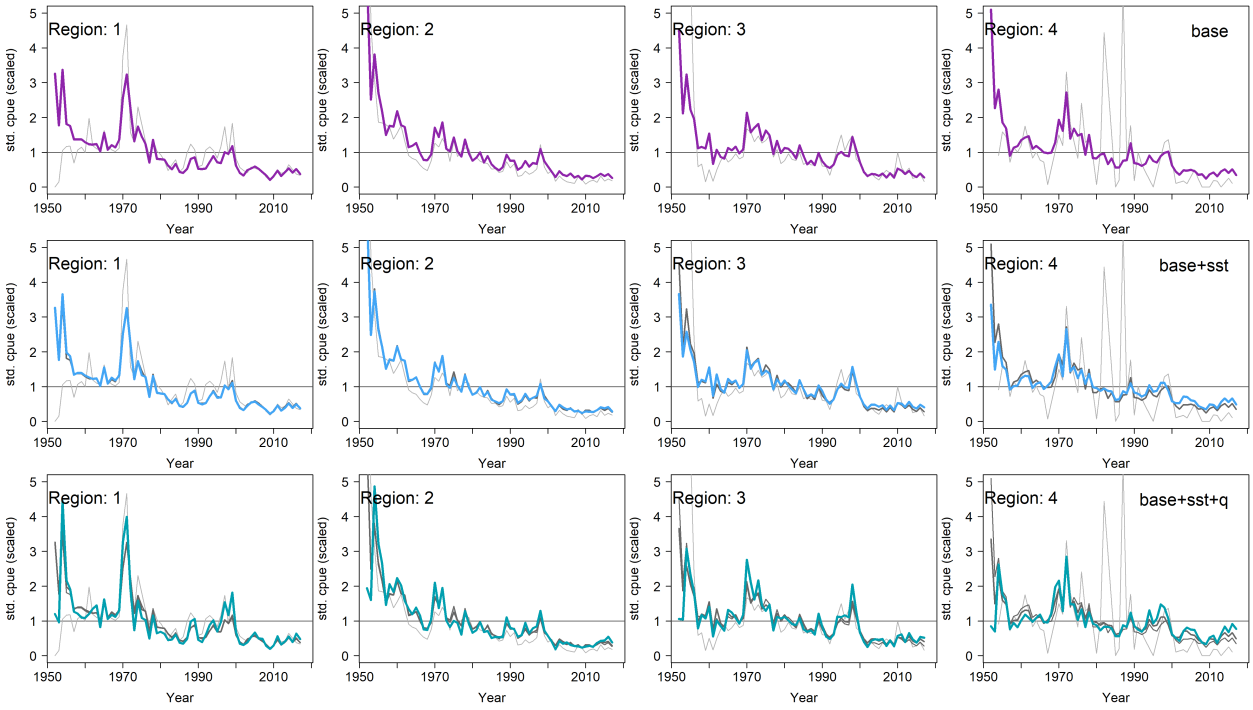

Figure 24: Standardized CPUE indices estimated from aggregated JPDW data showing the impact of the geostatistical model (purple, 1^{st} row), inclusion of SST (blue, 2^{nd}), and catchability covariates (teal, 3^{rd} row) in each of the 4 model sub-regions. All indices were rescaled to a mean of 1. In each row, the thin gray line is the nominal index and the thick gray line is the standardized index from the previous row.

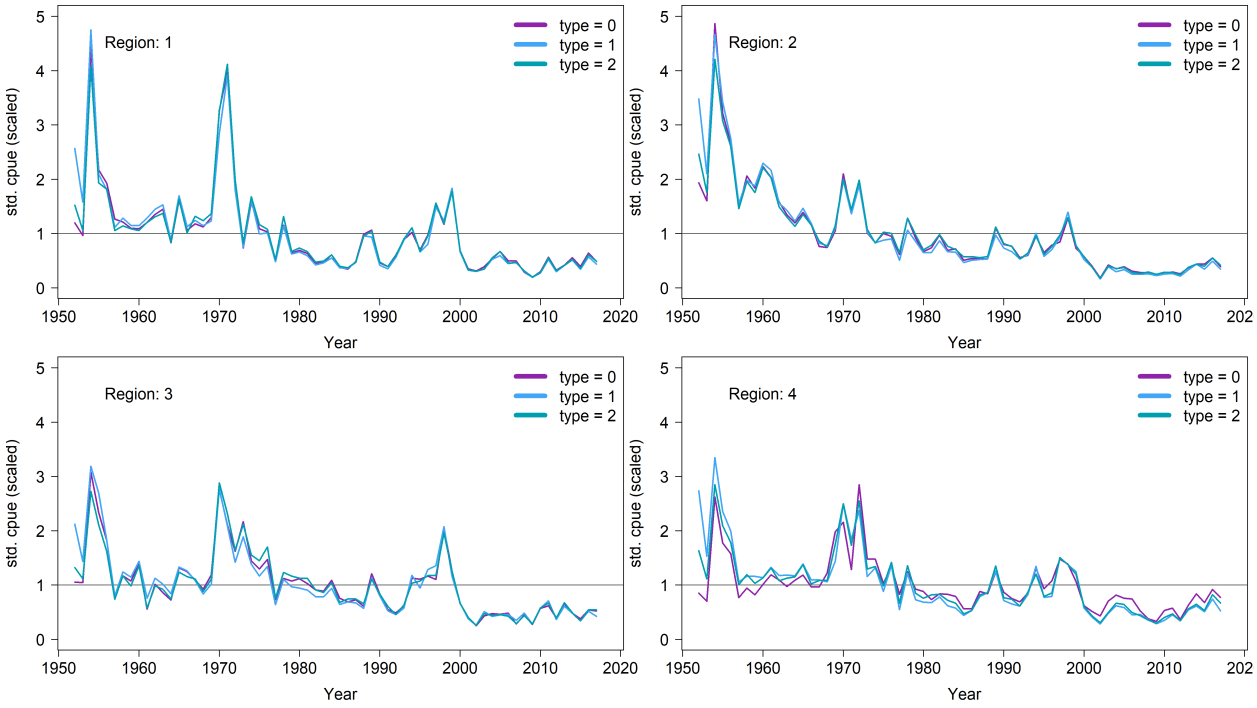

Figure 25: Standardized CPUE indices estimated from aggregated JPDW data with different methods used to define the geostatistical model's spatial knot structure: proportional to the density of the observations (type 0, purple), proportional to the $1^\circ \times 1^\circ$ grid cells within the assessment region (type 1, blue), and proportional to the sampled $1^\circ \times 1^\circ$ grid cells within the assessment region (type 2, teal). All indices were rescaled to a mean of 1.

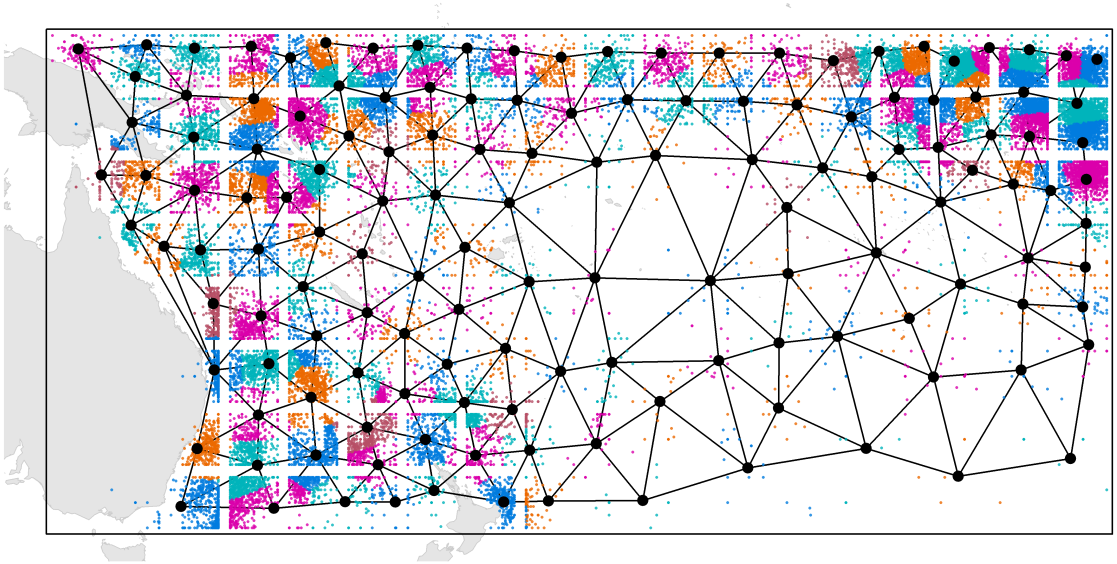

Figure 26: Triangular mesh and spatial knot structure used for the geostats model. Knots (black dots) were allocated using the type 2 method. The colored dots indicate locations of spatial observations within the $5° \times 5°$ grid shown in white.

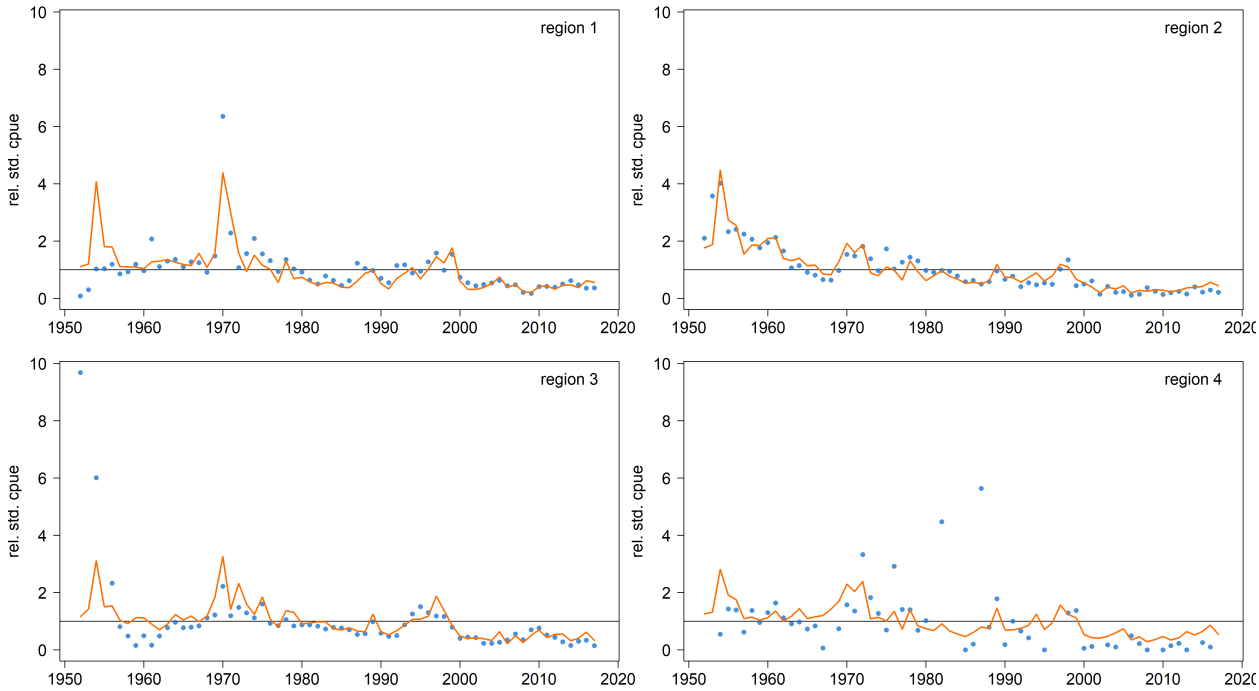

Figure 27: Standardized indices for the JP DW fleet. The standardized index used in the diagnostic case model for Fishery 2 is shown in the panel for region 2. In all panels the standardized CPUE is denoted by the orange line, and blue points denote the nominal CPUE observations. All indices were rescaled to a mean of 1.

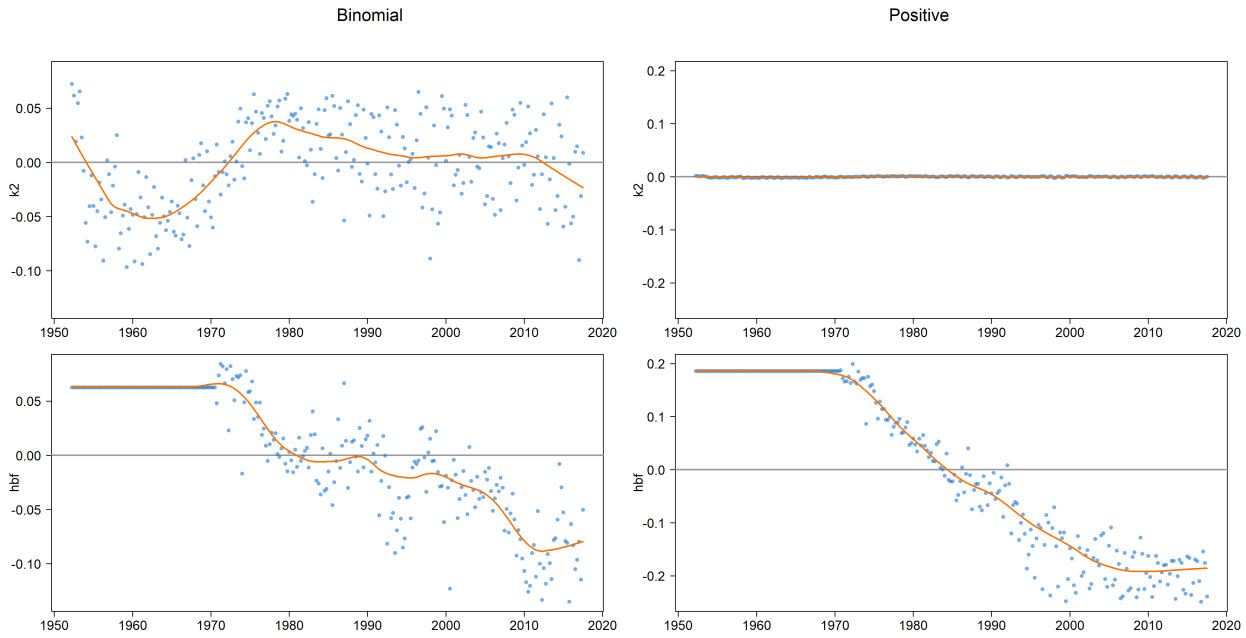

Figure 28: Influence plot showing the relative effect of each covariate over time for both the binomial and positive component of the geostats model. The colored dots represent the covariate effect for each year-quarter and the colored line is the loess trend through the data. The horizontal line indicates the mean effect for that covariate. Additionally the units are the same within each model component (binomial and positive) allowing for comparison of the magnitude of the effect between covariates.

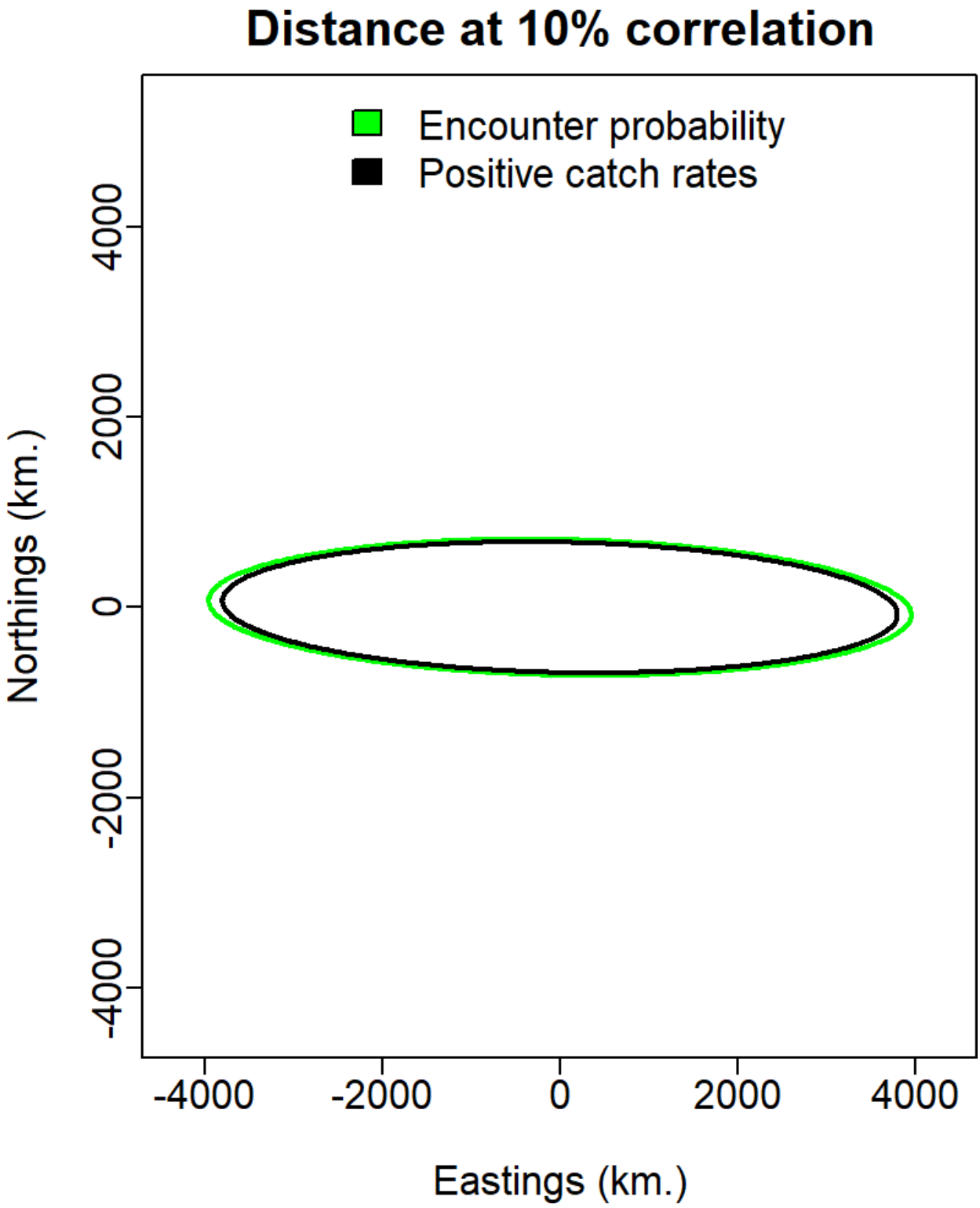

Figure 29: Estimated anisotropic spatial correlation. The 10% correlation distances are shown for the binomial component (encounter probability, green) and the positive component (positive catch rates, black).

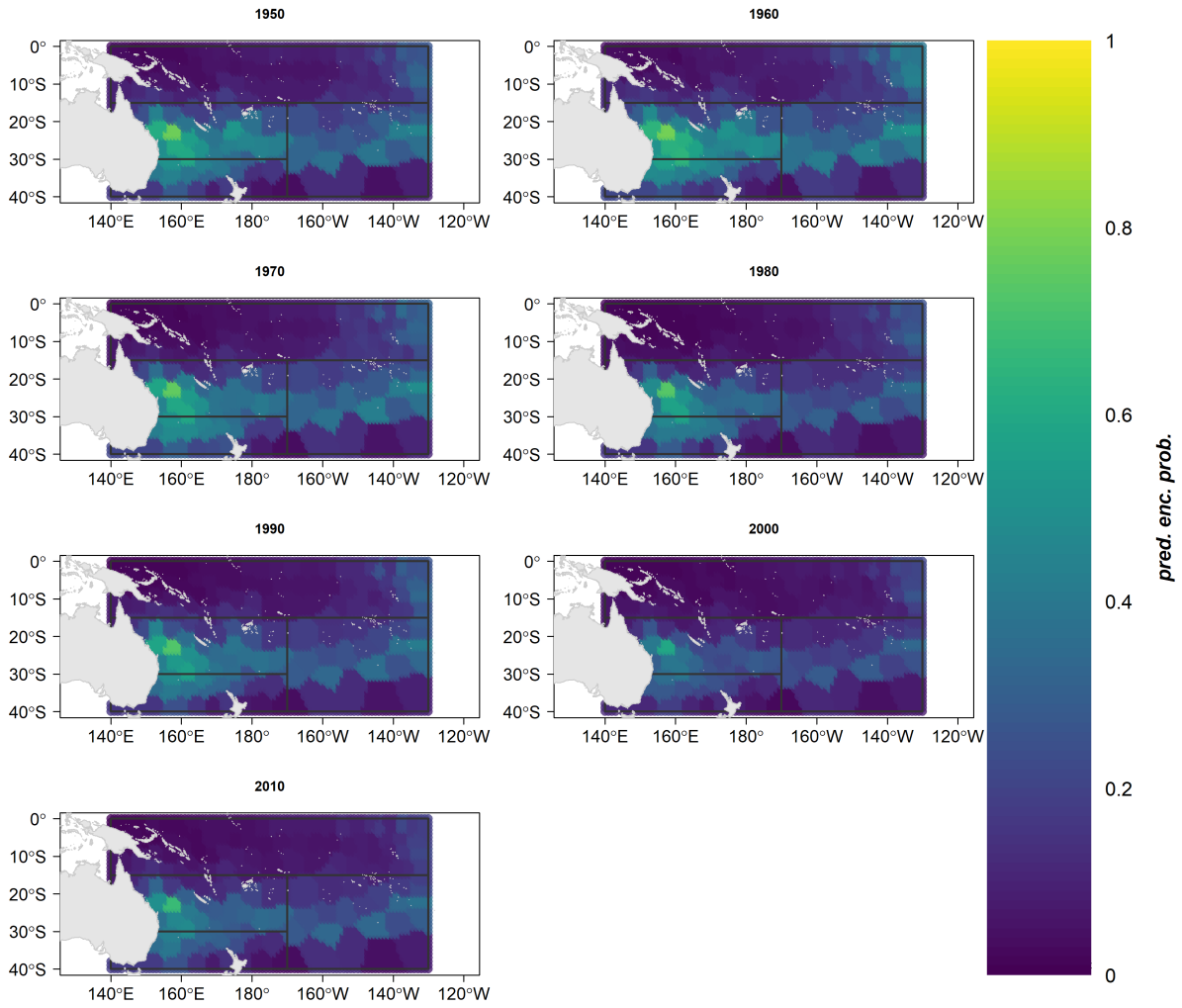

Figure 30: Predicted spatial probability of encounter (binomial component) of striped marlin by decade from the geostats model for each $1^\circ \times 1^\circ$ grid cell in the assessment region. Warmer colors indicate a greater probability of encounter, and cooler colors indicate a lower probability of encounter.

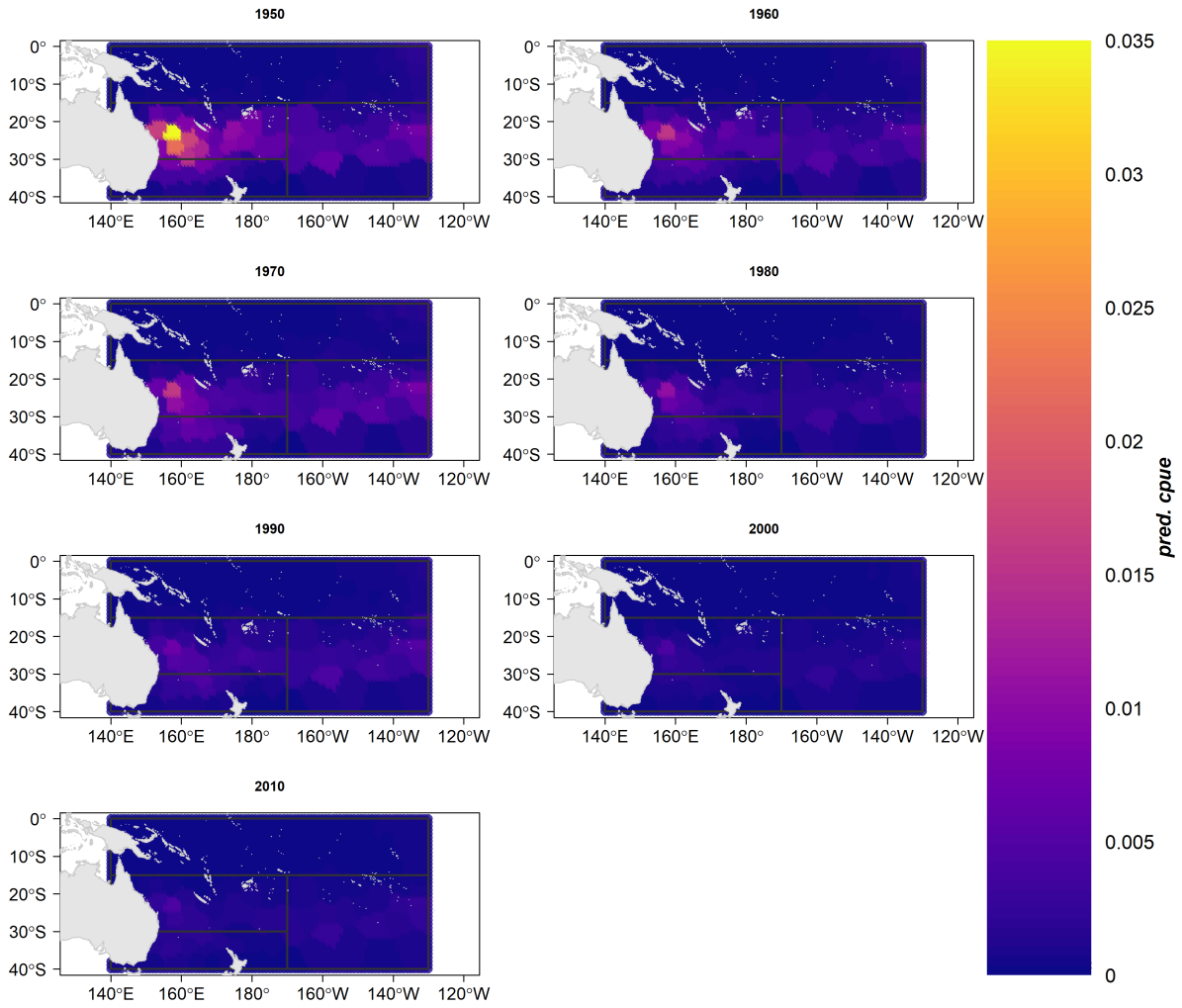

Figure 31: Predicted spatial CPUE of striped marlin by decade from the geostats model for each $1° \times 1°$ grid cell in the assessment region. Warmer colors indicate a greater probability of encounter, and cooler colors indicate a lower probability of encounter.

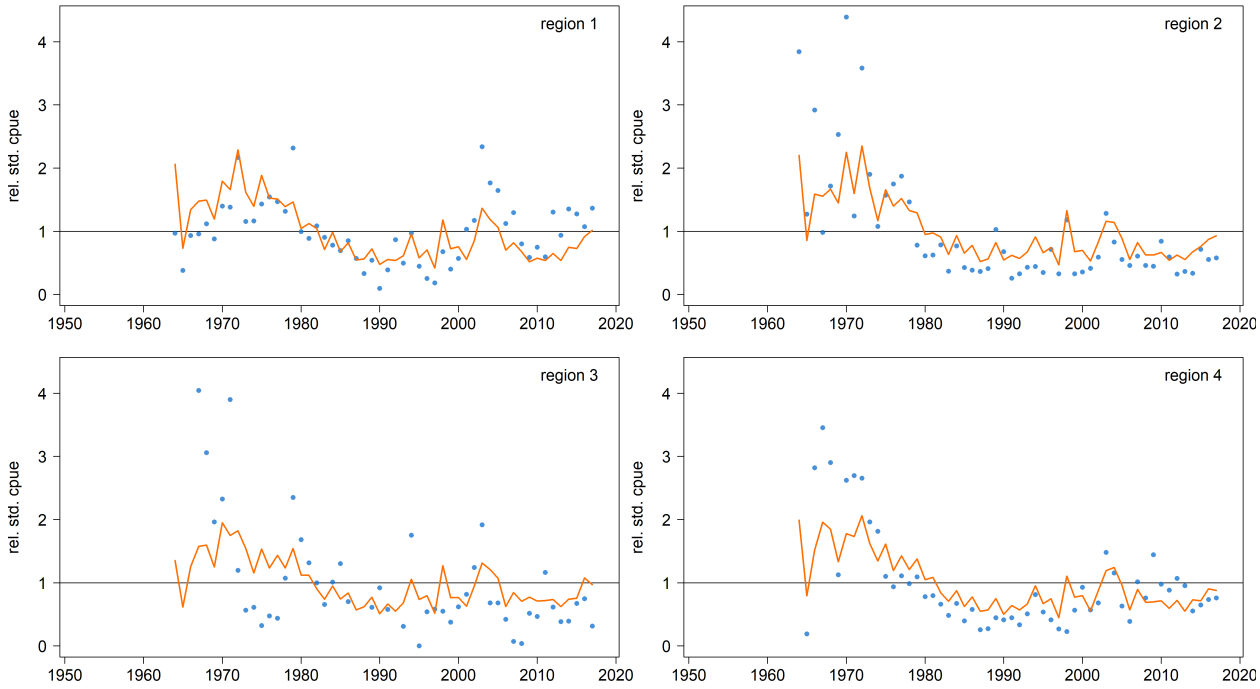

Figure 32: Standardized indices for the TW DW fleet. The standardized index used in structural uncertainty grid for Fishery 5 is shown in the panel for region 4. In all panels the standardized CPUE is denoted by the orange line, and blue points denote the nominal CPUE observations. All indices were rescaled to a mean of 1.

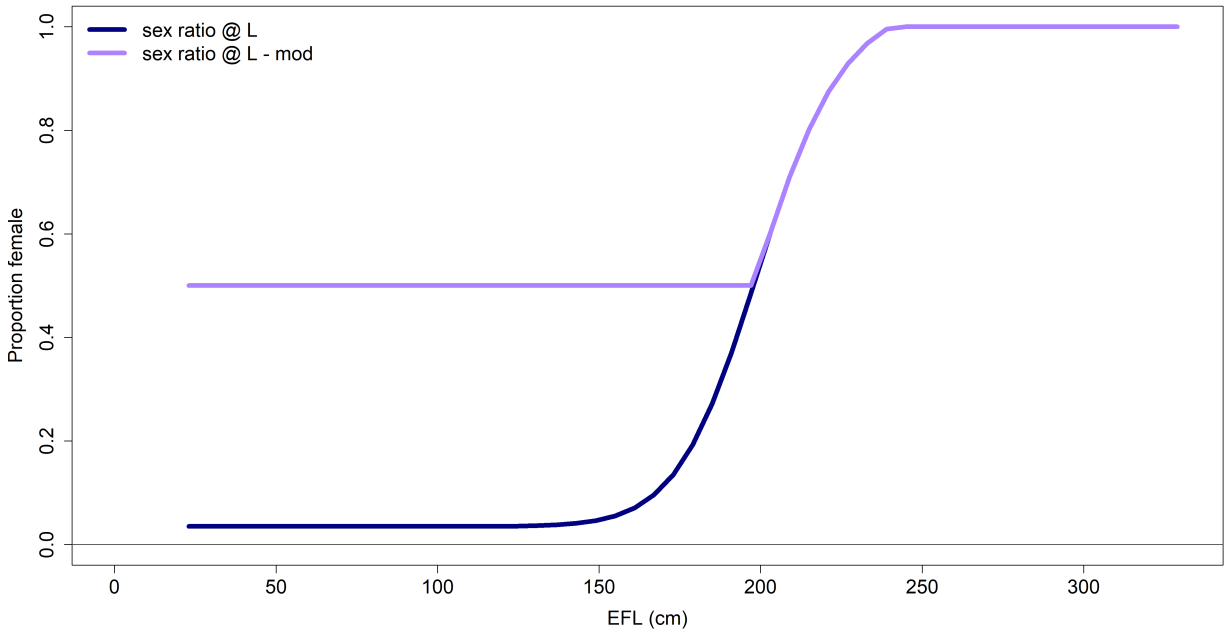

Figure 33: The calculated sex-ratio at length (eye-orbital fork length) based on Kopf et al. (2012) (dark purple) and the modified sex-ratio at length (light purple) used to define ρ_ℓ in the 2019 striped marlin stock assessment.

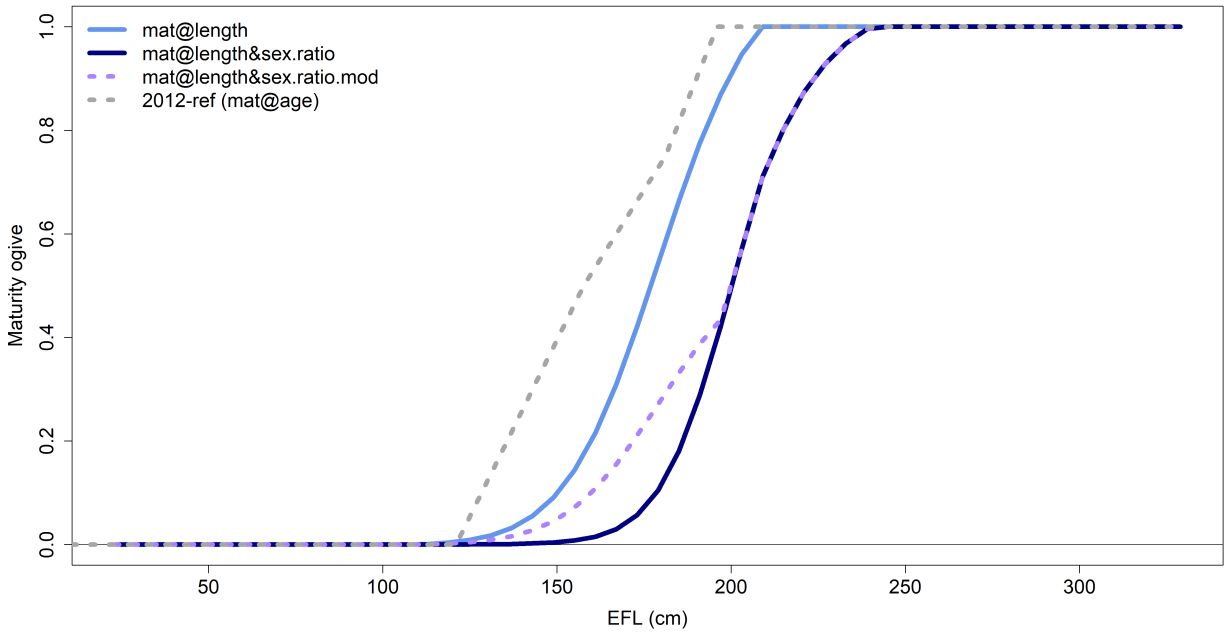

Figure 34: The derived maturity ogive, ρ_ℓ, at length (eye-orbital fork length) used in the 2019 striped marlin stock assessment (dotted light purple). The maturity ogive at age used in the 2012 stock assessment is shown in the dotted gray line. Additionally, the female maturity at length (PMF) used to calculate ρ_ℓ (light blue) and the maturity ogive derived without the modification to the sex-ratio (dark purple) are shown.

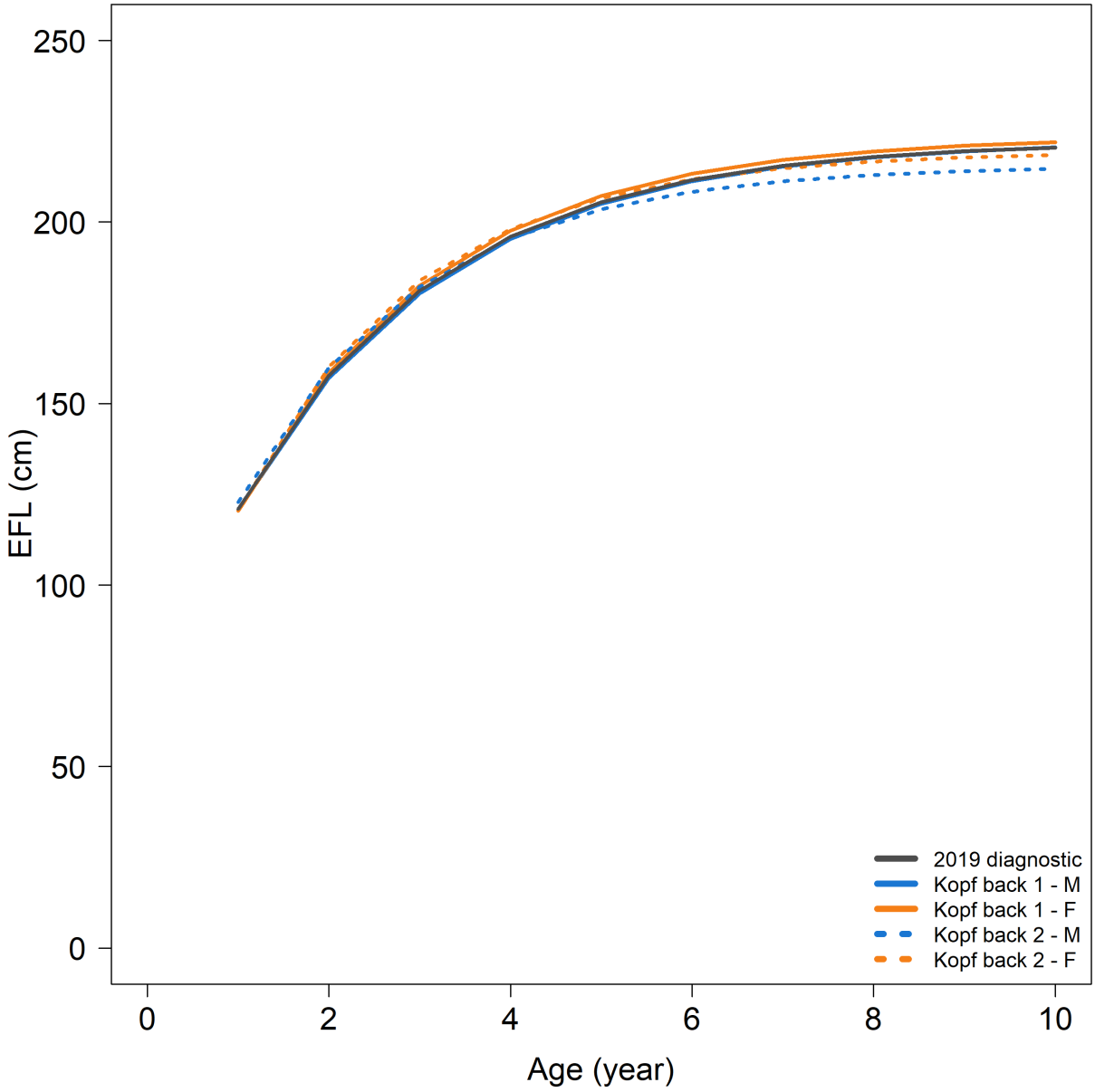

Figure 35: Sex specific growth curves considered for the sex-disaggregated model sensitivity runs. The 2019 diagnostic case growth is shown in gray. The male curves are in blue and the female growth curves are in orange. The "back-calculation 2" growth (dotted lines) is differentiated from the "back-calculation 1" growth by line type.

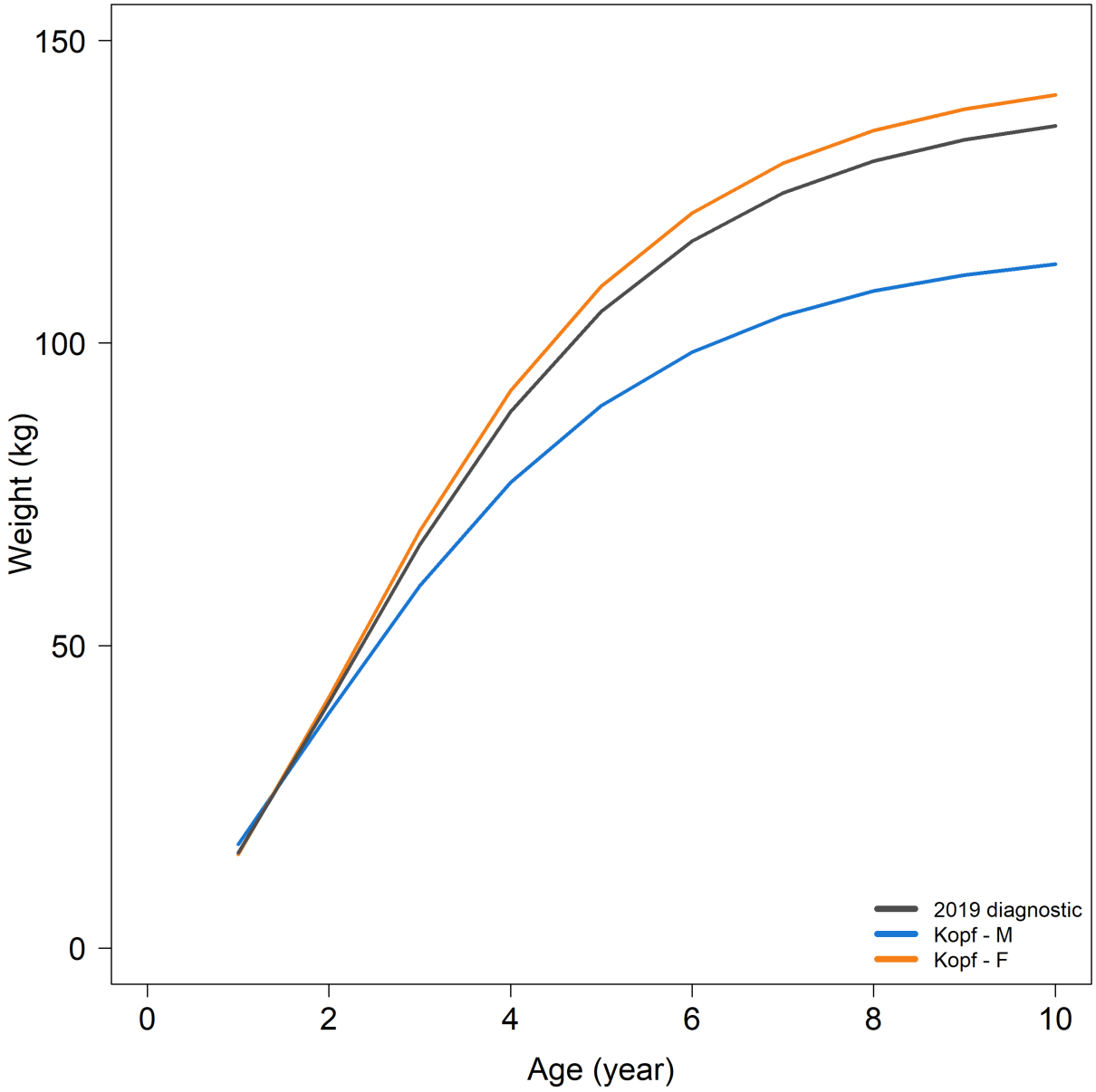

Figure 36: Sex specific weight-at-age considered for the sex-disaggregated model sensitivity runs. The 2019 diagnostic case growth is shown in gray. The male curves are in blue and the female growth curves are in orange.

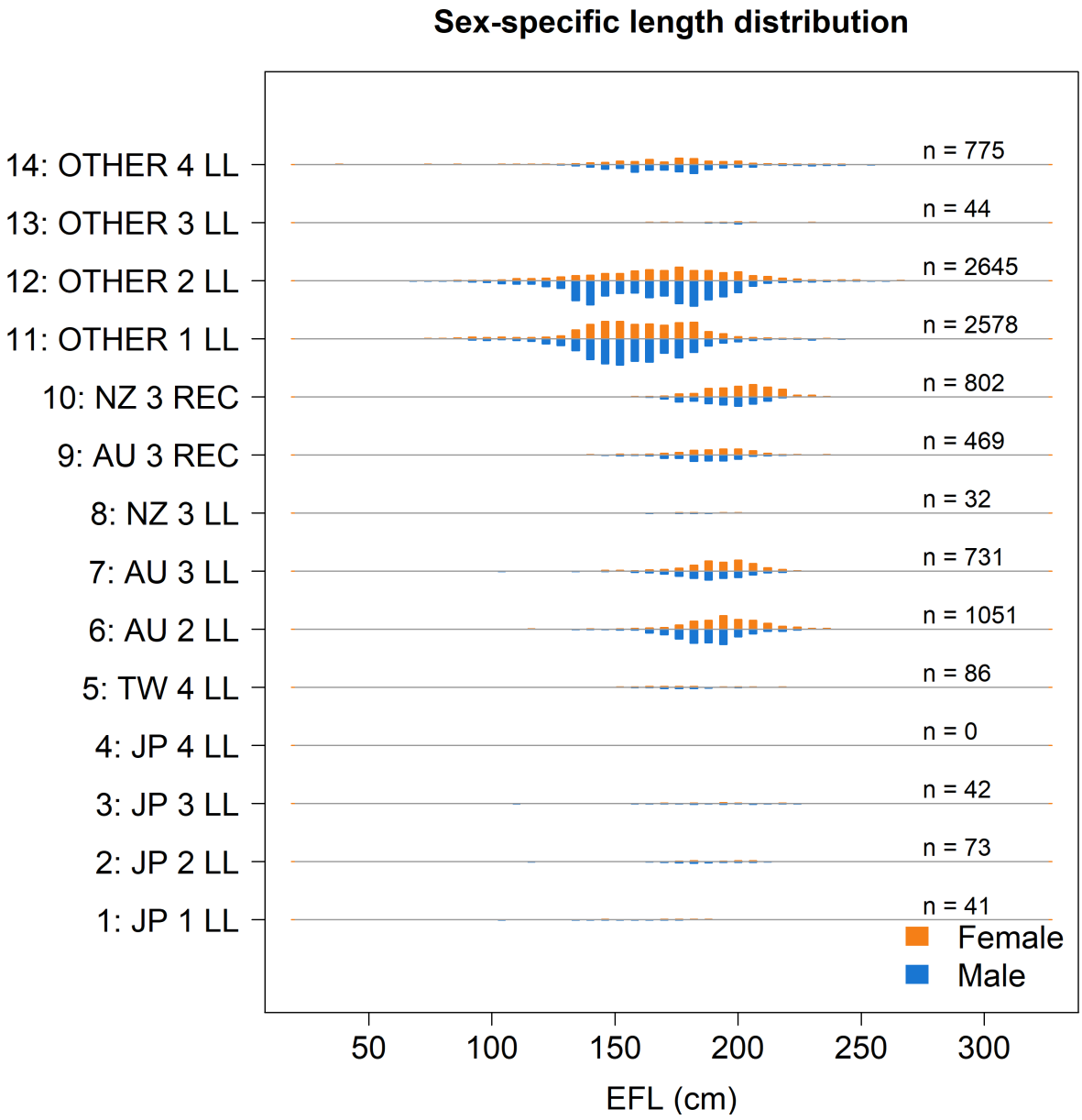

Figure 37: Sex specific *EFL* (cm) length frequency distributions for each fishery. The male observations are in blue and the female observations are in orange.

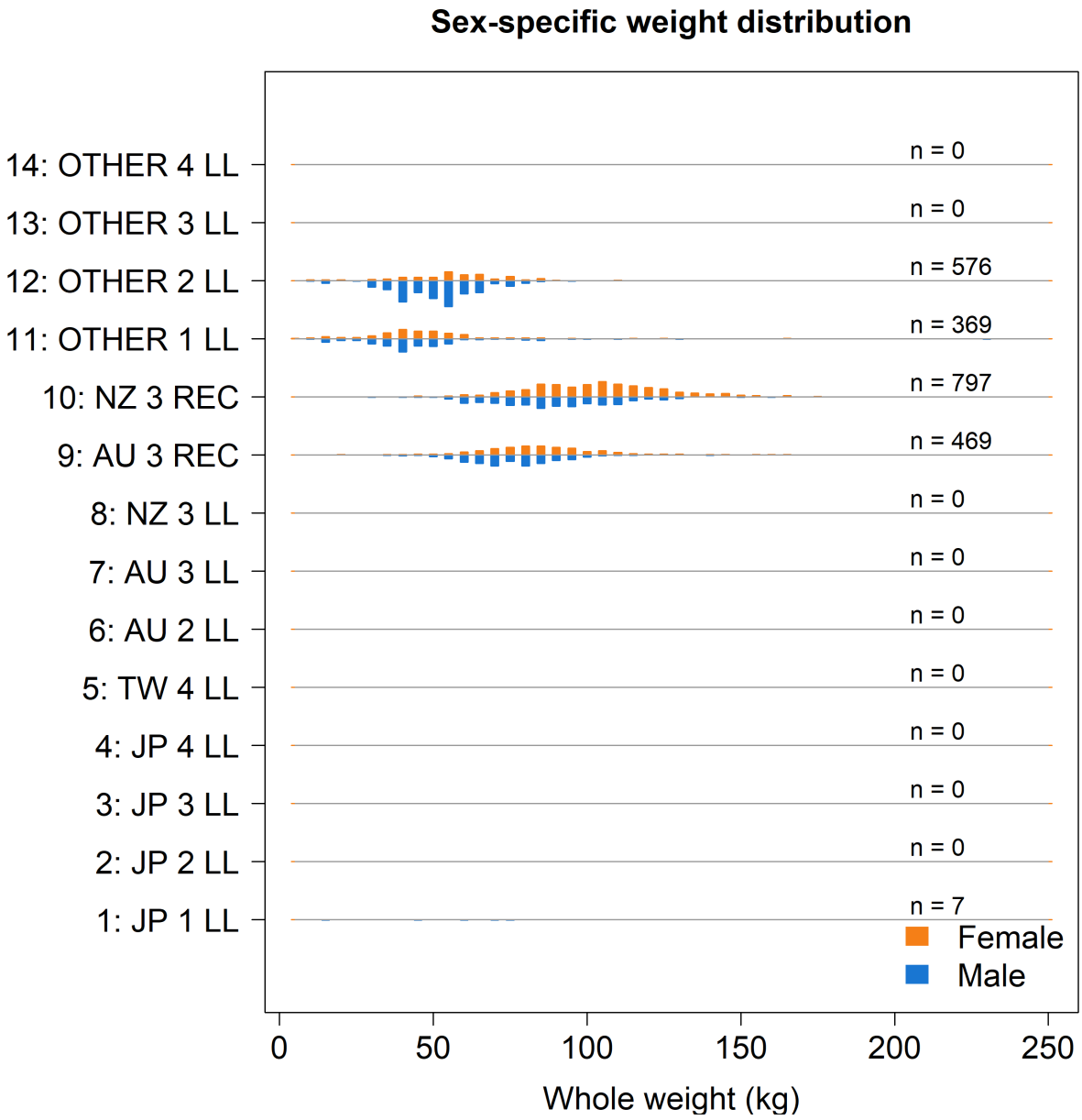

Figure 38: Sex specific whole weight (kg) frequncy distributions for each fishery. The male observations are in blue and the female observations are in orange.

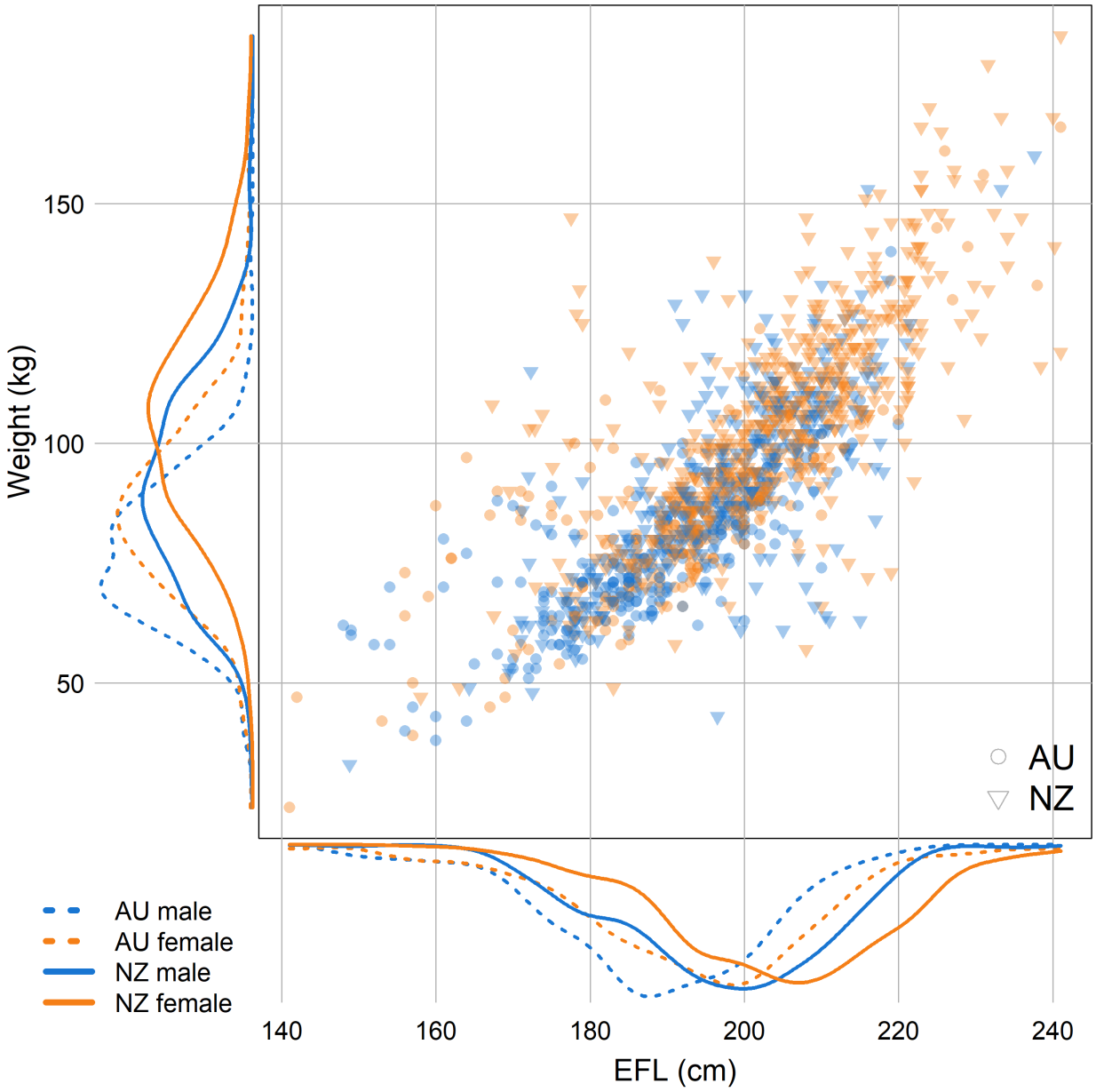

Figure 39: Bivariate distribution of striped marlin weight at length from the Australian (AU, circle) and New Zealand (NZ, triangle) recreational fisheries. The male observations are in blue and the female observations are in orange. The sex and fishery specific densities of *EFL* and whole weight are shown on each axis.

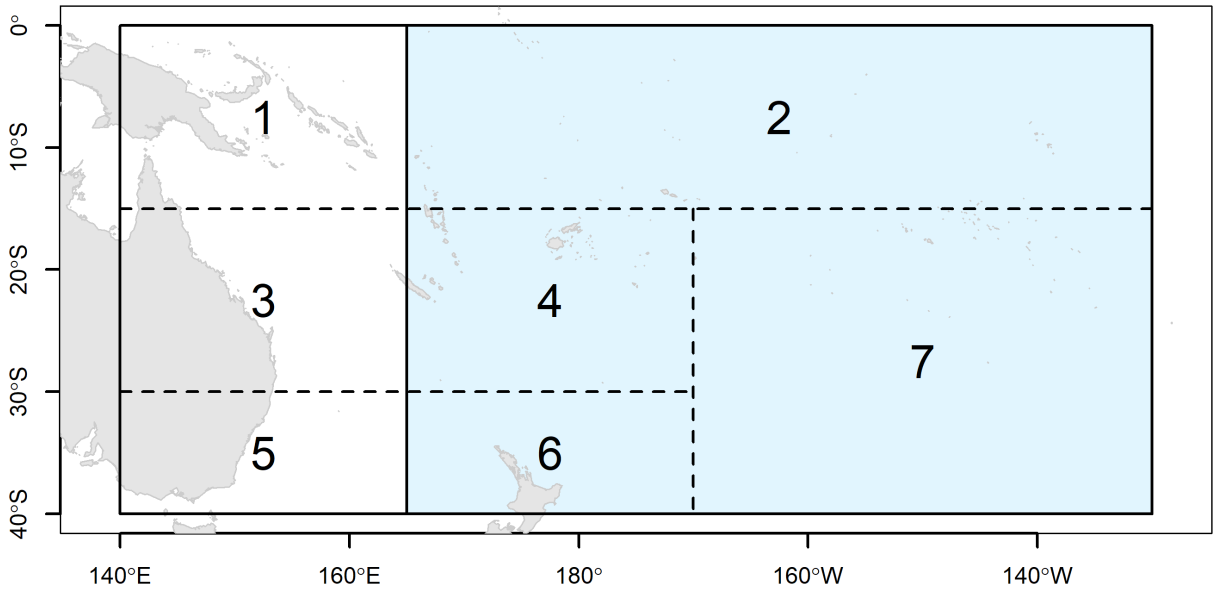

Figure 40: The model regions and sub-regions used to define the movement and fishery definitions for the spatially disaggregated model sensitivity runs. The solid line gives the regional boundary at 165°E with region 1 on the left and region 2 on the right (blue). The dotted lines denote the sub-regions used to define the fisheries.

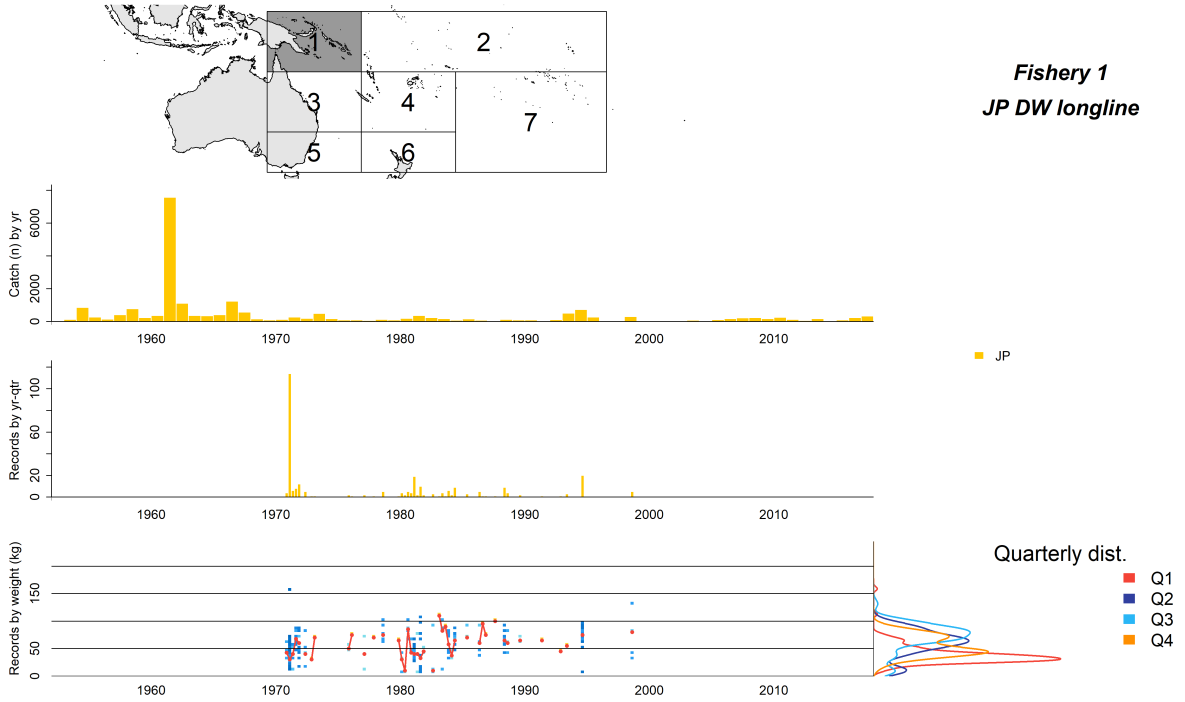

Figure 41: Summary plot showing the characteristics of the fisheries defined for the 2019 striped marlin stock assessment. The top panel indicates the sub-region the fishery was defined in. The middle two panels indicate the annual catch by country and the quarterly size composition records by country for the fishery (middle-top and middle-bottom, respectively). The lower panel shows the size composition data for the fishery by whole weight (kg) bin at a quarterly time scale with the median in each time period shown in red. To the right of this are the cumulative size composition distributions by quarter.

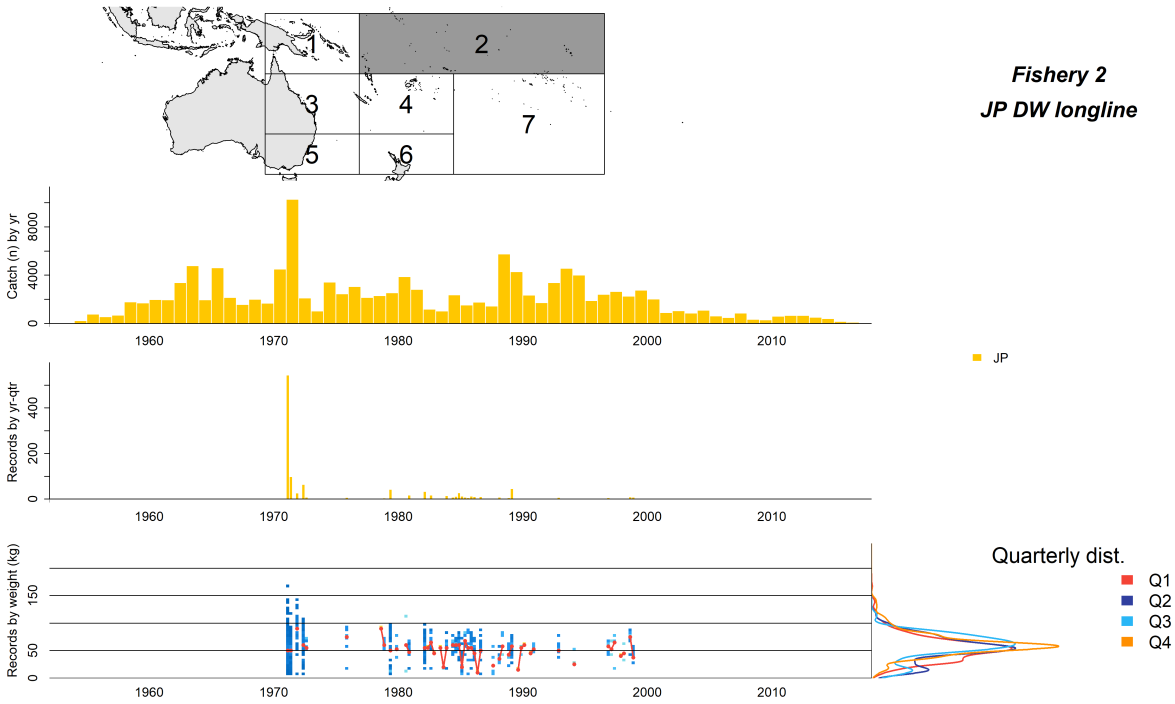

Figure 42: Summary plot showing the characteristics of the fisheries defined for the 2019 striped marlin stock assessment. The top panel indicates the sub-region the fishery was defined in. The middle two panels indicate the annual catch by country and the quarterly size composition records by country for the fishery (middle-top and middle-bottom, respectively). The lower panel shows the size composition data for the fishery by whole weight (kg) bin at a quarterly time scale with the median in each time period shown in red. To the right of this are the cumulative size composition distributions by quarter.

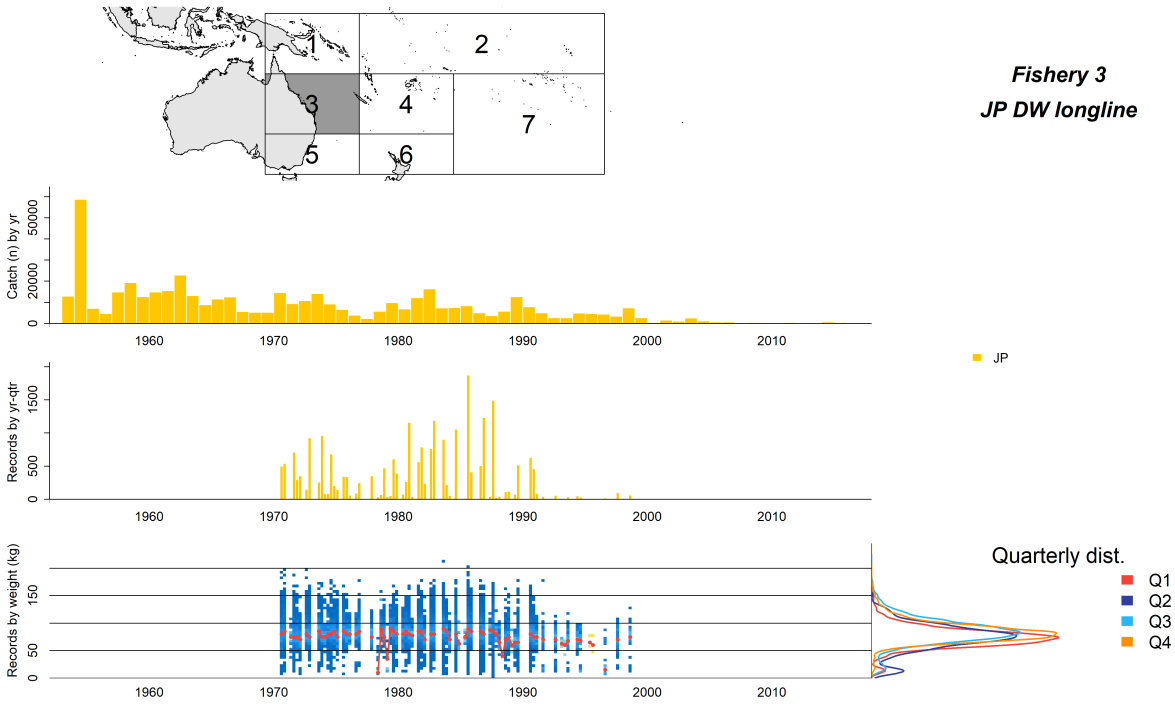

Figure 43: Summary plot showing the characteristics of the fisheries defined for the 2019 striped marlin stock assessment. The top panel indicates the sub-region the fishery was defined in. The middle two panels indicate the annual catch by country and the quarterly size composition records by country for the fishery (middle-top and middle-bottom, respectively). The lower panel shows the size composition data for the fishery by whole weight (kg) bin at a quarterly time scale with the median in each time period shown in red. To the right of this are the cumulative size composition distributions by quarter.

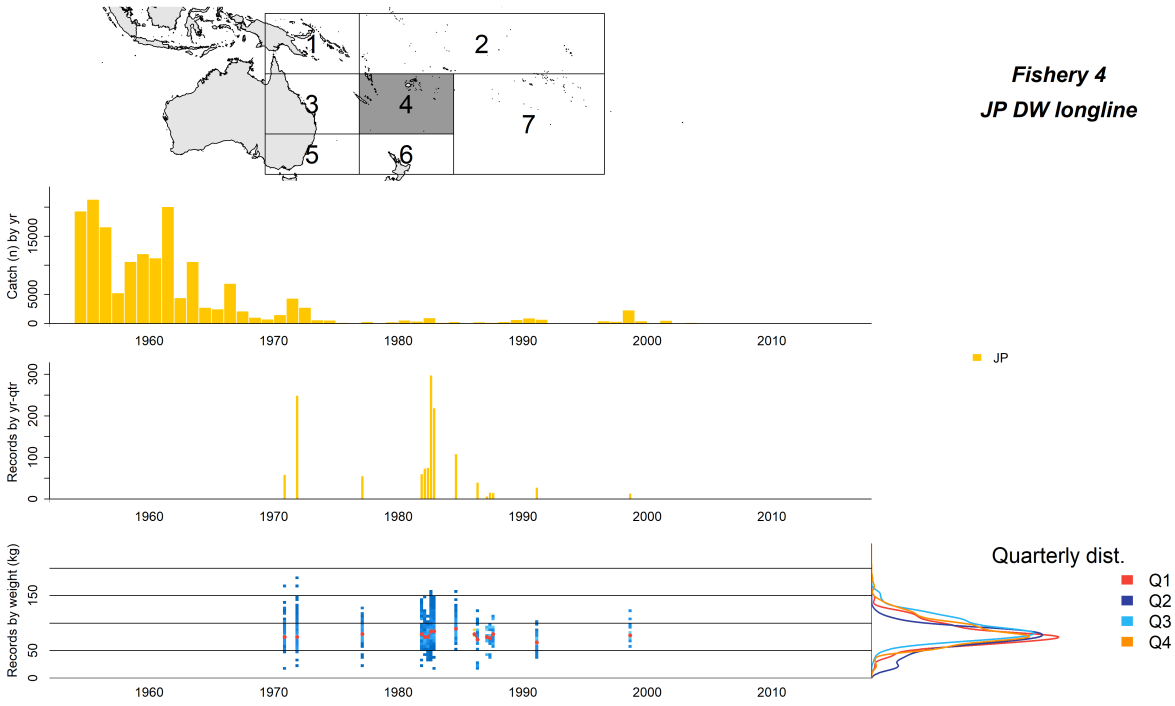

Figure 44: Summary plot showing the characteristics of the fisheries defined for the 2019 striped marlin stock assessment. The top panel indicates the sub-region the fishery was defined in. The middle two panels indicate the annual catch by country and the quarterly size composition records by country for the fishery (middle-top and middle-bottom, respectively). The lower panel shows the size composition data for the fishery by whole weight (kg) bin at a quarterly time scale with the median in each time period shown in red. To the right of this are the cumulative size composition distributions by quarter.

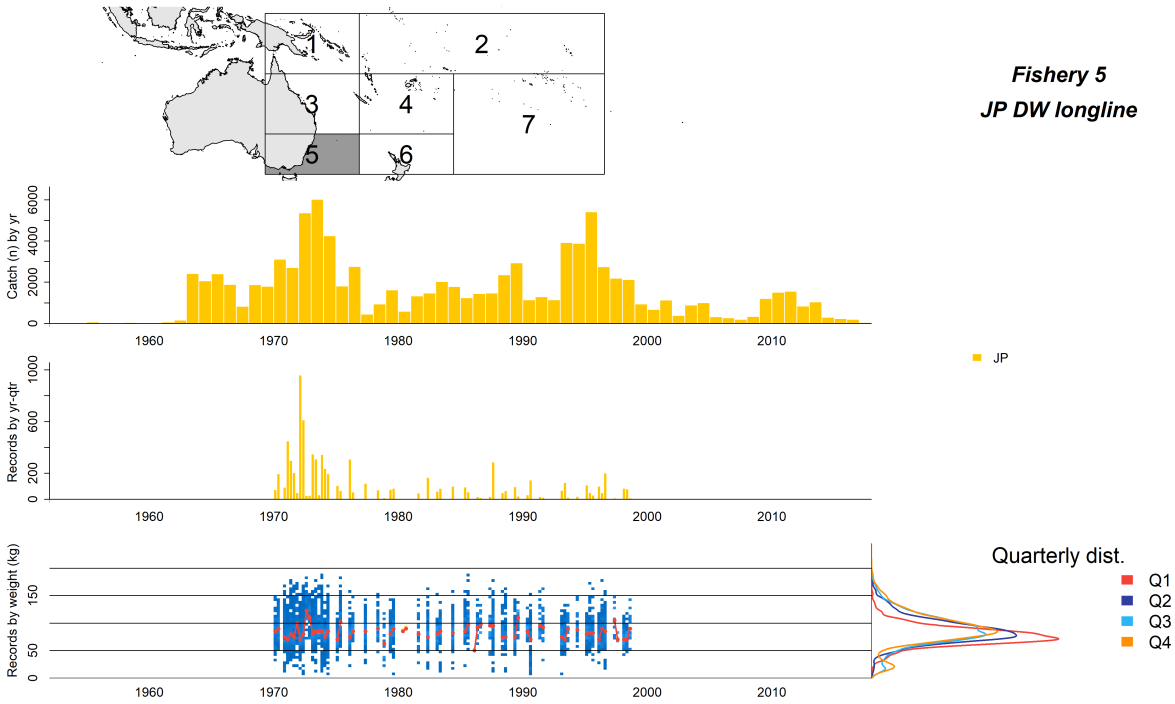

Figure 45: Summary plot showing the characteristics of the fisheries defined for the 2019 striped marlin stock assessment. The top panel indicates the sub-region the fishery was defined in. The middle two panels indicate the annual catch by country and the quarterly size composition records by country for the fishery (middle-top and middle-bottom, respectively). The lower panel shows the size composition data for the fishery by whole weight (kg) bin at a quarterly time scale with the median in each time period shown in red. To the right of this are the cumulative size composition distributions by quarter.

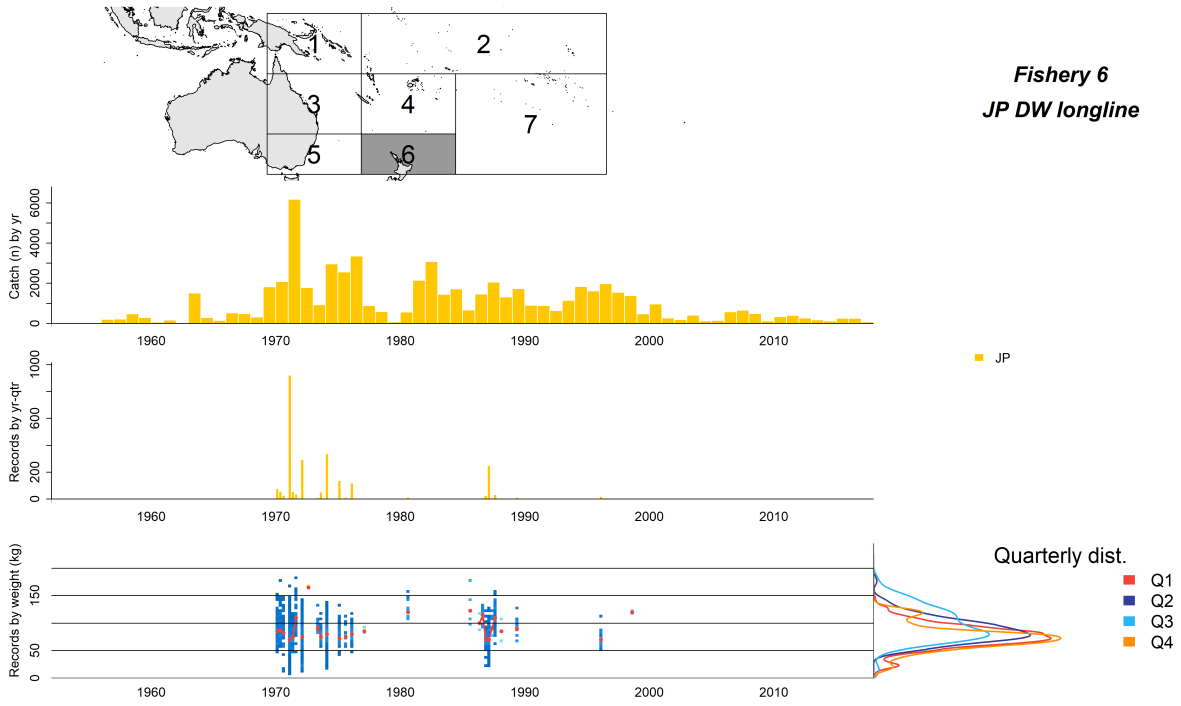

Figure 46: Summary plot showing the characteristics of the fisheries defined for the 2019 striped marlin stock assessment. The top panel indicates the sub-region the fishery was defined in. The middle two panels indicate the annual catch by country and the quarterly size composition records by country for the fishery (middle-top and middle-bottom, respectively). The lower panel shows the size composition data for the fishery by whole weight (kg) bin at a quarterly time scale with the median in each time period shown in red. To the right of this are the cumulative size composition distributions by quarter.

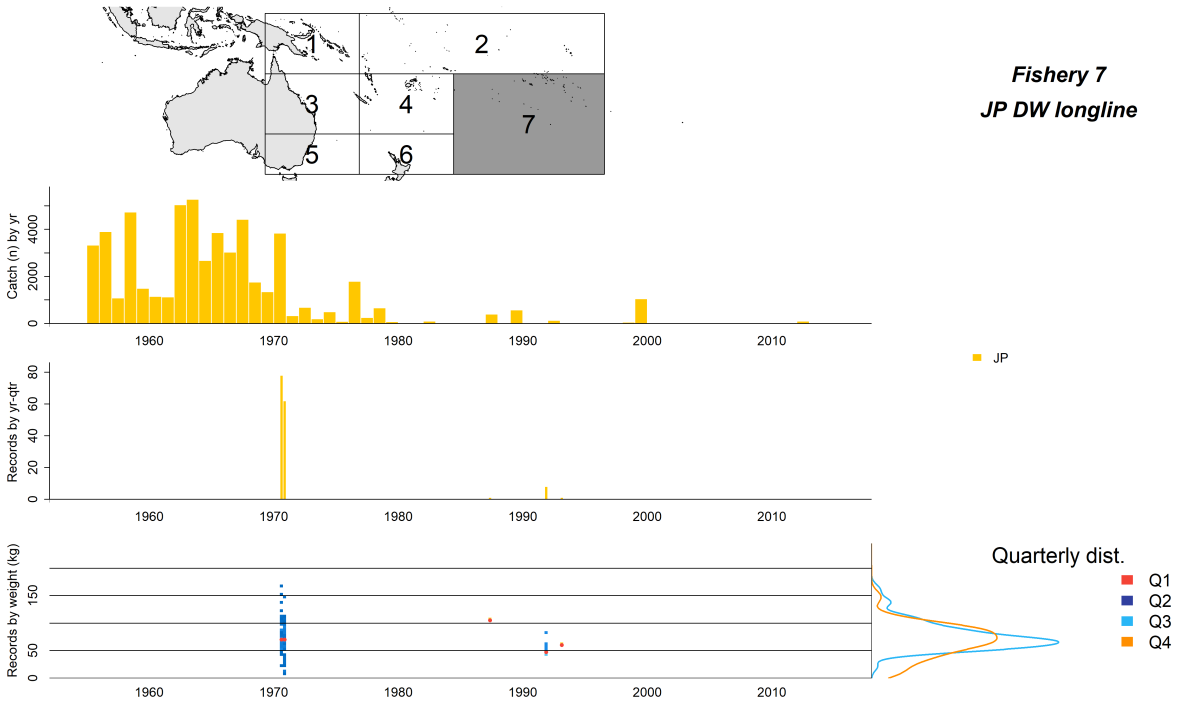

Figure 47: Summary plot showing the characteristics of the fisheries defined for the 2019 striped marlin stock assessment. The top panel indicates the sub-region the fishery was defined in. The middle two panels indicate the annual catch by country and the quarterly size composition records by country for the fishery (middle-top and middle-bottom, respectively). The lower panel shows the size composition data for the fishery by whole weight (kg) bin at a quarterly time scale with the median in each time period shown in red. To the right of this are the cumulative size composition distributions by quarter.

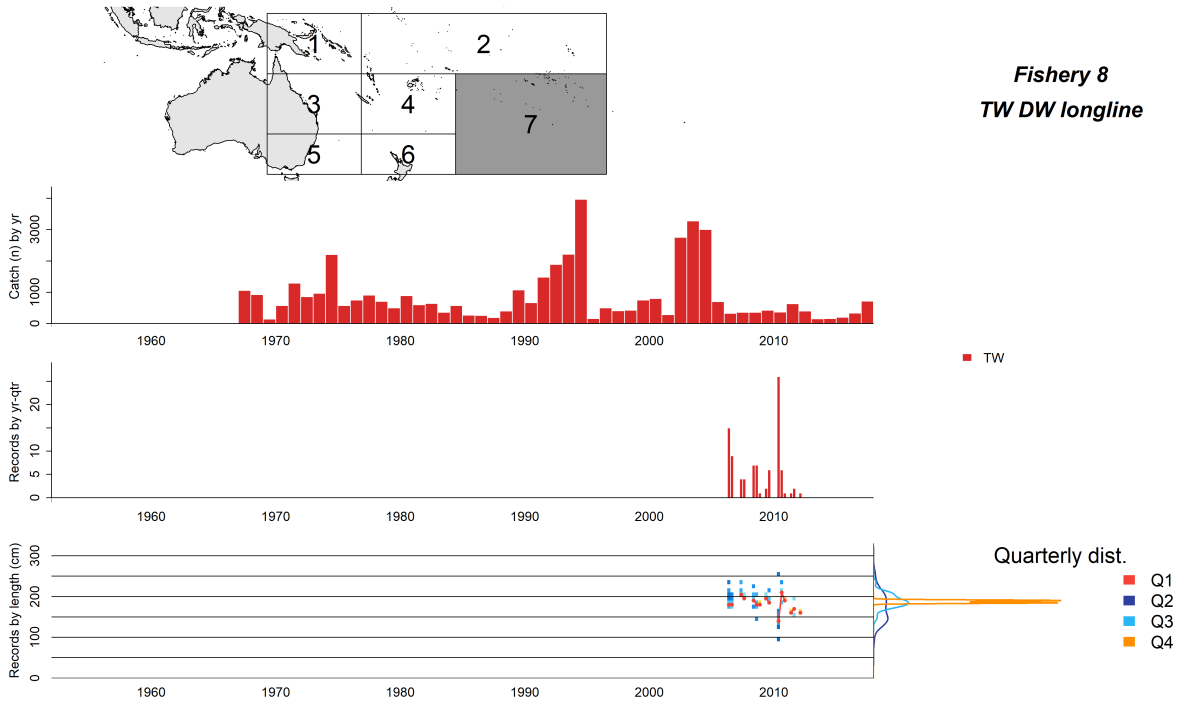

Figure 48: Summary plot showing the characteristics of the fisheries defined for the 2019 striped marlin stock assessment. The top panel indicates the sub-region the fishery was defined in. The middle two panels indicate the annual catch by country and the quarterly size composition records by country for the fishery (middle-top and middle-bottom, respectively). The lower panel shows the size composition data for the fishery by eye-fork length (cm) bin at a quarterly time scale with the median in each time period shown in red. To the right of this are the cumulative size composition distributions by quarter.

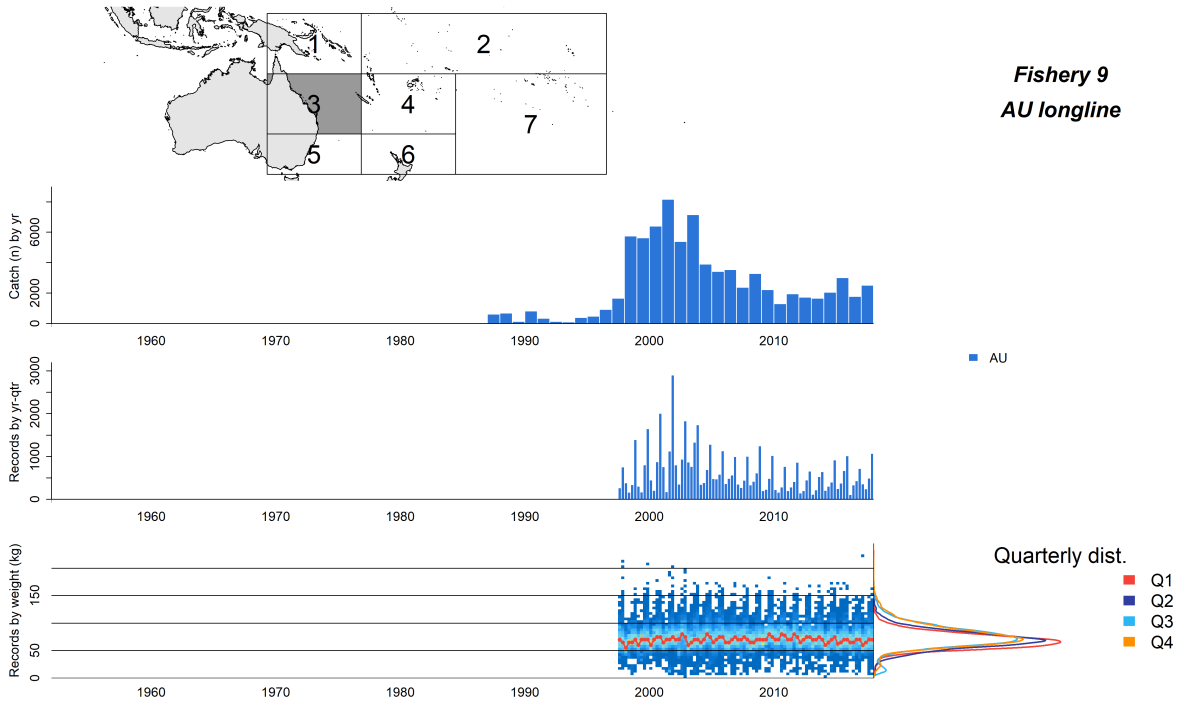

Figure 49: Summary plot showing the characteristics of the fisheries defined for the 2019 striped marlin stock assessment. The top panel indicates the sub-region the fishery was defined in. The middle two panels indicate the annual catch by country and the quarterly size composition records by country for the fishery (middle-top and middle-bottom, respectively). The lower panel shows the size composition data for the fishery by whole weight (kg) bin at a quarterly time scale with the median in each time period shown in red. To the right of this are the cumulative size composition distributions by quarter.

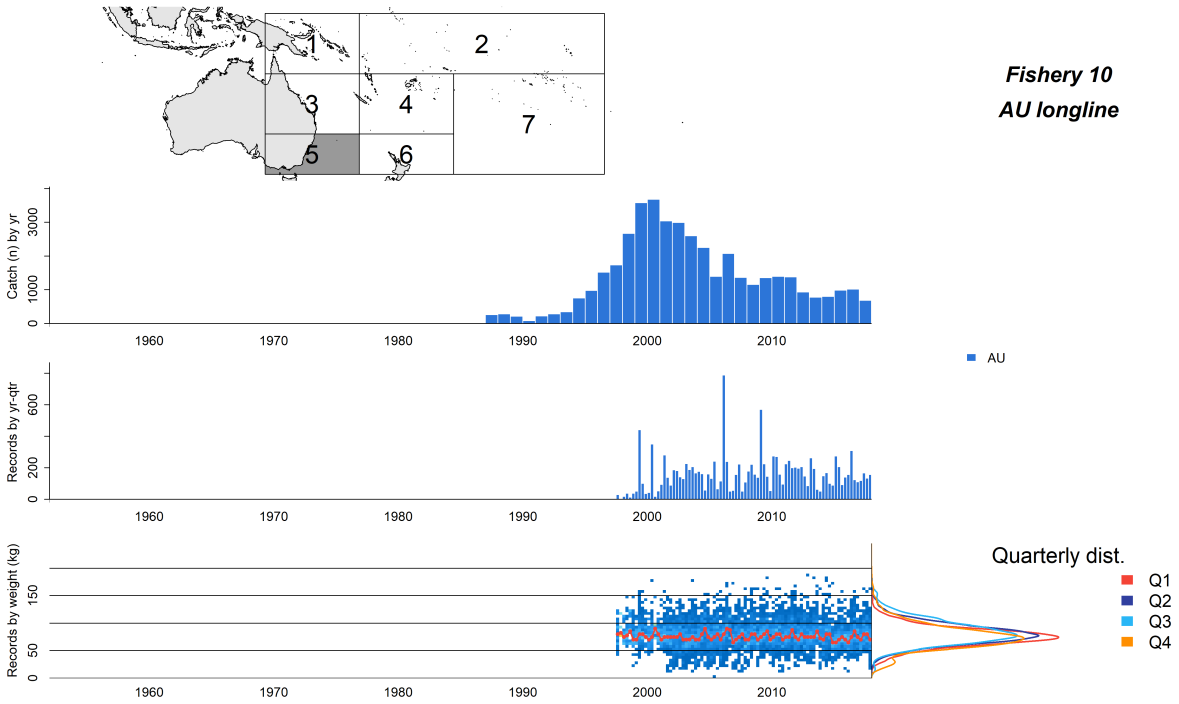

Figure 50: Summary plot showing the characteristics of the fisheries defined for the 2019 striped marlin stock assessment. The top panel indicates the sub-region the fishery was defined in. The middle two panels indicate the annual catch by country and the quarterly size composition records by country for the fishery (middle-top and middle-bottom, respectively). The lower panel shows the size composition data for the fishery by whole weight (kg) bin at a quarterly time scale with the median in each time period shown in red. To the right of this are the cumulative size composition distributions by quarter.

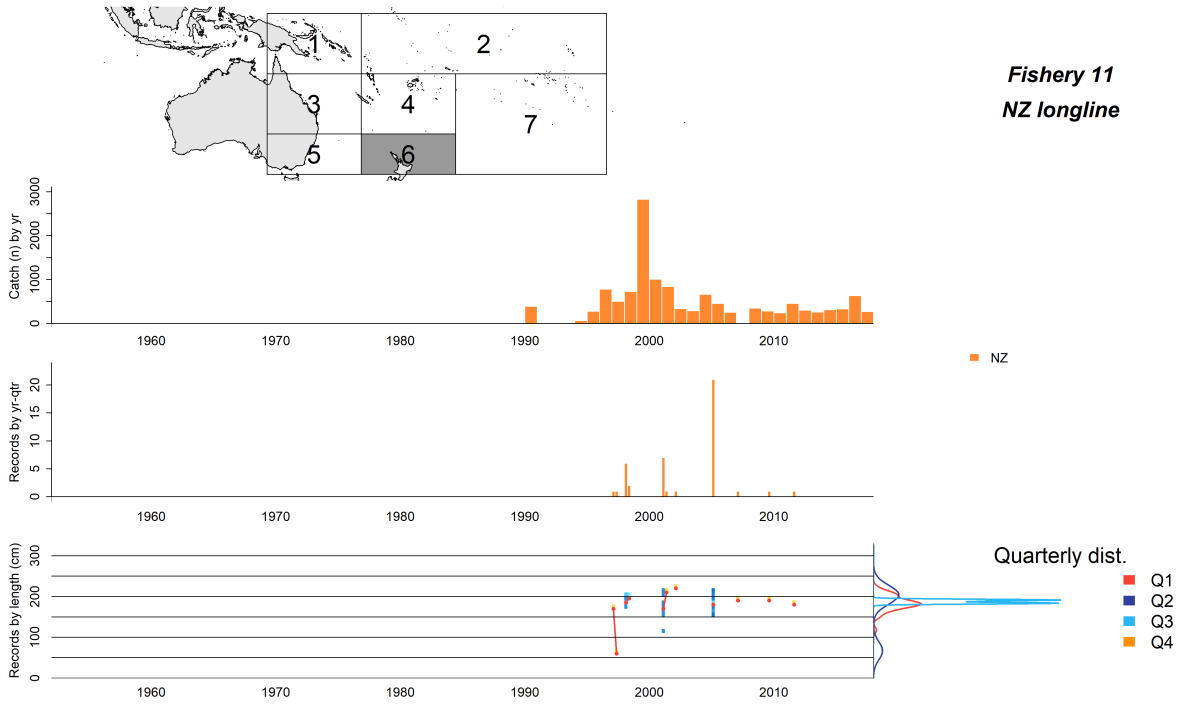

Figure 51: Summary plot showing the characteristics of the fisheries defined for the 2019 striped marlin stock assessment. The top panel indicates the sub-region the fishery was defined in. The middle two panels indicate the annual catch by country and the quarterly size composition records by country for the fishery (middle-top and middle-bottom, respectively). The lower panel shows the size composition data for the fishery by eye-fork length (cm) bin at a quarterly time scale with the median in each time period shown in red. To the right of this are the cumulative size composition distributions by quarter.

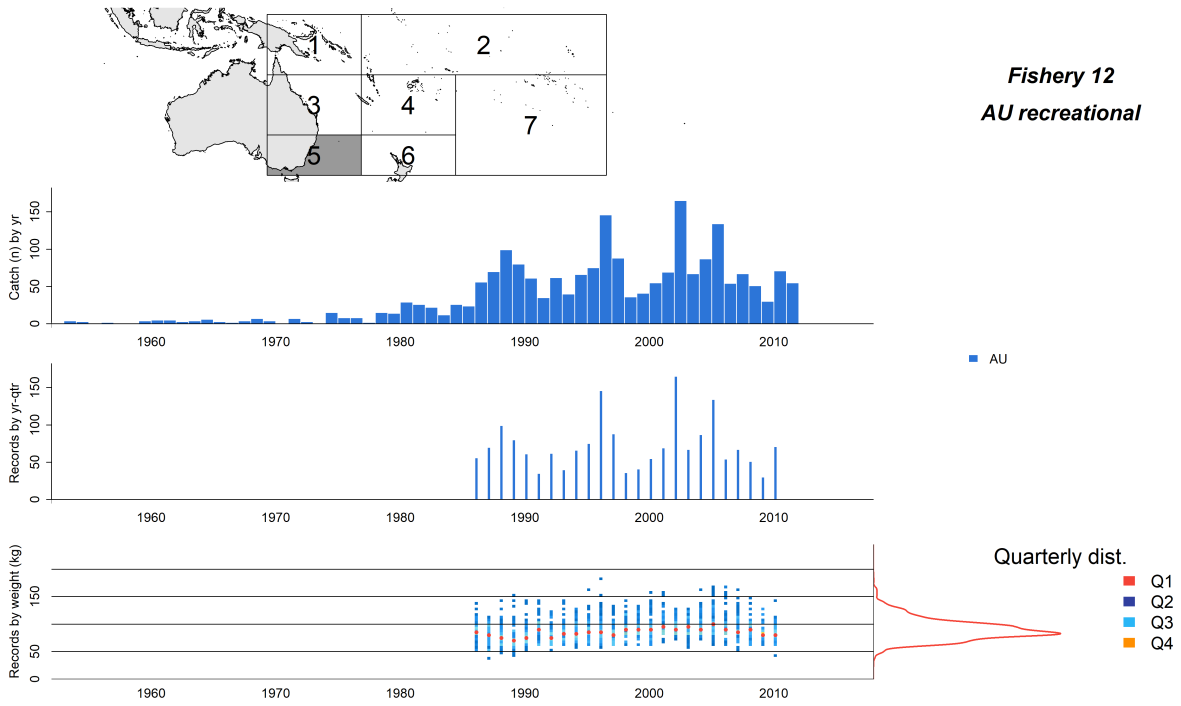

Figure 52: Summary plot showing the characteristics of the fisheries defined for the 2019 striped marlin stock assessment. The top panel indicates the sub-region the fishery was defined in. The middle two panels indicate the annual catch by country and the quarterly size composition records by country for the fishery (middle-top and middle-bottom, respectively). The lower panel shows the size composition data for the fishery by whole weight (kg) bin at a quarterly time scale with the median in each time period shown in red. To the right of this is the cumulative size composition distributions by quarter. Note that in the model the recreational fisheries are assumed to occur only in the first quarter of each year.

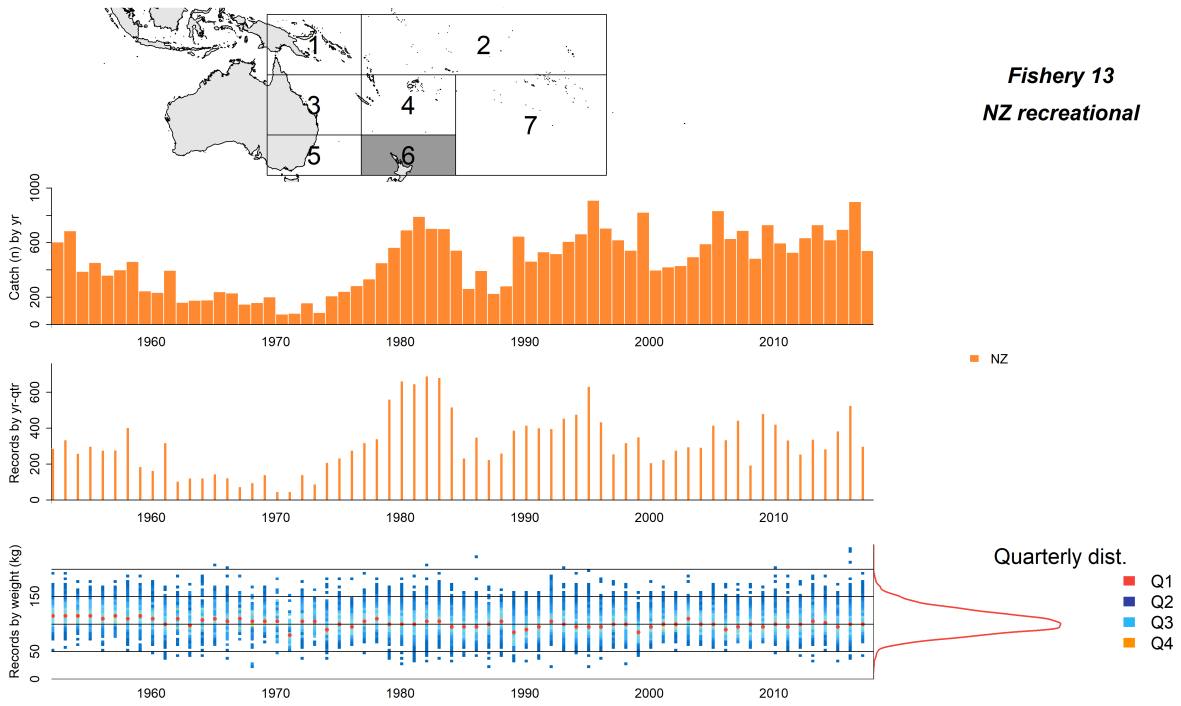

Figure 53: Summary plot showing the characteristics of the fisheries defined for the 2019 striped marlin stock assessment. The top panel indicates the sub-region the fishery was defined in. The middle two panels indicate the annual catch by country and the quarterly size composition records by country for the fishery (middle-top and middle-bottom, respectively). The lower panel shows the size composition data for the fishery by whole weight (kg) bin at a quarterly time scale with the median in each time period shown in red. To the right of this is the cumulative size composition distributions by quarter. Note that in the model the recreational fisheries are assumed to occur only in the first quarter of each year.

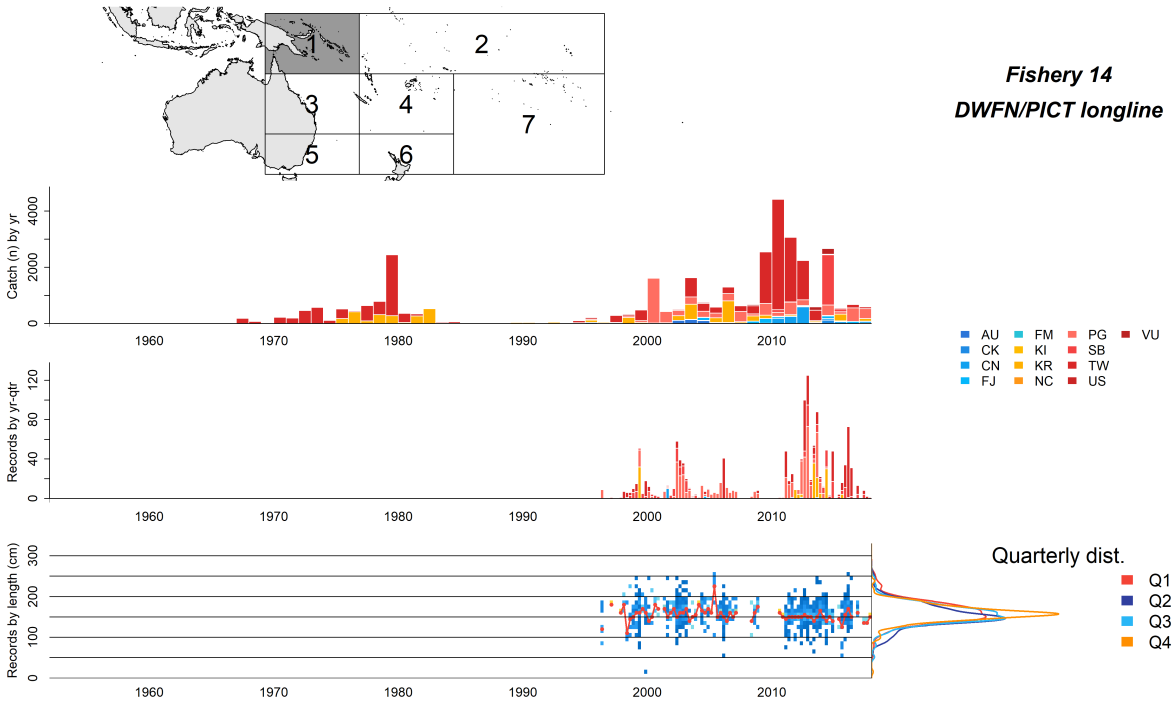

Figure 54: Summary plot showing the characteristics of the fisheries defined for the 2019 striped marlin stock assessment. The top panel indicates the sub-region the fishery was defined in. The middle two panels indicate the annual catch by country and the quarterly size composition records by country for the fishery (middle-top and middle-bottom, respectively). The lower panel shows the size composition data for the fishery by eye-fork length (cm) bin at a quarterly time scale with the median in each time period shown in red. To the right of this are the cumulative size composition distributions by quarter.

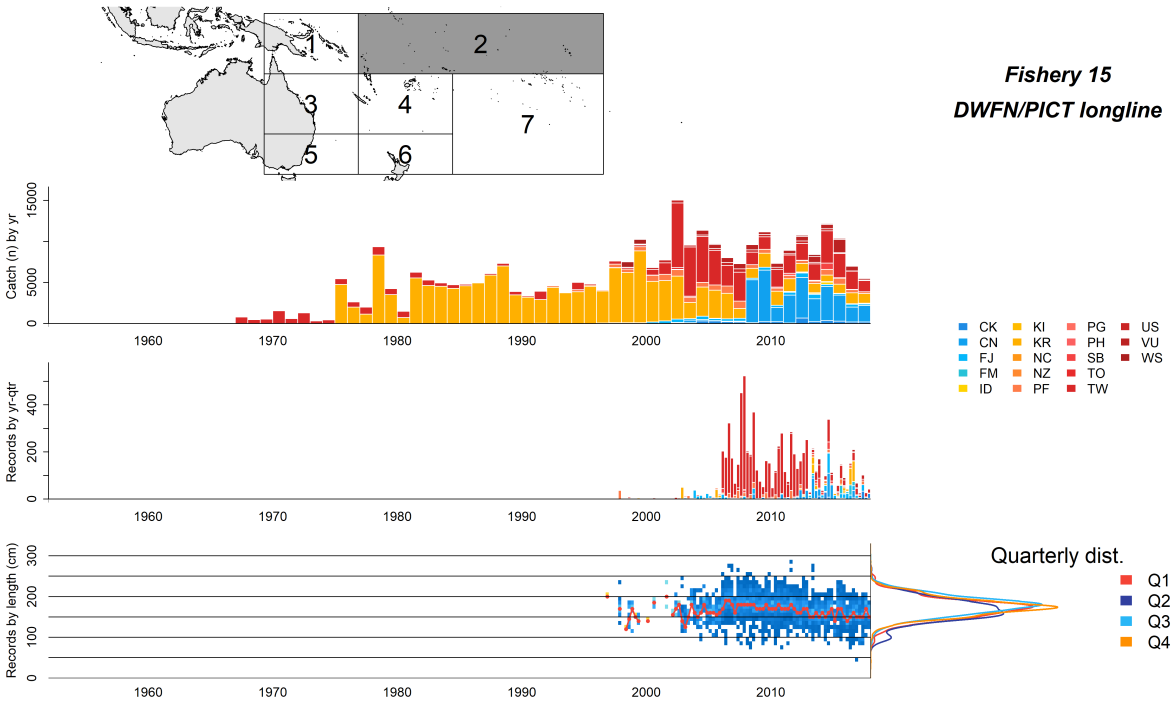

Figure 55: Summary plot showing the characteristics of the fisheries defined for the 2019 striped marlin stock assessment. The top panel indicates the sub-region the fishery was defined in. The middle two panels indicate the annual catch by country and the quarterly size composition records by country for the fishery (middle-top and middle-bottom, respectively). The lower panel shows the size composition data for the fishery by eye-fork length (cm) bin at a quarterly time scale with the median in each time period shown in red. To the right of this are the cumulative size composition distributions by quarter.

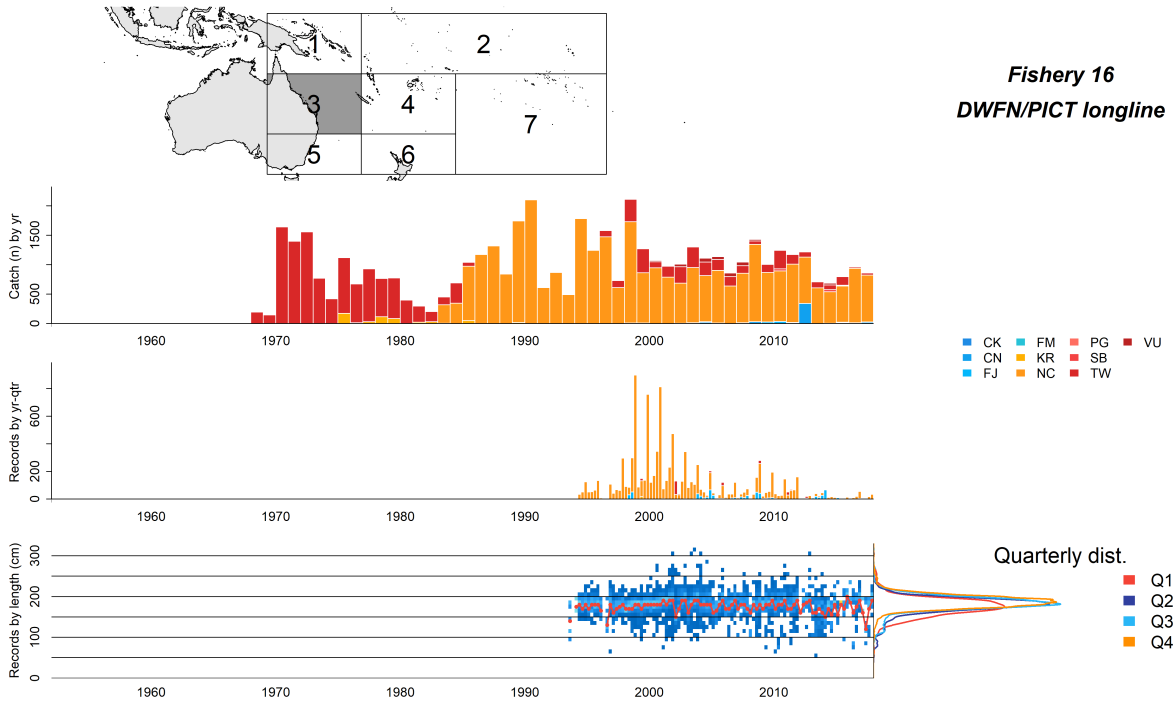

Figure 56: Summary plot showing the characteristics of the fisheries defined for the 2019 striped marlin stock assessment. The top panel indicates the sub-region the fishery was defined in. The middle two panels indicate the annual catch by country and the quarterly size composition records by country for the fishery (middle-top and middle-bottom, respectively). The lower panel shows the size composition data for the fishery by eye-fork length (cm) bin at a quarterly time scale with the median in each time period shown in red. To the right of this are the cumulative size composition distributions by quarter.

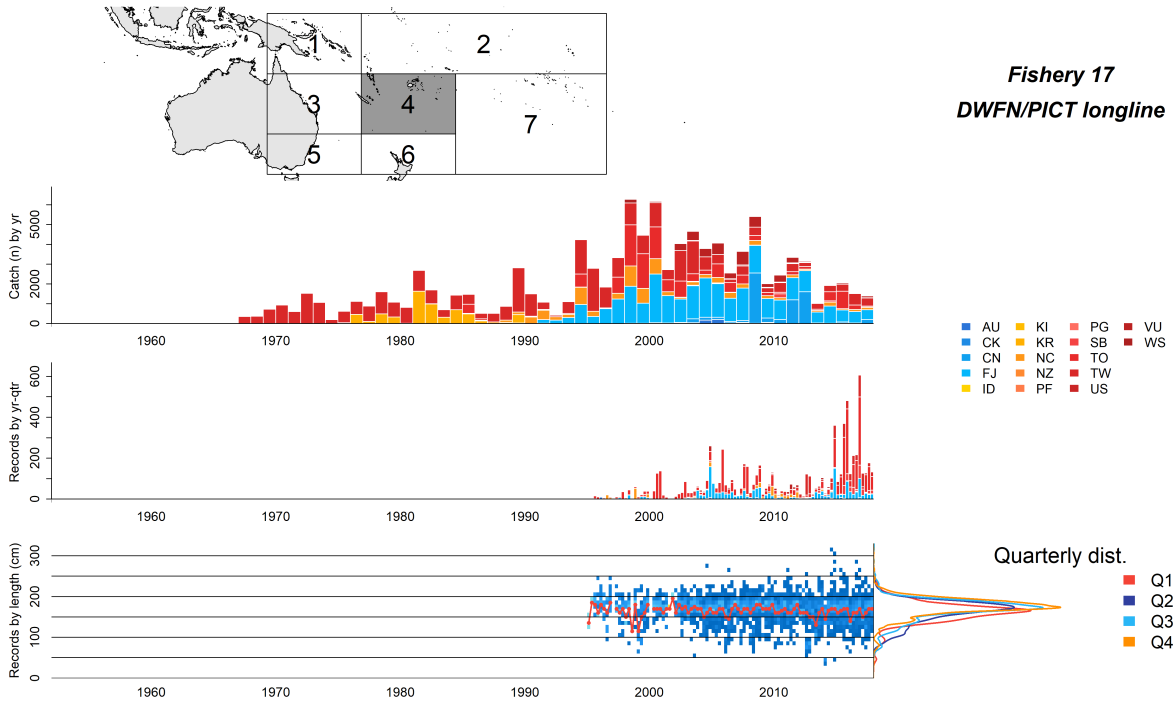

Figure 57: Summary plot showing the characteristics of the fisheries defined for the 2019 striped marlin stock assessment. The top panel indicates the sub-region the fishery was defined in. The middle two panels indicate the annual catch by country and the quarterly size composition records by country for the fishery (middle-top and middle-bottom, respectively). The lower panel shows the size composition data for the fishery by eye-fork length (cm) bin at a quarterly time scale with the median in each time period shown in red. To the right of this are the cumulative size composition distributions by quarter.

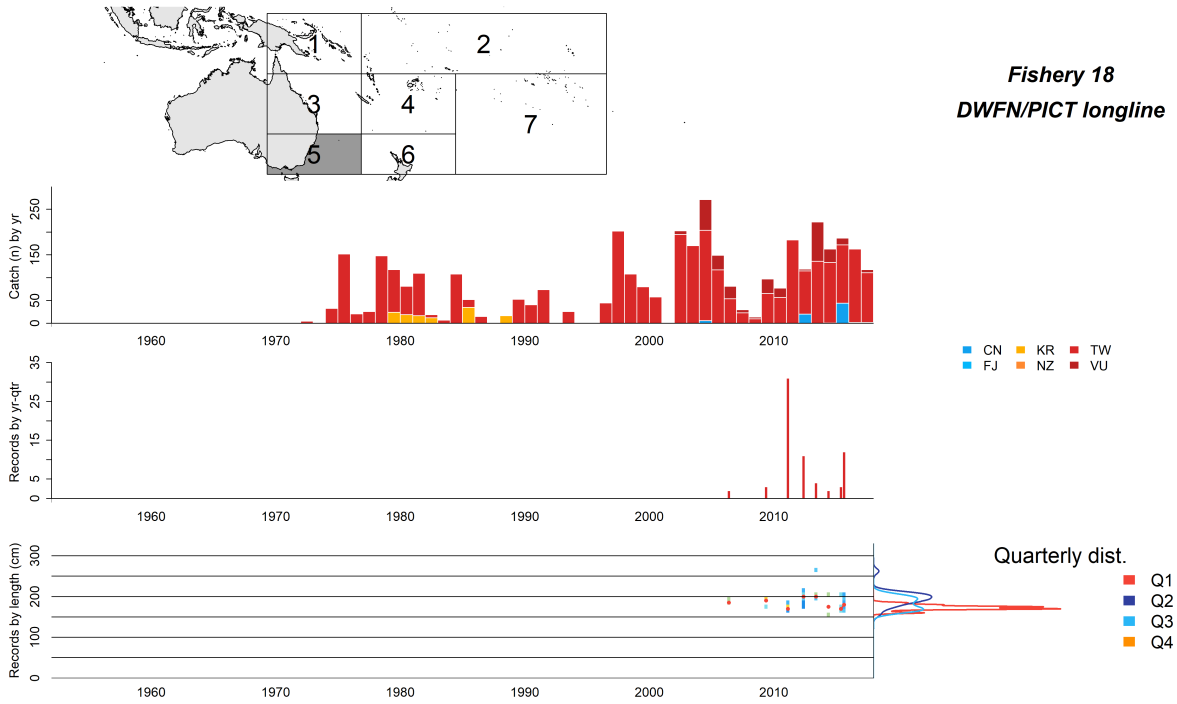

Figure 58: Summary plot showing the characteristics of the fisheries defined for the 2019 striped marlin stock assessment. The top panel indicates the sub-region the fishery was defined in. The middle two panels indicate the annual catch by country and the quarterly size composition records by country for the fishery (middle-top and middle-bottom, respectively). The lower panel shows the size composition data for the fishery by eye-fork length (cm) bin at a quarterly time scale with the median in each time period shown in red. To the right of this are the cumulative size composition distributions by quarter.

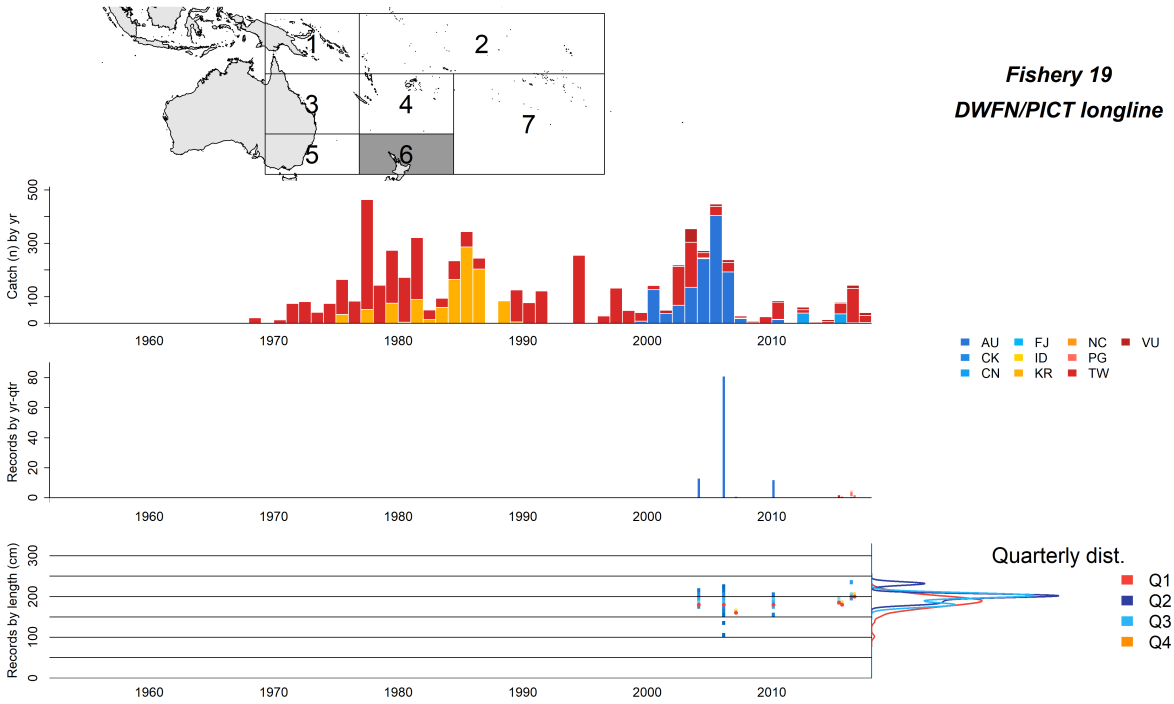

Figure 59: Summary plot showing the characteristics of the fisheries defined for the 2019 striped marlin stock assessment. The top panel indicates the sub-region the fishery was defined in. The middle two panels indicate the annual catch by country and the quarterly size composition records by country for the fishery (middle-top and middle-bottom, respectively). The lower panel shows the size composition data for the fishery by eye-fork length (cm) bin at a quarterly time scale with the median in each time period shown in red. To the right of this are the cumulative size composition distributions by quarter.

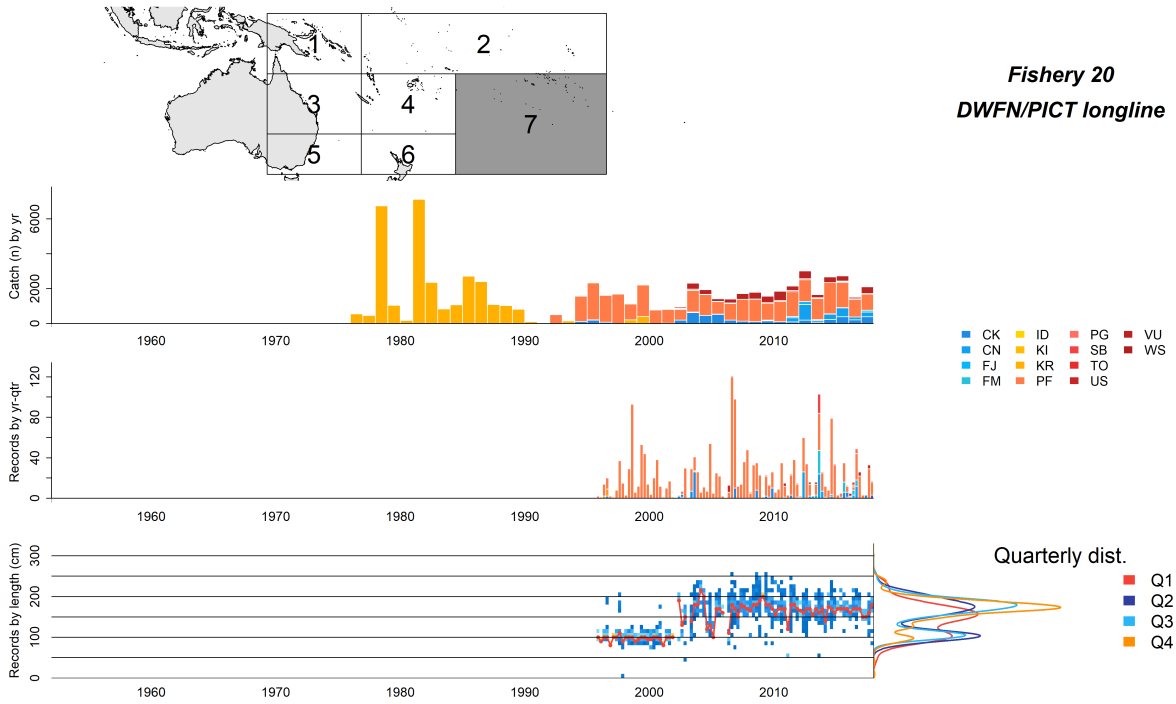

Figure 60: Summary plot showing the characteristics of the fisheries defined for the 2019 striped marlin stock assessment. The top panel indicates the sub-region the fishery was defined in. The middle two panels indicate the annual catch by country and the quarterly size composition records by country for the fishery (middle-top and middle-bottom, respectively). The lower panel shows the size composition data for the fishery by eye-fork length (cm) bin at a quarterly time scale with the median in each time period shown in red. To the right of this are the cumulative size composition distributions by quarter.

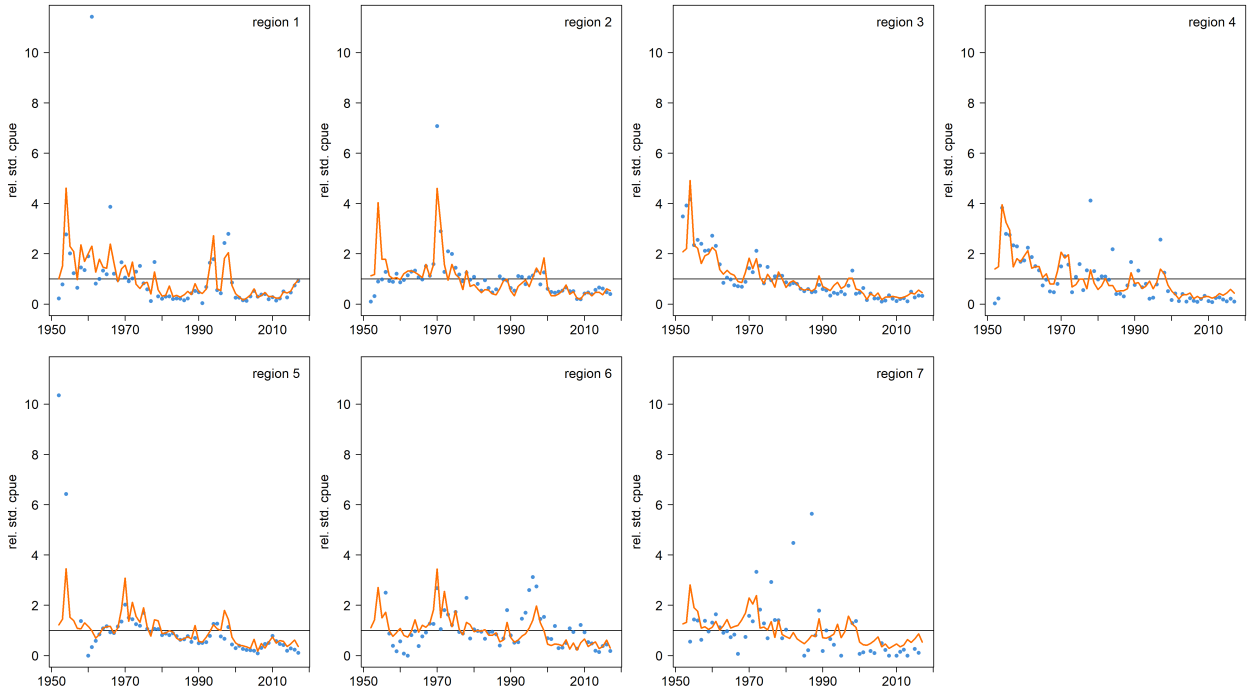

Figure 61: Standardized indices for the JP DW fleet. The standardized index used in the spatially disaggregated sensitivity runs for Fishery 3 is shown in the panel for region 3. In all panels the standardized CPUE is denoted by the orange line, and blue points denote the nominal CPUE observations. All indices were rescaled to a mean of 1.